Technische Universität München

Wissenschaftszentrum Weihenstephan für Ernährung, Landnutzung und Umwelt
Lehrstuhl für Atmosphärische Umweltforschung

Emission and abundance of biogenic volatile organic compounds in wind-throw areas of upland spruce forests in Bavaria

Benjamin S. J. Wolpert

Vollständiger Abdruck der von der Fakultät Wissenschaftszentrum Weihenstephan für Ernährung, Landnutzung und Umwelt der Technischen Universität München zur Erlangung des akademischen Grades eines

Doktors der Naturwissenschaften (Dr. rer. nat.)

genehmigten Dissertation.

Table of contents

1.   Introduction

1.1.   Motivation

On 18th and 19th January 2007, the hurricane-strength storm "Kyrill" caused widespread damage across central and western Europe. Kyrill caused 47 fatalities and in addition extensive damages of transport systems and buildings. Millions of households were temporary without electricity. The wind-storm uprooted more than 62 million trees in central Europe (Fink et al., 2009). Particularly affected regions were the upland forests in northern and eastern Bavaria, where the cyclone caused huge wind-throw areas.
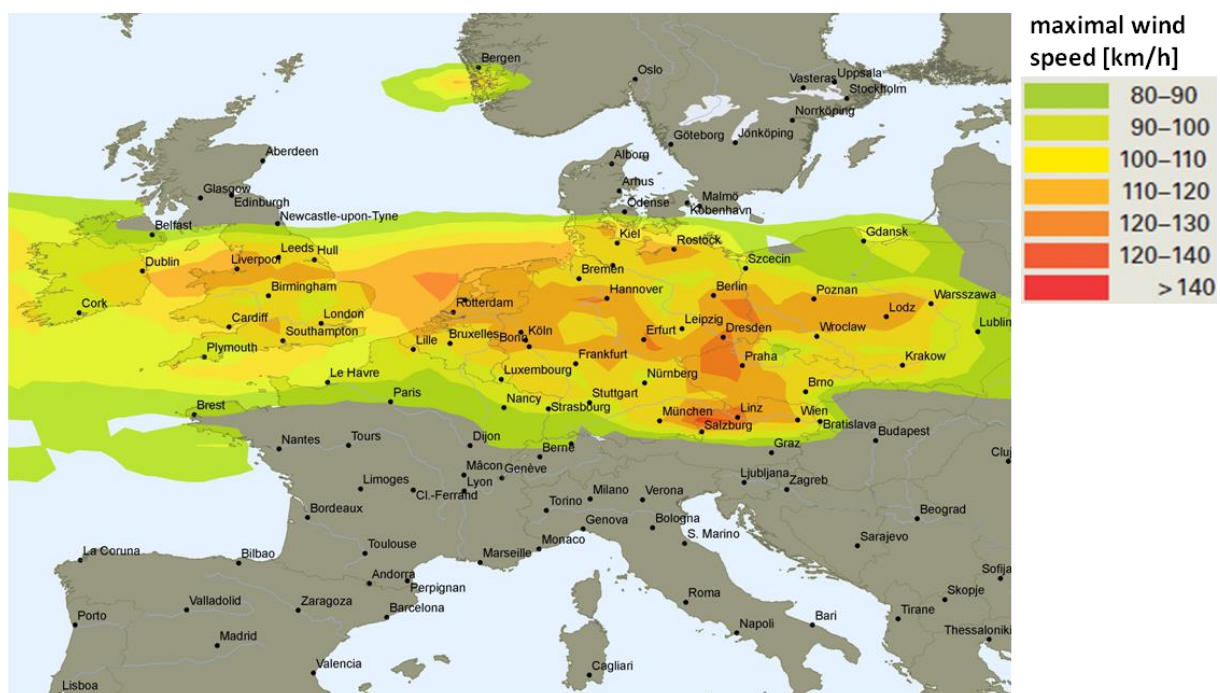
Figure 1. Track of the wind-storm Kyrill on 18/19.1.2007. Figure from Munich RE, 2007.

In commercial forest management, the salvage lumber is cleared for economic reasons to sell it on the market and partially mitigate the storm damage and the dead wood is removed to prevent infestation by pests and diseases. According to the maxim "let nature be nature", in contrast to this traditional forest management, the wind-throw areas were not cleared in the national parks Bavarian Forest and Berchtesgaden and the dead wood was left on the ground where it fell. This led to a unique opportunity for the investigation of trace gas emissions and natural rebuilding processes of disturbed forest ecosystems, where the role of dead wood can be studied in detail (Bark beetle project I, 2007; Bark beetle project II, 2008). In this work the emission of biogenic volatile organic compounds (BioVOCs) originating from the
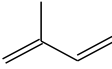
dead wood in the wind-throw areas is examined. BioVOCs emitted by vegetation have various fundamental effects on the atmospheric chemistry and physics, changing the climate sensitivity of the atmosphere. Thus, volatile organic compounds are contributors to climate change, but their variability and dynamics still represent high uncertainties and up to our knowledge no investigation of the VOC emission characteristics of dead wood has been done yet.

1.2.   Biogenic volatile organic compounds

Biogenic volatile organic compounds (BioVOCs) are a very heterogeneous group of reactive secondary natural products. Common characteristics of these chemical substances are their low vapor pressure, their biological origin and their organic structure, consisting mainly of carbon and hydrogen. BioVOCs include alkanes, alkenes, alcohols, ketones, aldehydes, ethers, esters and carboxylic acids (Kesselmeier and Staudt, 1999). In general, biogenic methane is not included in the compound mixture of BioVOCs, because it is primarily produced by microorganism not by higher plants, which is why BioVOCs are also called non methane hydrocarbons (NMHC). On a global scale, the annual BioVOC emission (more than $1200 * 10^{12}$ g carbon per year) (Guenther et al., 1995) far exceeds the anthropogenic VOC emission ($150 * 10^{12}$ g carbon per year) (Singh and Zimmermann, 1992). Still, there are high uncertainties in the global BioVOC emission budgets, even in the highly investigated fluxes of isoprene ($440-660 * 10^{12}$ g carbon per year) and monoterpenes ($33-480 * 10^{12}$ g carbon per year) to the atmosphere (Laothawornkitkul et al., 2009). In the last few years, these estimates could be confirmed by remote sensing methods of VOC oxidation products in the atmosphere (Guenther et al., 2006). The atmospheric mol fractions of biogenic organic compounds range between ppt (nmol/mol) and several ppb (μmol/mol) (Table 1).

BioVOCs emitted by vegetation very often contain C-C double bonds or functional groups like alcohol or ketones, so they are very easily oxidized by OH, NO_x or ozone in the atmosphere (Atkinson and Arey, 2003). This high chemical reactivity and the high emission of the biogenic volatile organic compounds from vegetation lead to a significant effect on atmospheric chemistry and physics (see chapter 1.7 and Laothawornkitkul et al., 2009). In general, BioVOCs are of high ecological importance to the interaction of biosphere and atmosphere (Fuentes et al., 2000).

Table 1. Estimated annual BioVOC emission rates, atmospheric mol fractions and prominent examples (Laothawornkitkul et al., 2009); p: pico (10^{-12}); n: nano (10^{-9}).

Compound	Global emission (Tg C/a)	Atmospheric levels	Examples
Isoprene	400-600	pmol/mol-nmol/mol	
Monoterpenes	35-500	pmol/mol-nmol/mol	α-pinene , β-pinene, eucalyptol
other VOC	~ 500	nmol/mol	methanol, acetone, 2-methyl-3-buten-ol

Within the globally emitted BioVOCs the group of terpenoids, also called isoprenoids, dominates and consists of more than 40000 compounds. They are ubiquitous in plants, animals and microorganisms (Bohlmann and Keeling, 2008).

The most prominent isoprenoids emitted by vegetation are isoprene (2-methyl-1,3-butadiene), monoterpenes (e.g. α-pinene, β-pinene, eucalyptol) and sesquiterpenes (e.g. caryophyllene). They can be classified by the number of isoprene (C_5) units in the molecule: hemiterpenoids (1 unit = C_5), monoterpenoids (C_{10}), sesquiterpenoids (C_{15}), diterpenoids (C_{20}), triterpenoids (C_{30}), tetraterpenoids (C_{40}) and polyterpenoids ($>C_{45}$).

In this work, isoprenoids from Norway spruce (*Picea abies* (L.) Karst.) (Janson, 1993; Lindfors et al., 2000), mainly monoterpenoids, are of particular interest.

1.3.   Monoterpenoids

In 1910, Otto Wallach won the Nobel Prize in chemistry for the systematic analysis of essential oils, which are hydrophobic and aromatic extracts from plants, and first investigations on monoterpenes. In contrast to the previous existing notion, Wallach proved that essential oils isolated from different plants consist of similar chemical compounds, mainly monoterpenes (Wallach, 1891). His results opened a new branch of organic chemistry and changed the traditional chemical industry, especially the perfume and medicine production.

Monoterpenes are oils or solids at room temperature (Table 2), which are hardly soluble in water and show a high solubility in organic solvents like chloroform or ether.

Table 2. Boiling points, molar masses and chemical formulas of selected monoterpenes (S.Dev et al., 1982)

Monoterpene	Boiling point [°C]	Molar mass [g/mol]	Chemical formula
α-pinene	155	136.24	$C_{10}H_{16}$
camphene	159	136.24	$C_{10}H_{16}$
β-pinene	163	136.24	$C_{10}H_{16}$
Δ^2-carene	167	136.24	$C_{10}H_{16}$
Δ^3-carene	165	136.24	$C_{10}H_{16}$
limonene	176	136.24	$C_{10}H_{16}$
p-cymene	175	134.22	$C_{10}H_{14}$
eucalyptol	173	154.24	$C_{10}H_{17}OH$
α-terpineol	104	154.24	$C_{10}H_{17}OH$
menthol	216	156.27	$C_{10}H_{19}OH$
carvone	230	150.22	$C_{10}H_{14}O$
(-)-verbenone	227	150.21	$C_{10}H_{14}O$
cis-verbenol	88 (at 1.2 kPa)	152.24	$C_{10}H_{15}OH$

Another characteristic of monoterpenes is their very strong but mostly pleasant odor. For example thioterpineol (grapefruit mercaptan), a terpineol in which the hydroxyl group (-OH) is replaced by a thiol group (-SH), is most likely the substance with the lowest odor detection threshold known for humans (Buettner and Schieberle, 1999). It can be detected in a concentration of 0.1 ng/l in water (Demole et al., 1982).

a)

b)
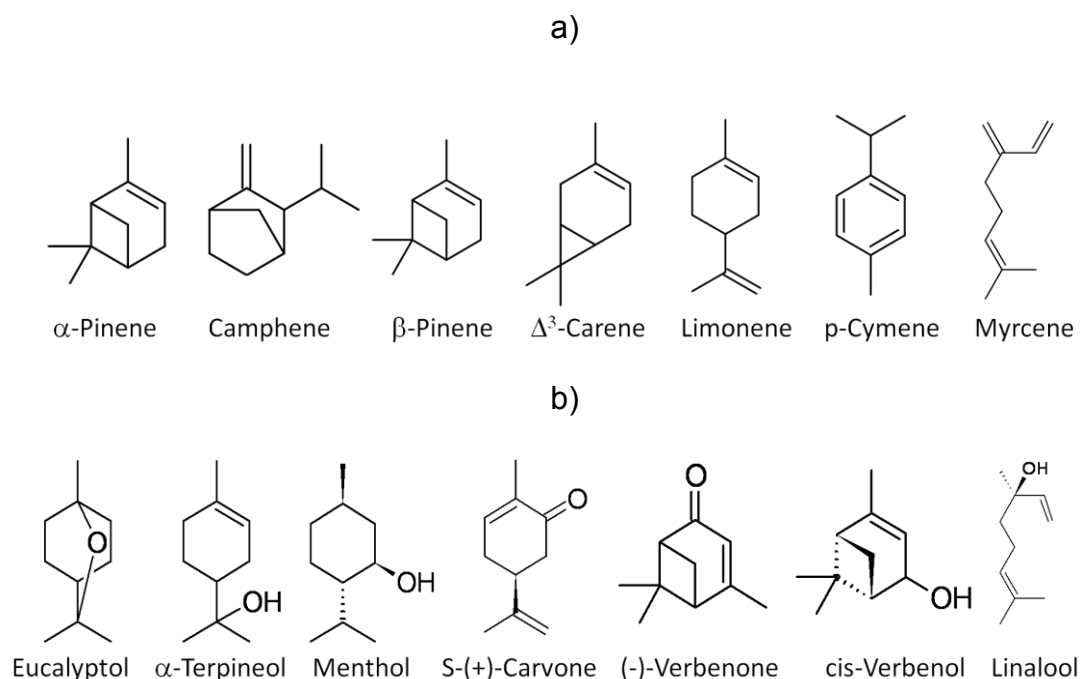
Figure 2. Typical examples of non oxygenated (a) and oxygenated (b) monoterpenes

Best known monoterpenes are limonene (for example in citrus fruits or ginger), menthol (peppermint), carvone (caraway, dill), eucalyptol (eucalyptus) and α- and β-pinene (conifers).

According to their molecular geometry, the group of monoterpenoids are classified into acyclic (myrcene, linalool), cyclic (limonene, α-terpineol, menthol, carvone) and bicyclic structures (pinenes, carene, eucalyptol, verbenone, verbenol). They are also divided into oxygenated (usually containing alcohols or ketones as functional groups) or non-oxygenated (containing only carbon and hydrogen) substances (Figure 2).

1.4.   Functional relationship of monoterpenes and plants

The functional role of monoterpenes for the emitting plant is not totally clear in all cases, but they certainly play an important role in biotic and abiotic stress protection of the plant (Loreto and Schnitzler, 2010), in defense mechanisms, and in signaling interaction with their surrounding environment (Figure 3). In other words, volatile organic compounds can be considered as a kind of language of plants (Penuelas et al., 1995).
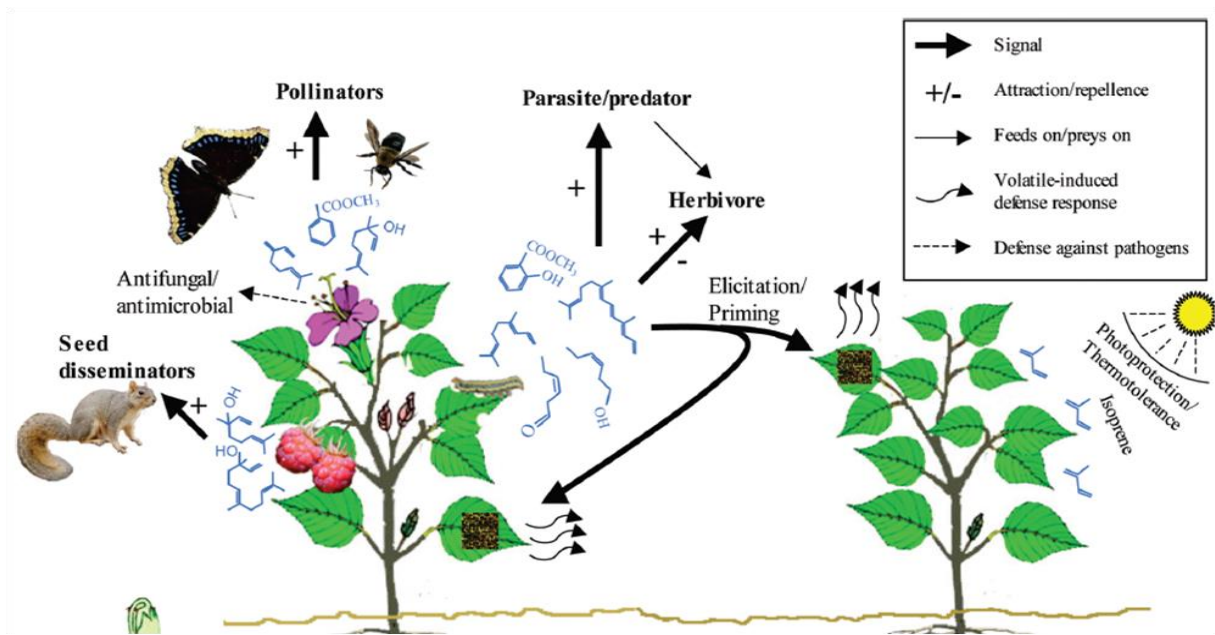
Figure 3. Overview of plant-environment interactions mediated by volatile organic compounds. Figure from Dudareva et al. 2006.

1.4.1. Protection of plants against oxidative stress and heat

Monoterpenes can protect the photosynthetic apparatus and the tissue of plants from damage caused by oxidative stress and high temperature (Loreto et al., 1998; Vickers et al., 2009a).

The thylakoid membrane in the chloroplast can become leaky at elevated temperatures (Gounaris et al., 1984), resulting in a decrease of the photosynthetic rate. To prevent this, the stability of a cellular membrane can be enhanced by incorporation of the lipophilic terpenes into the fluid-crystalline phase of the membrane (Sharkey, 1996).

Copolovic et al. (2005) suppressed the monoterpene emission in oak (*Quercus ilex*) leaves by fumigation with fosmidomycin, resulting in a decrease of the photosynthetic thermotolerance. This effect could be partly reversed by applying a relatively low concentration of α-pinene.
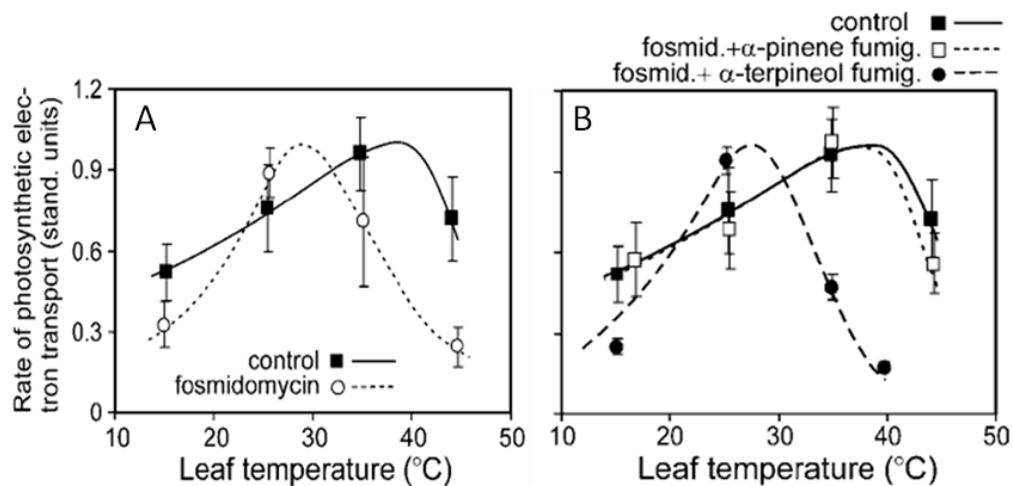
Figure 4. Photosynthetic electron transport as a function of temperature for nonfumigated versus fosmidomycin-fed leaves (A) and versus fosmidomycin-fed leaves that were fumigated with 3.5 to 5 nmol mol^{-1} α-pinene or α-terpineol (B). Figure from Copolovic et al., 2005.

The anti-oxidizing effect of terpenoids can protect the leaves and needles against stress, caused by reactive oxidizing compounds like ozone or hydrogen peroxide (Loreto et al., 2004). This quenching of ozone happens either inside the plant cells or outside at the surface of the leaves by scavenging oxidizing agents (Calfapietra et al., 2009; Vickers et al., 2009b). Behnke et al. (2007) demonstrated reduced photosynthetic electron transfer and net assimilation of transgenic, isoprene free grey poplar plants during heat stress. This result was explained by an isoprene enhanced protection of the photosynthetic apparatus during brief episodes of temperatures above 40°C.

1.4.2. VOC mediated plant defense

BioVOCs can directly repel (Kessler and Baldwin, 2001) and intoxicate (Vancanneyt et al., 2001; Keeling and Bohlmann, 2006) microbes or predators, or defend the plant indirectly by attracting natural enemies of herbivores (Arimura et al., 2005; Dicke, 2009), or by interfering the attraction chemosensors of parasites (Loivamaeki et al., 2008). The release of these signaling volatiles in the ambient air can also induce defense reactions in healthy leaves of the same plant or neighboring plants of the same species of upcoming attacks of pests (Shulaev et al., 1997). These airborne warnings also provide the basis for a fast response on future attacks of herbivores (Kessler et al., 2006). Herbivore attacks can drastically change the quantity and quality of BioVOC emissions (e.g., Dicke et al., 1990; Van Den Boom et al., 2004).

1.4.3. Plant reproduction and signaling

Many flowering plants emit between 20-60 different volatile compounds in which the substance class of monoterpenes is the most common one (Knudsen et al., 2006). This high variety in the floral scent allows pollinators and disseminators to distinguish between specific plant species and find their preferred target plants (Pichersky and Gershenzon, 2002; Reinhard et al., 2004).

Plants are also able to increase their evolutionary success by releasing phytotoxic volatile compounds in the soil, which have an allelophatic effect on competitive neighboring plants or attract predators such as the nematode (*Heterorhabditis megidis* Poinar) attacking and killing the western corn rootworm (*Diabrotica virgifera virgifera* LeConte) (Singh et al., 2002; Nishida et al., 2005).

1.5. Synthesis of terpenes in plants

Terpenoids are produced and stored in specific structures; resin ducts, glandular trichomes, or resin channels of conifers. These are located in stem and needle tissue (Fall R., 1999; Franceschi et al., 2005).

In the end of the 19th century Otto Wallach (Wallach, 1887) postulated that these terpenes can be seen as being built of two or more isoprene units (C_5) to form molecules of the general formula $(C_5H_8)_n$ where n is the number of linked isoprene units (Figure 5).
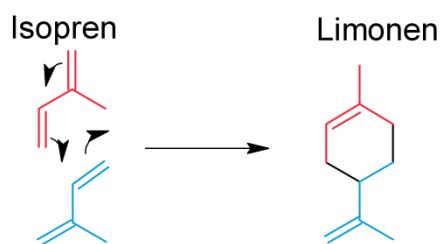
Figure 5. Simplified scheme of the isoprene rule; the formation of one monoterpene (e.g. limonene) out of two isoprene units.

In the 1920s Leopold Ružička formulated this postulation as the famous "isoprene rule" which could later be verified in the plant metabolism (Ruzicka, 1953). The biosynthesis of monoterpenes is based on isopentenyl diphosphate (IDP) and its allylic isomer dimethylallyl diphosphate (DMADP). These C_5 units are considered as

activated isoprenes, which react to the monoterpene precursor geranyl diphosphate (GDP) by head-to-tail condensation (Figure 6).
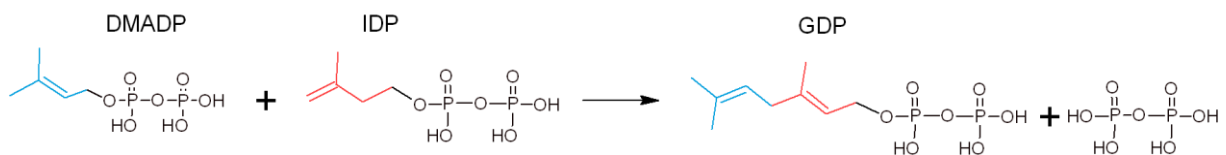
Figure 6. Formation of geranyl diphosphate (GDP) from head-to-tail condensation of isopentenyl diphosphate (IDP) and dimethylallyl diphosphate (DMADP).

IDP and DMADP are produced by two independent mechanisms, the cytosolic mevalonate (MVA) pathway (Mcgarvey and Croteau, 1995) and the plastidic 2-C-methyl-D-erythritol 4-phosphate (MEP) pathway (Flesch and Rohmer, 1988; Lichtenthaler, 1999) (Figure 7). These two key substances are synthesized in the plastidic MEP pathway from a condensation of pyruvate and glyceraldehyde-3-phosphate, while the cytosolic MVA pathway starts with acetyl-CoA.
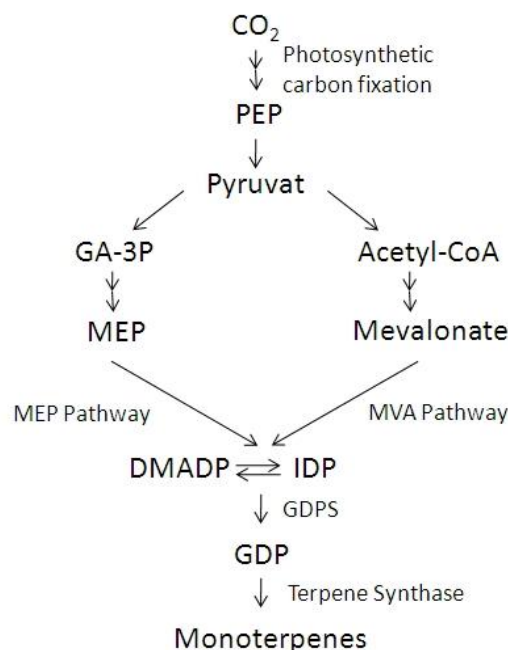
Figure 7. Simplified schematic of the monoterpene biosynthesis via the MEP and MVA pathway. [Acronyms: Acetyl-CoA = acetyl coenzyme-A; DMADP = dimethylallyl diphosphate; GA-3P = glyceraldehyde-3-phosphate; GDP = geranyl diphosphate; GDPS = GDP synthase; IDP = isopentenyl diphosphate; MEP = 2-*C*-methyl-D-erythritol 4-phosphate; MVA = mevalonate; PEP = phosphoenolpyruvate]

The formation of monoterpenes from GDP is catalyzed by various terpene synthases via an intermediate highly reactive α-terpinyl cation. Proton elimination and cyclication leads to cyclic and bicyclic monoterpenes, nucleophilic addition to this carbocation leads to oxygen containing terpenes (Kreuzwieser et al., 1999).

Originating from the same pathways, isoprene is directly synthesized by isoprene synthase from DMADP (Monson et al., 1992; Schnitzler et al., 1996). A successive condensation of other activated multiple C_5 units leads to higher isoprenoids like sesquiterpenes, diterpenes, carotenoids and steroids (Bohlmann et al., 1998).

1.6.   Environmental control of monoterpene emission

The emission of terpenoids from plants into the air results from diffusion along a concentration gradient from high concentrations inside the plant to relatively low concentrations in the surrounding atmosphere. Therefore, the emission is controlled by internal (genetic and biochemical) and external (abiotic and biotic) factors that influence the VOC concentration and vapor pressure in the plant and the diffusion resistance of the volatile organic compounds from inside the plant (1) through the cell membranes, epidermis and cuticula either directly into the atmosphere or (2) through the cell membranes into the intercellular airspace and then through the stomata into the atmosphere.

The best known and most investigated monoterpene emission controlling factor is temperature. As mentioned above, monoterpenes are stored in specific pools inside the plants, so the release of the volatile compounds is primarily controlled by the temperature dependent vapor pressure and the diffusion resistance of a specific substance. Consequently, BioVOC emission source strength is calculated with a temperature dependent algorithm (Guenther et al., 1995; Simpson et al., 1999):

$$E_{MT} = \gamma E_{MT}{}^{*} \qquad\qquad (1)$$

$$\gamma = exp(\beta(T - T_S)) \qquad\qquad (2)$$

$E_{MT}{}^{*}$; Monoterpene emission capacity at standard temperature (T_S = 30°C)

E_{MT}; Emission of monoterpene ($\mu g\ m^2\ h^{-1}$)

γ; Temperature correction factor

β; Empirical factor, usually 0.09 but variable (e.g. Dominguez-Taylor et al., 2007)

In contrast to this, recent studies indicate, that a large fraction of the emission of conifer trees may originate directly from *de novo* synthesis of monoterpenes (Steinbrecher, 1999; Schnitzler et al., 2002; Ghirardo et al., 2010). This monoterpene emission type is temperature and light dependent as it uses precursors resulting

directly from *in situ* photosynthesis. This *de novo* emission also has been implemented in some current models (Lindfors et al., 2000; Steinbrecher et al., 2009; Schurgers et al., 2009).

The temperature and light dependence algorithm to compute monoterpene emissions considers only short term (in the range of minutes to hours) variations of the emission. On a longer timescale the source strength is affected by additional factors which have to be considered in models. The concentration and therefore the vapor pressure of terpenoids inside the plant can be influenced on the one hand by phenological events, like leaf development stage and seasonality (Staudt et al., 2000; Hakola et al., 2003; Pio et al., 2005) and senescence of the plant (Llusia and Penuelas, 2000), which are already used in some extended model algorithms (Steinbrecher et al., 2009) and on the other hand by factors influencing the vitality of the plant, like water (Lerdau et al., 1997), CO_2 (Constable et al., 1999; Raisanen et al., 2008) and nutrient availability.

The dominating controlling factors temperature and light availability are highest in summer, so the BioVOC source strength follows the annual cycle of these factors (Figure 8).
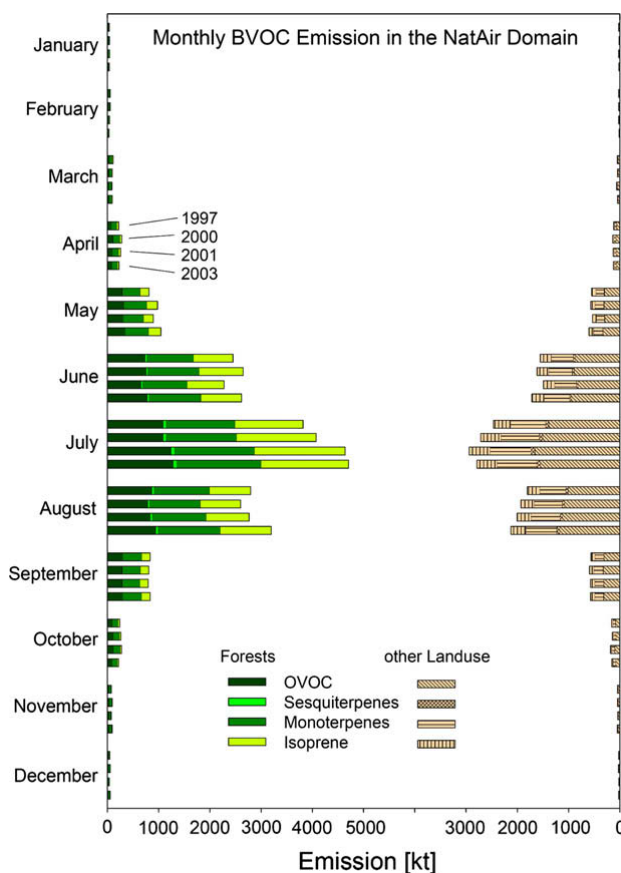
Figure 8. Estimated monthly emissions of isoprene, mono-, sesquiterpenes, and OVOC (volatile organic compounds with heteroatoms of oxygen) in Europe, including neighbouring areas (domain area: 22.56 Tm^2) in the years 1997, 2000, 2001, and 2003. Other land use: all land use categories except for forests. Figure from Steinbrecher et al., 2009.

In addition, damage caused by herbivore or mechanical wounding can lead to a several orders of magnitude increased terpene release (Prieme et al., 2000; Staudt and Lhoutellier, 2007; Arneth and Niinemets, 2010; Schaub et al., 2010) and different terpene emission patterns (Litvak and Monson, 1998). The mechanical wounding drastically reduces the diffusion barrier from the cellular material to the atmosphere, resulting in a short term increase of the emission, whereas an herbivore feeding can also increase the enzyme activity and the synthesis of defense related terpenes can stay at elevated levels.

1.7.   Scientific interest in biogenic volatile organic compounds

Reactive hydrocarbons play a fundamental role in the chemistry and physics of the atmosphere (Figure 9) (Penuelas and Staudt, 2010). Within these hydrocarbons, the fluxes of biogenic compounds far exceed the anthropogenic VOC emission on a global scale. Even in industrial areas like Germany, the BioVOC emission can be

higher than the anthropogenic one on warm and sunny summer days (Friedrich et al., 2002). The importance of a precise knowledge of the source strength of biogenic volatile organic compounds has even increased, as the release of man-made hydrocarbons was reduced in the last decade (e.g., Steinbrecher, 2011). Apart from that, BioVOCs show a higher reactivity compared to anthropogenic ones (Atkinson, 2000). Within the group of biogenic trace gases, monoterpenes are emitted in the second largest quantity after isoprene, with profound effects on air quality and climate. When monoterpenes are released to the atmosphere they are rapidly oxidized through different radicals, in particular the hydroxyl-radical, leading finally to CO_2. Although this monoterpene derived CO_2 has a almost negligible effect on the ecosystem carbon budget (Guenther, 2002), the intermediate products of the oxidation process are important, due to their manifold participation in atmospheric chemistry and physics.
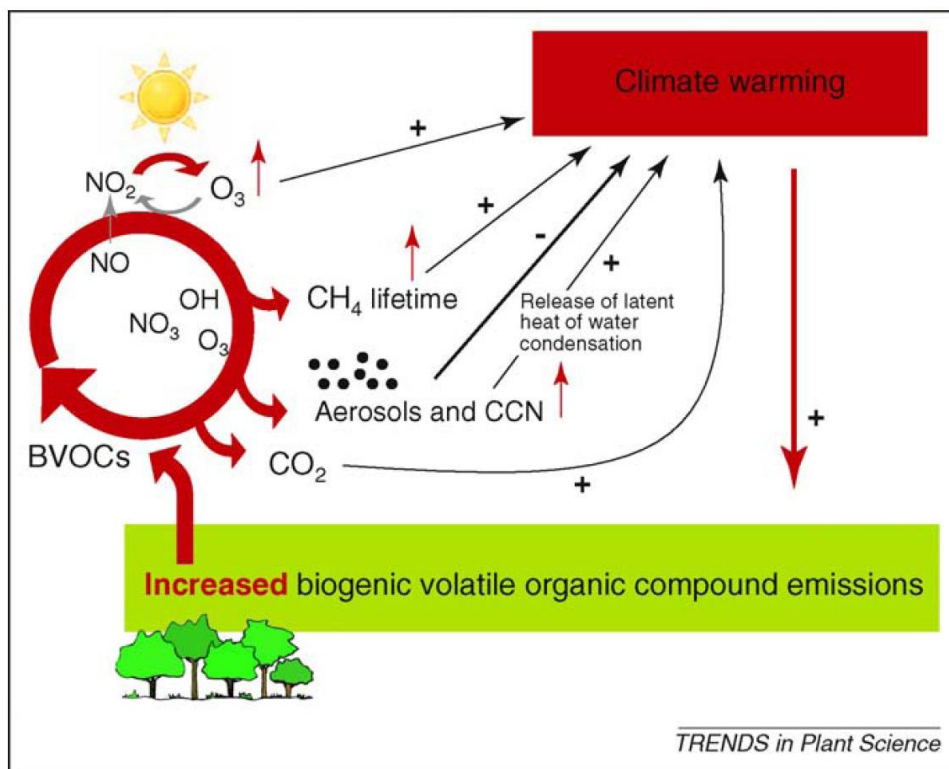
Figure 9. Schematic figure of the influence of BioVOC emissions on atmospheric chemistry and climate. Figure from Penuelas and Staudt, 2010.

1.7.1.   Oxidation capacity of the atmosphere

Major tropospheric oxidizing agents are the hydroxyl radical (OH), ozone and the nitrate radical (NO_3) (Table 3). The hydroxyl radical is a very effective oxidant, also called the "detergent" of the atmosphere. The oxidation reaction of biogenic

hydrocarbons and OH may decrease the concentration of the hydroxyl radical in the troposphere and thus may impact the oxidation capacity of the atmosphere. In consequence, the lifetime and thus the concentration of the important greenhouse gas methane may be increased by this depletion of the hydroxyl radical (Wang et al., 1998; Jockel et al., 2006). This way the greenhouse effect of the Earth could indirectly be enhanced, because of a lower potential of the atmosphere to oxidize the pollutant gases.

Table 3. Calculated atmospheric lifetimes of biogenic volatile organic compounds. Data from Atkinson and Arey 2003.

Biogenic VOC	Lifetime for reaction with		
	OH	O_3	NO_3
camphene	2.6 h	18 day	1.7 h
Δ^2-carene	1.7 h	1.7 h	4 min
Δ^3-carene	1.6 h	11 h	7 min
limonene	49 min	2.0 h	5 min
myrcene	39 min	50 min	6 min
α-pinene	2.6 h	4.6 h	11 min
β-pinene	1.8 h	1.1 day	27 min
sabinene	1.2 h	4.8 h	7 min
terpinolene	37 min	13 min	0.7 min
1,8-cineole	1 day	> 110 day	1.5 year

Assumed radical concentrations: OH: $2.0*10^6$ molecules cm^{-3}, 12-h daytime average.

O_3: $7*10^{11}$ molecules cm^{-3}, 24-h daytime average.

NO_3: $2.5*10^8$ molecules cm^{-3}, 12-h daytime average.

However, a recent study showed a less negative influence of VOC concentration on atmospheric oxidation capacity than expected previously (Lelieveld et al., 2008). In this field experiment and associated models in the unpolluted tropical area of the Amazon, the VOC oxidation recycles OH with an assumed efficiency of 40 - 80%. In a recent publication (Montzka et al., 2011), results based on methyl-chloroform (CH_3CCl_3) measurements showed a smaller interannual variability of the global mean OH concentration than expected, explained by a buffering of the global hydroxyl level on this time scale.

1.7.2. Ozone

Through its chemical and physical nature, ozone plays an important role in the atmosphere. In addition to chemical processes it also impacts atmospheric energy transfer processes. Next to CO_2 and methane, it is the third most important greenhouse gas (IPCC, 2007). In high radiation and stable weather conditions combined with high concentrations of NO_x and hydrocarbons, surface ozone levels frequently exceed air quality standards (e.g. WHO 100 mg/m^3; 8-hour average) (EEA, 2010), despite the implemented air quality control measures.

The first step in daytime atmospheric oxidation of terpenoids initiated by the OH radical leads to the formation of peroxide radicals (Figure 10 step 1) (Jenkin et al., 1997). In nitrous oxide polluted air these peroxides can oxidize NO to NO_2. (Figure 10 step 2). The generated oxide radicals react with molecular oxygen in the air to form a carbonyl product and a HO_2 radical (Figure 10 step 3). The new hydrocarbon can undergo the cycle again until its total oxidation to CO_2. One of these oxidation cycles starting from one molecule of reactive hydrocarbon depletes one molecule of NO, O_2 and OH and produces water, NO_2 and the hydroperoxyl radical HO_2 (Figure 10).
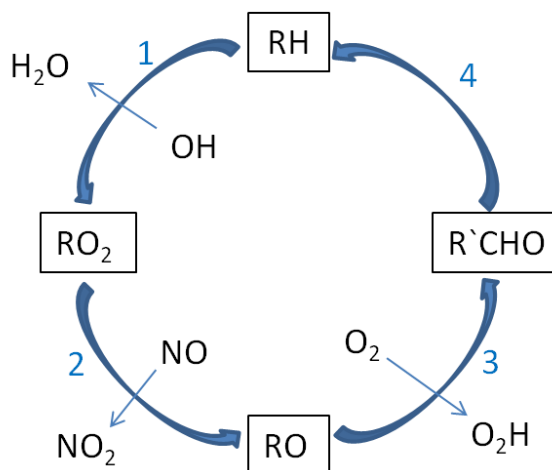
Figure 10. Simplified scheme for the OH radical initiated degradation of volatile hydrocarbons (RH) in the atmosphere.

The oxidizing agent OH is recycled in the reaction of the formed product HO_2 and NO, leading to the production of nitrogen dioxide NO_2 (Equation 3 a). The photochemical dissociation of NO_2 at a wavelength of 193 nm leads to active oxygen, which forms ozone with molecular oxygen while recycling one nitric oxide (Equation 3 b+c).

a) Generation of NO_2

$$HO_2 + NO \longrightarrow OH + NO_2$$

b) Photolysis of NO_2:

$$NO_2 \xrightarrow{193 \text{ nm}} NO + O \qquad\qquad (3)$$

c) Formation of ozone:

$$O + O_2 \longrightarrow O_3$$
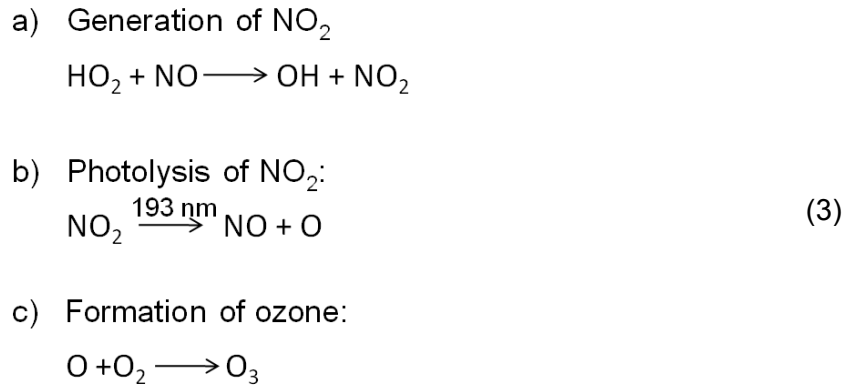
Equation 3. Generation of nitrogen dioxide (NO_2) (a) and subsequent formation of Ozone from active oxygen (b+c).

The nitrogen oxides are acting as a catalyst. In total, the photochemical degradation of volatile organic compounds in the atmosphere leads to the formation of two ozone molecules in each oxidation cycle (Equation 4).

$$RH + 4\,O_2 \longrightarrow R'CHO + 2O_3 + H_2O \qquad\qquad (4)$$
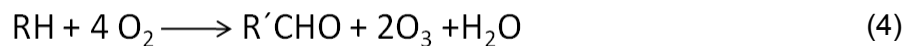
Equation 4. Net reaction for the ozone formation in the atmosphere based on the hydrocarbon degradation.

Without reactive hydrocarbons oxidizing NO, an equilibrium between NO, NO_2 and O_3 would adjust in the daytime atmosphere, what cannot explain the observed high ozone concentrations. Therefore, the ozone formation especially near industrial polluted areas (strong NO_x sources) is strongly determined by the prevailing VOC mixture (Derwent et al., 2007). The O_3 production is proportional to the VOC concentration, the light intensity, and the concentration of the catalyst NO. Depending on whether the hydrocarbons or the nitrogen oxides are present in deficiency, the reaction speed of the ozone formation is determined by volatile organic compounds or NO_x. The ratio of both compounds is therefore crucial for the kinetics and type of limitation of the net reaction. A dependency of the ozone formation rate from the initial VOC/NO_x ratio is shown in Figure 11 (Barnes et al., 2011). The area marked in red corresponds to typical rural air masses originating from forest, where the biogenic emission of volatile organic compounds is dominant. The ozone production rate is NO_x limited, i.e. an increase of the NO_x concentration leads to an increase in O_3 formation. The blue area in the graph characterizes air in cities or polluted regions, with a high NO_x loading. In this case the kinetics is determined by the VOC concentration. The VOC/NO_x ratio depends on the age of the

air masses, since the lifetimes of nitrogen oxides are usually shorter than the ones of VOCs, and on the emission pattern of biogenic organic compounds, due to the fact that different VOCs are degraded at different rates according to their chemical reactivity.
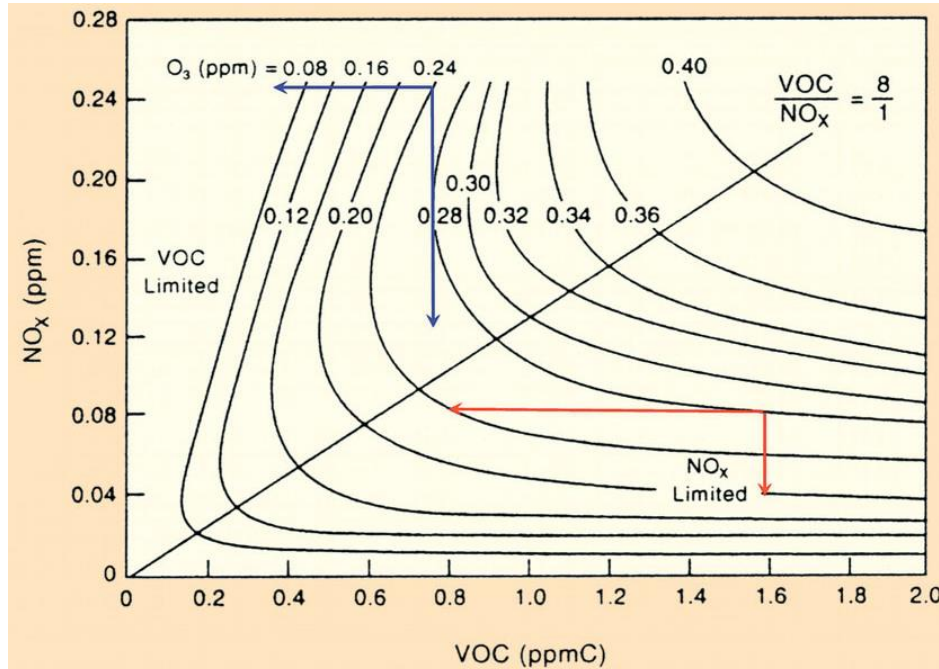
Figure 11: Model calculation of the dependence of the ozone level in air of the NO_x and VOC concentration. Figure from Barnes et al., 2011.

As the levels of hydrocarbons originating from vegetation are particularly high in the atmosphere during warm and sunny periods, biogenic VOCs can strongly contribute to the formation of ozone during summer in Europe, in particular in the Mediterranean basin (Curci et al., 2009) (Figure 12).
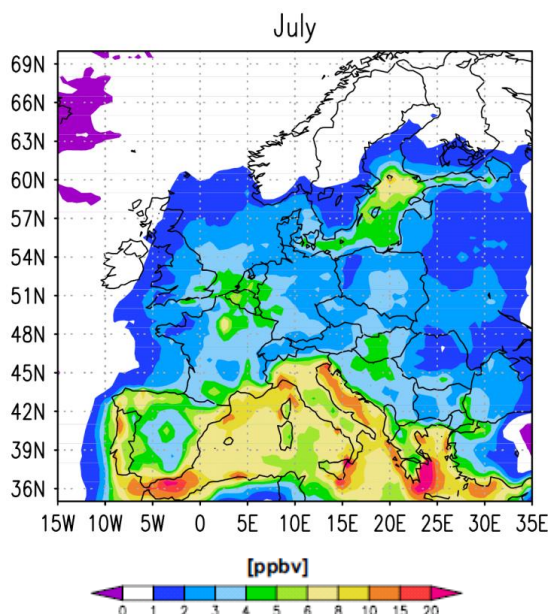
Figure 12. BioVOC impact on monthly mean daily ozone maxima over Europe using NatAir BioVOC emissions. Figure from Curci et al., 2009.

Instead of the hydroxyl radical, ozone itself can act as an oxidizing agent for VOCs. O_3 can be added to the double bonds of unsaturated terpenes leading to the formation of unstable ozonids, the Molozonid or Criegee-intermediate (Alvarado et al., 1998; Cataldo et al., 2010), cleaving to an aldehyde or a ketone and an organic peroxide radical, feeding further oxidation cycles in the atmosphere. Considering this, due to atmospheric conditions monoterpenes can reduce the ozone concentration in ambient air.

1.7.3. Secondary organic aerosols (SOA)

Due to their introduced functional groups BioVOC oxidation products typically have lower vapor pressures than the primary substances and thus can easily condense and deposit on existing nuclei (Went, 1960; Calogirou et al., 1999; Joutsensaari et al., 2005; Jimenez et al., 2009). Field studies and smog chamber experiments suggest terpenes as the most important precursor of secondary organic aerosols (Hoffmann et al., 1998; Leaitch et al., 1999; Kanakidou et al., 2000), with a predicted global annual SOA production of 19 Tg per year, whereas that from anthropogenic hydrocarbons is only 2 Tg (Chung and Seinfeld, 2002; Kanakidou et al., 2005). However, several publications (reviewed in Hoyle et al. 2001) pointed out an enhancement of the formation of SOA from biogenic precursors through

anthropogenic emission. In spite of the effort used to get precise results of the magnitude of SOA formation, the differences in the predictions are still huge, ranging from 2.5 to 79 Tg per year for biogenic SOA (Andreae et al., 2009).

The underlying mechanism of this aerosol formation is not totally clear (Kulmala, 2003), but recent publications (Kerminen et al., 2010; Metzger et al., 2010) used a new semi-empirical parameterization to explain nucleation rates. They are based on a proportionality of the nucleation to the product of the concentrations of sulfuric acid and volatile organic molecules, suggesting that only one molecule H_2SO_4 and one organic molecule are involved in the initiating step of the nucleation process. This behavior is explained by the formation of organosulfate clusters as starting nuclei.

Aerosol particles affect the climate by direct and indirect alteration of the radiation budget of the Earth and act as substrates for heterogeneous reactions in the troposphere (Fuentes et al., 2001).

The direct effect of aerosols is based on the reflection (e.g. sulfate, organics) or absorption (e.g. black carbon) of solar radiation (Kurten et al., 2003). Black carbon aerosols (soot) are emitted through incomplete combustion of biomass and fossil fuels and absorb shortwave radiation causing a net warming and changes in the vertical temperature gradient of the atmosphere (Ito and Penner, 2005; Moosmüller et al., 2009). Contrary to these light absorbing aerosols, most SOA are cooling the atmosphere by reflection of the incoming radiation (Carslaw et al., 2010). The indirect impact on the climate is based on the ability of SOA from monoterpenes to act as cloud condensation nuclei (CCN) (Engelhart et al., 2008). The resulting clouds have an increased optical thickness and enhance the reflection of the earth, additionally cooling the atmosphere (Ramanathan et al., 2001). The total radiative forcing effect of direct and indirect cooling from aerosols is -0.5 W/m^2 respectively -0.7 W/m^2 on global average and this value shows the highest uncertainty of all radiative forcing components influencing the climate of the Earth (IPCC, 2007). A better understanding of the aerosol formation is therefore crucial for the understanding of the climate change.

1.7.4. Carbon balance

The average terrestrial emission of BioVOCs is estimated to 7 g Carbon/m^2 per year but could exceed 100 g/m^2 per year at some tropical locations (Guenther, 2002). This

sums up to 1-2% of the total global carbon assimilation by terrestrial ecosystems (Grace and Rayment, 2000). Particularly under stress conditions, the "carbon loss" of plants due to BioVOC release could locally be up to 5–10% of the total net carbon exchange or even more (Kesselmeier et al., 2002; Ghirardo et al., 2011).

In particular during periods when plants suffer from environmental stress, BioVOC emissions should be considered in calculations of at least regional carbon budgets. As the emission of volatile compounds from vegetation is most likely to increase in a future presumable warmer climate (Penuelas and Staudt, 2010), the influence of BioVOCs might even become more important in global carbon models.

1.7.5. Plant insect interaction

In addition to the intended attraction of pollinators and disseminators for reproduction also herbivores are unintentionally directed to their preferred host plants (Dudareva et al., 2006). One of the most important pests in coniferous forest around the world is the bark beetle (*Scolytinae)* attack, which is responsible for huge areas of dead trees in America, Europe and Asia. In Central Europe one of the most affected areas is the combined national park Šumava/ Bavarian Forest, where in particular in the high altitude regions almost all trees were killed by the European bark beetle *(Ips typographus* L.*).* The primary attraction of this beetle is most probably related to monoterpenes emitted from spruce, in particular α-pinene (Seybold et al., 2000; Pureswaran et al., 2004). After the infection of a tree, the beetle oxidizes α-pinene in his bowel to form the strong aggregation pheromone cis-verbenol, which leads to a further assembling of the herbivores. (-)-Verbenone is used as a repellent pheromone to disperse the bark beetle to attack not yet infected trees (Figure 13) (Klimetzek and Francke, 1980; Reddemann and Schopf, 1996; Bohlander and Schopf, 1999).
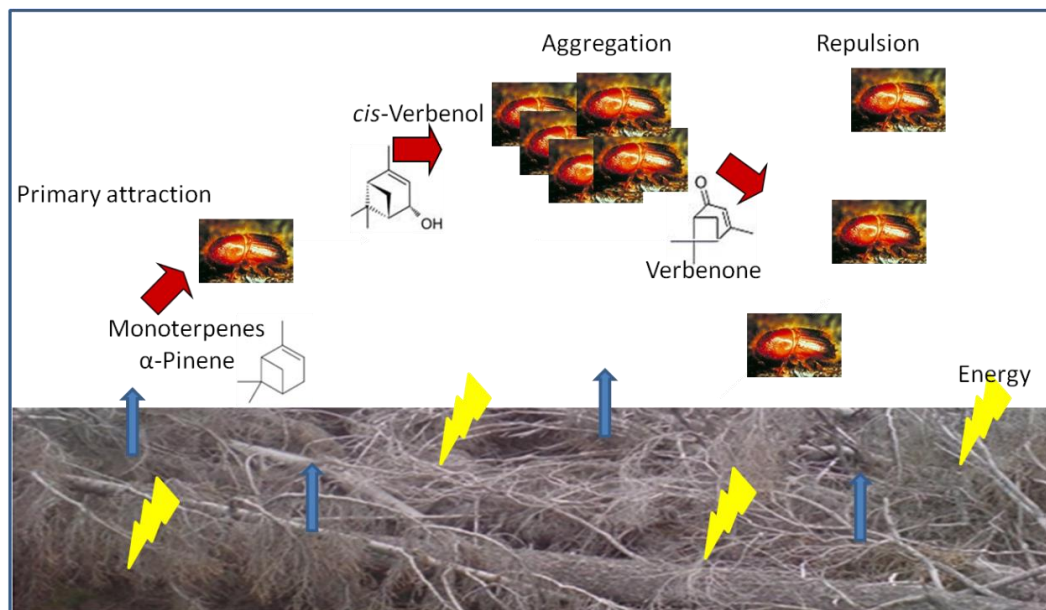
Figure 13. Control on the bark beetle (*Ips typographus*) colonization behavior. Yellow flashes represent energy input (i.e. solar radiation), blue arrows the emission of monoterpenes from the dead wood.

To understand the dispersion and feeding behavior of the bark beetle in forests as well as to develop efficient procedures for forest protection against the attack of *Scolytinae,* it is vital to quantify the emission and distribution of monoterpenes in forest ecosystems (Jakus et al., 2003).

1.8. Objectives

According to the UN forest resources assessment 46% of the total land area of Europe is forested. Natural disturbances (wind-throw, fire, insects, snow break) are crucial for the functioning of forest ecosystems (FAO, 2000). In the period 1950 – 2000, an annual average of 35 million m^3 wood was damaged by these disturbances, whereas storms were responsible for 53% of the total damage (Schelhaas et al., 2003).

Since 1990, eight severe winter storms have caused a total of 10.9 billion € damage only in Germany with more than 1 billion m^3 of dead wood (Munich RE, 2007). The huge wind-throw areas resulting from these storms are poorly investigated with respect to volatile organic compounds.

Figure 14: Volumes of wood damaged by storms as reported in European countries for 1850–2000. Figure from Schelhaas et al., 2003.
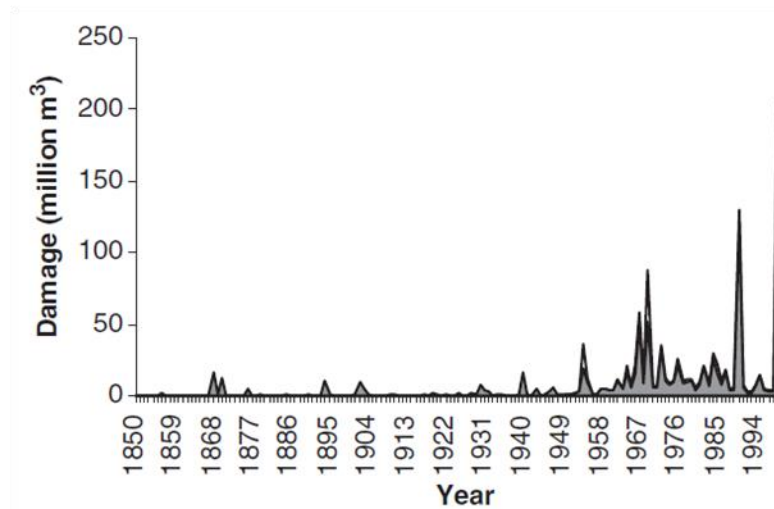
The storm activity in central, northern and western Europe has increased from the end of the nineteenth century until present days (Donat et al., 2011). In a changing climate the frequency of extreme weather events including strong storms is likely to rise (IPCC, 2007; Usbeck et al., 2010; Scaife et al., 2011). Particularly in the winter time an increase in mean storminess of up to 20% is supposed to occur in western Europe (Scaife et al., 2011). The reported damage from storms increased from 1850 to 2000, both in frequency and in magnitude, although this increase may be partially an artifact due to increased reporting (Figure 14) (Schelhaas et al., 2003). Even though there is little agreement among model predictions, whether storm strength and frequency will increase in the near future (IPCC, 2007), there are some publications linking climate change to an intensification of the north Atlantic oscillation (Ulbrich and Christoph, 1999; Easterling et al., 2000; Bengtsson et al., 2006; Ulbrich et al., 2008) which may cause increased storm track activity towards Northern Europe. An increase in the severity of storms due to higher maximum wind speeds and growth of the spatial extent of winter storms in central Europe are reported (Gardiner et al., 2010).

Even if the storm intensity and frequency will not change much, forests may become weakened through longer and more intense draught, and high temperature periods often associated with a high load of air toxics such as ozone in the future. A stressed forest is less resistant to strong wind events. In Europe, forest ecosystems which are specifically affected by a warming climate are spruce forests, namely the boreal forests in Northern Europe and forests in mountainous high altitude regions.

For these reasons, an increasing amount of trees in these forest ecosystems may become uprooted through strong wind events, and thus, the fraction of wind-throw areas will increase. Regarding VOC research in wind-throw areas, the following questions will be addressed in this thesis:

- Are wind-throw areas a significant source of BioVOCs?
- How do the concentrations of these trace gases change on a daily and seasonal time scale?
- Which environmental factors control BioVOC levels in ambient air over wind-throw areas?
- Are there any differences regarding the composition of biogenic volatile organic compounds in the air over different wind-throw types?

To find answers to these questions, measurements of biogenic volatile organic compounds were conducted in two different kinds of wind-throw areas of Norway spruce forest in the upland of the national parks "Bavarian Forest" and "Berchtesgaden" in the years 2008 – 2011. The levels of BioVOCs in ambient air were analyzed by gas chromatography - mass spectroscopy (GC-MS) after pre-concentration on adsorption tubes. The emissions of these reactive hydrocarbons were determined by the modified Bowen ratio (MBR) method and the surface layer gradient (SLG) technique. The research sites were additionally equipped with measurement stations collecting meteorological data, which are relevant for the emission strength and distribution of monoterpenes, or which are required for the quantification of atmospheric exchange rates.

2. Site description

The investigations where conducted in the nearly pristine area of two national parks in Bavaria. They provide great opportunities for scientists of various fields to investigate ecosystems in different altitudinal zones. The partly pristine spruce forests including their natural disturbances offer excellent conditions for the experimental analysis of monoterpene air concentrations and emissions.

Figure 15: The location of the Bavarian national parks in Germany.

2.1. The Bavarian Forest National Park

The Bavarian Forest National Park, founded in 1970, was the first national park in Germany and is combined with the Ŝumava National Park in the Czech Republic, the largest contiguous forest area in Central Europe. On approximately 1000 km^2 forests, meadows and bogs are protected against excessive human exploitation. Surrounded by a mainly rural countryside, the Bavarian Forest National Park offers unique possibilities for the investigation of almost untouched nature. 98% of the total area of the national park is forested.

It is covered by three different kinds of forest, depending on altitude and slope of the area. Because of temperature inversion, the valleys are often colder than the surrounding slopes. This leads to an accumulation of cold air and growth of the

lowland spruce forest in the valleys. On the warmer slopes of the hills, the mixed mountain forest with spruce, fir and beech trees dominates. In the higher regions above 1200 m (a.s.l.), a forest consisting almost only of Norway spruce is the native vegetation. The climate in the national park is rather cold with an average annual temperature of 5 - 6° Celsius and snow coverage of 5 - 6 month. The average annual precipitation is 1100 – 1300 mm but can reach values of 1800 mm near the top of the hills.

2.1.1.   The wind-throw situation in the Bavarian Forest National Park

At the 18th and 19th of January 2007 the hurricane-strength windstorm Kyrill caused widespread damage in Europe, including an uprooting of approximately 62 million trees in Central Europe (Fink et al., 2009).

In the upper area (above 1000 m a.s.l.) of the Bavarian Forest National Park, the storm produced windfalls of huge dimensions, with a total quantity of 160.000 m^3 of dead wood (Figure 16). According to the maxim "Let nature be nature" the administration of the Bavarian Forest National Park decided not to clear away storm damaged trees in the core area and in some of the outer parts of the national park.
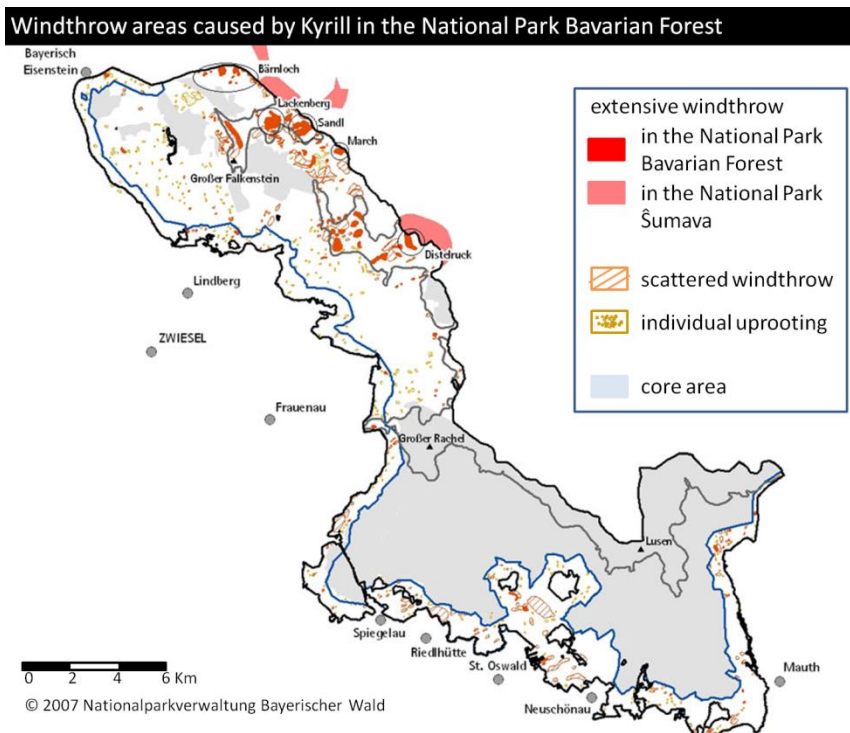

Figure 16: Wind-throw areas caused by the storm Kyrill in January 2007 in the Bavarian Forest National Park. No data was collected in the core area. (after http://www.nationalpark-bayerischer-wald.bayern.de/aktuelles/pic/karte_windwurfflaechen.jpg)

Outbreaks of the European bark beetle (*Ips Tipographus* Linnaeus), a pest, which preferably infests Norway spruce, in the fresh wind-throw areas caused additional dead wood in spruce forests in the high altitude regions of the park. Contrary to traditional forest management strategies in Europe, the deadwood is left in the forest, which makes an observation of natural rebuilding processes in a long time period after a wind-throw possible. This is a unique situation in Central Europe for the investigation of disturbed forests.

2.1.2. Measurement site Lackenberg

A site which is particularly suitable for the investigations on biogenic organic compounds produced by a disturbed spruce forest was identified in the large wind-throw area of 268000 m^2 on the slope of the Lackenberg mountain (1337 m a.s.l), close to the boarder of the Czech Republic. Almost all spruce trees in the area were uprooted by the storm in January 2007 (Figure 17, 2007). In the subsequent years, the area sourrounding the wind-throw was heavily affected by attacs of bark beetles, and most of the still standing spruces were killed. To prevent a further spreading of the beetle, these areas were cleared in the years 2009 and 2010 (Figure 17, 2009). Since the reflection properties of the dead wood differs strongly from the one of living vegetation or ground material, particularly in the near infrared, an optical interpretation of the aerial photo is possible. Therefore, the wind-throw area was cut out and analysed by a pixel based method (Figure 17, 2010 b). 10 training site polygons for two classes (wind-throw or non wind-throw) were manually established in the aerial photo. The wind-throw class includes stems, crowns and woody parts of the root plates. The non wind-throw class was mainly grassland and stones. Due to the different color spectrum of dead wood and other material in the three channels (near infrared, green and blue) of the picture, each pixel was automatically assigned to one of the two predefined classes. This analysis was done by the use of the geospatial processing program ArcGis (Esri, Redlands, CA, USA). The projected area of the dead wood in the wind-throw region was determined to be approximately 50% ± 9% or 137000 m^2 ± 24700 m^2 of the total area. No differences in this value between the years 2007 – 2010 could be observed within the uncertainty.
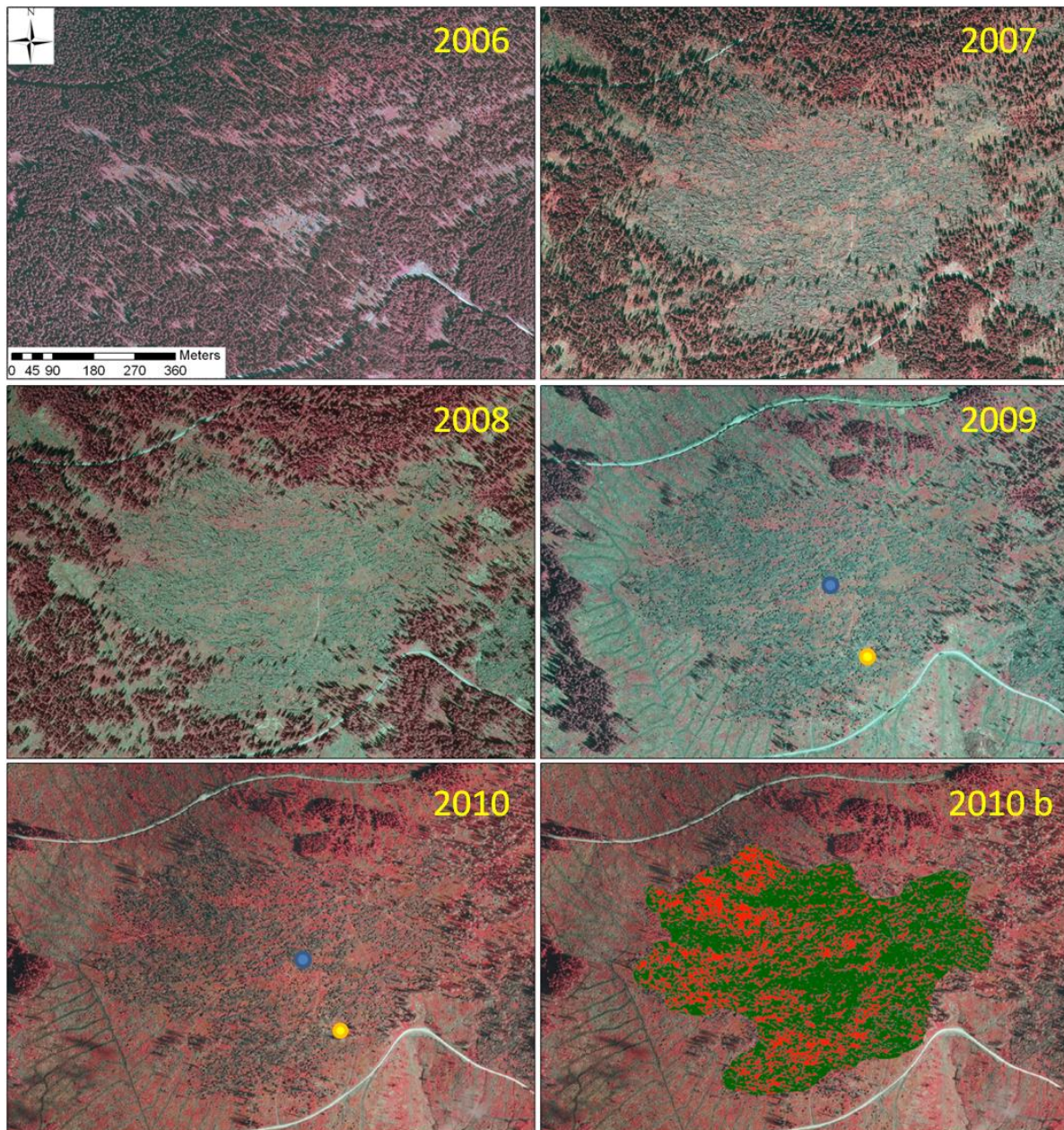
Figure 17: Pictures of the Lackenberg site in the period 2006 – 2010. The blue dot represents the central observation station; the yellow dot the satellite station, both installed in 2009. 2010b shows an analysis of the amount of dead wood in the wind-throw area by maximum likelihood classification; red color indicates dead wood, green color indicates living vegetation/soil. The aerial photos were kindly provided by the Bavarian Forest National Park. Photos taken by the Digital Mapping Camera (DMC, Intergraph Holding Deutschland GmbH, Ismaning, Germany). The red channel of the RGB composite is replaced by the near infrared (675 – 850 nm).

2.1.3. Inventory of the dead wood material at the Lackenberg

An inventory of the dead wood in the wind-throw area Lackenberg was done by analysis of the aerial photo of 2010. Four representative sample plots of 66 m * 66 m in the 4 cardinal directions of the wind-throw area were selected and the number, length and diameter of the lying stems recorded. Average stem length was 18 m, the

standard deviation of the length of these 169 trees was 3.6 m, the range was 8 m to 30 m. Mean diameter was 31 cm ± 7 cm, with a minimum of 15 cm and a maximal diameter of 60 cm. These estimated tree characteristics were converted into stem, bark, branch, root stump, and fine root mass by allometric functions (Repola, 2009). The averaged total tree biomass was 4.3 kg dry-weight per square meter wind-throw area (2.6 kg/m^2 for stem mass and 1.6 kg/m^2 for branch mass). Details of the allometric functions are listed in the appendix. Results of this inventory are shown in Table 4 and Table 5. The density of only 100 trees per hectare indicated the rather sparse stock (see also Figure 17, 2006).

Table 4. Number of trees, average length and diameter and calculated total biomass dry-weight at each sample point. Each sample point represents an area of 4356 m^2.

sample point	trees	mean length [m]	mean diameter [cm]	total mass [kg]	mass per m^2 [kg/m^2]
1	40	17.8	31	18065	4.2
2	44	18.4	31	19880	4.6
3	35	16.3	32	16090	3.7
4	50	18.1	32	21020	4.8
average	42.25	17.7	31.5	18764	4.3

Table 5. Average calculated dry-weight of single tree structures at each sample plot.

sample point	stem mass [kg]	bark [kg]	branches [kg]	stump [kg]	root [kg]
1	192	27	94	30	109
2	213	25	88	27	99
3	184	27	106	31	112
4	209	22	78	24	87
average	200	25	92	28	102

2.1.4. Vegetation at the Lackenberg

By an optical evaluation of the aerial images of the years 2007 to 2010 no relevant increase of the living woody vegetation was detectable. This is not surprising, because the cold climate and the long period of snow coverage inhibit a fast recovery

of the disturbed vegetation. Some young spruces have been growing on the dead wood of the fallen spruces, especially on the root plates, but to date their volume is small. Most of the living vegetation consists of grasses (*Deschampsia flexuosa* (L.) Trin.)*, Luzula sylvatica* (Huds.) Gaudin, *Juncus effuses* L.), fern (*Athyrium distentifolium* Tausch ex Opiz), few blue berries (*Vaccinium myrtillus* L.), and very few rowan berries (*Sorbus aucuparia* L.) (Raimund Henneken, TUM, personal communication, 2011). None of these species is known to be a monoterpene emitter, so they should not contribute to the monoterpene exchange rates in the wind-throw area.

2.1.5. Instrumentation of the measurement site Lackenberg

To interpret the concentrations and emissions of monoterpenes from vegetation correctly, it is important to know the environmental factors which control the release and distribution of the volatile compounds (see section 1.6). To obtain such background data in the remote region of the Bavarian Forest National Park, the measurement area was equipped with two meteorological observation stations in February 2009, in the center (Figure 17, blue dot) and at the edge of the wind-throw area (Figure 17, yellow dot), respectively.

The central station is located at 49°, 5.977′ N; 13°, 18.28′ E at an altitude of 1308 m (a.s.l.). The satellite station is located 228 m south-east of the central station (49°, 5.854′ N; 13° 18.29′ E) at 1269 m above sea level. The mean terrain slope between the measurement stations is thus 17%. The triangular lattice towers (GS 270 M, UKW-Berichte, Baiersdorf, Germany) are 9 m high, consist of three sections with a length of 3 m and a width of 30 cm and are made of zinc galvanized steel. Each of the three sections is braced three times via steel guy wires and pegs to the ground to obtain suitable stability (see Figure 18, Figure 19 and Figure 20).

The 12 V power supply at the central station was provided by twelve solar panels (0.66 m^2, Kyocera KC85T-1;Udomi, Neuenstein, Germany) yielding 87 W each, supported by three 65 W fuel cells (EFOY 1600, Udomi, Neuenstein, Germany) and buffered by three specially designed industrial 12 V batteries (Sonnenschein dryfit, Udomi, Neuenstein, Germany). The satellite station is powered by two solar panels and one battery.

Figure 18. Instrumentation of the central station Lackenberg, 16.-20.02.2009. Clockwise from the upper left corner: Installation of the eddy covariance system (with Rainer Steinbrecher); an example for data loss due to riming of sensors; installation of the power supply (Carsten Jahn); data collection (Matthias Mauder).

The instrumentation of these 9 m high towers are shown in Figure 19, Figure 20 and Table 6 and Table 7. Eddy covariance system parameters (3-d wind velocity, CO_2, water and temperature fluctuations, used for the VOC flux calculations, see section 3.2) are measured every 10 Hz and stored directly. The other meteorological parameters are measured every 10 seconds and averaged and stored as 10 minute mean values on the data logger. Additional storage, first processing and online transfer of data to the Institute (IMK-IFU), is done by an onsite minicomputer (MSEP 800/L, Kontron, Eching, Germany).
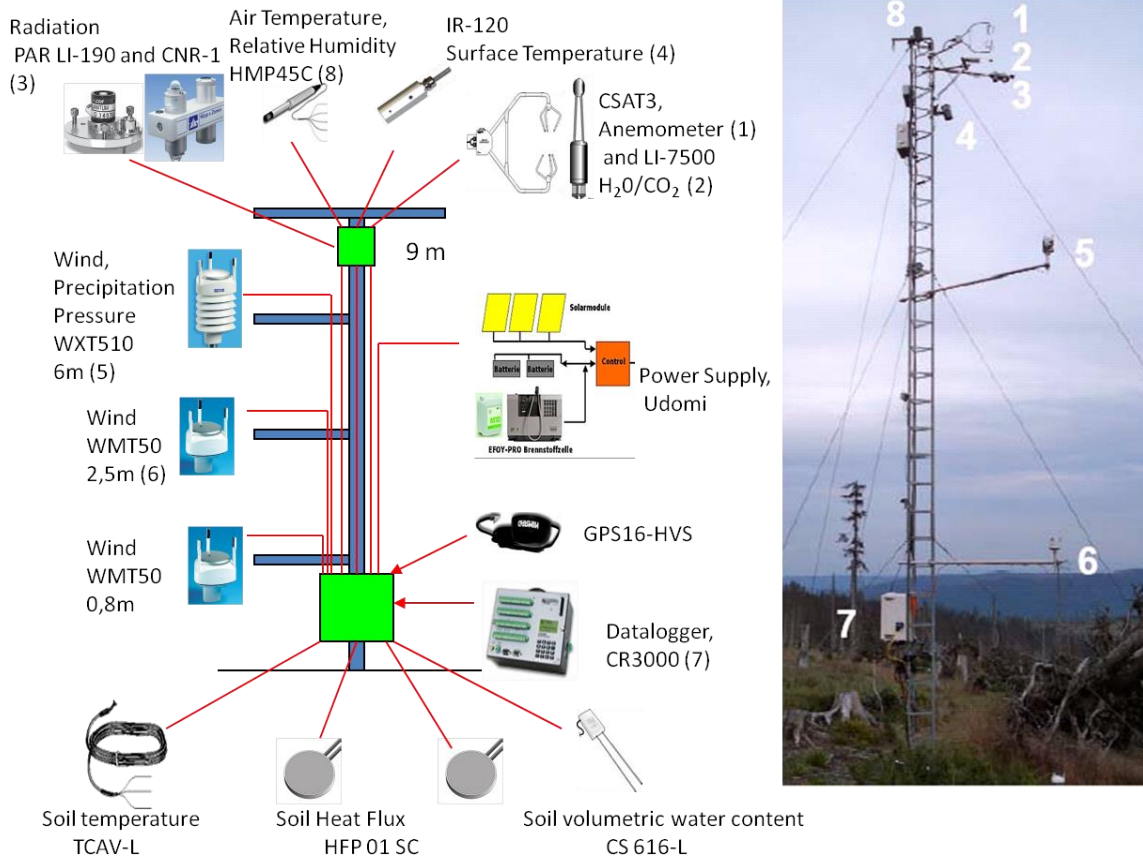
Figure 19: Instrumentation of the central station Lackenberg. Photo of the station taken from western direction. Numbers in the photo correspond to numbers in brackets in the schematic figure.
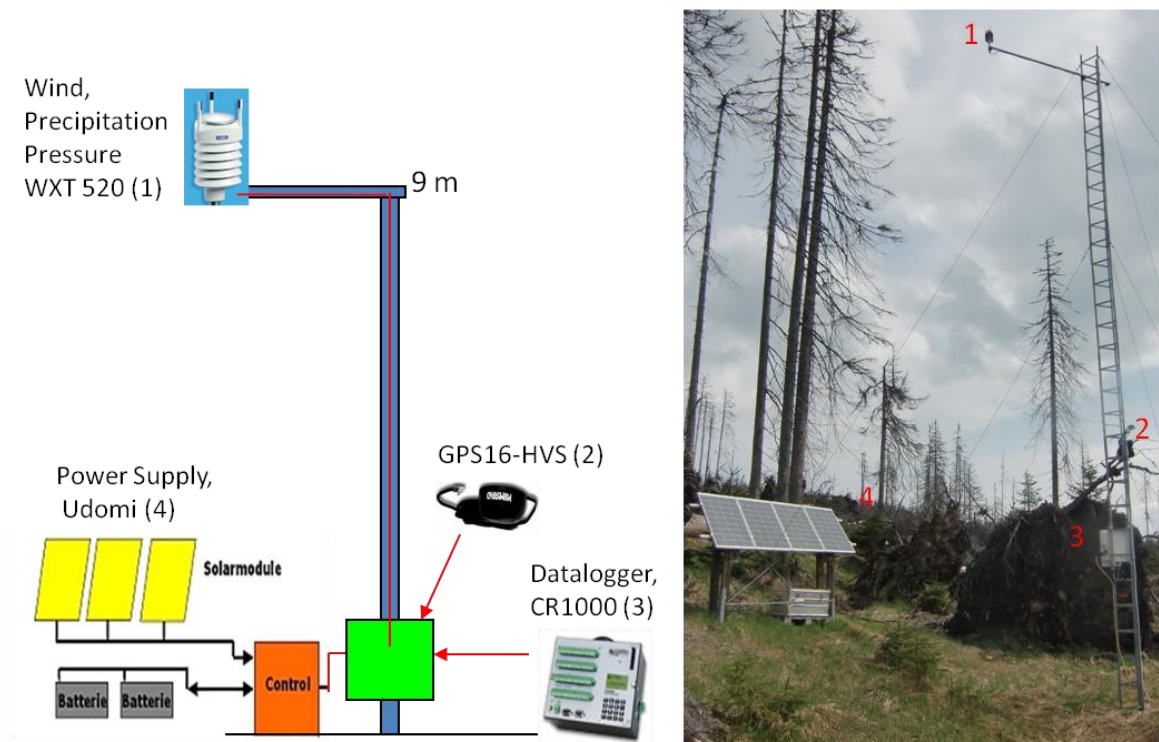

Figure 20: Instrumentation of the satellite station Lackenberg. Photo of the station taken from southwestern direction. Numbers in the photo correspond to numbers in brackets in the schematic figure.

Table 6. Setup of the central station Lackenberg and the corresponding measured variables.

Parameter	Unit	Temporal Resolution	Sensor Height	Instrument	Company*
wind speed in 3 dimensions	$m\ s^{-1}$	10 Hz	9 m	CSAT-3	Campbell
H_2O	$g\ m^{-3}$	10 Hz	9 m	Li-7500	Li-Cor
CO_2	$mg\ m^{-3}$	10 Hz	9 m	Li-7500	Li-Cor
air temperature	°C	10 Hz	9 m	HMP 45 C	Vaisala
relative air humidity	%	10 Hz	9 m	HMP 45 C	Vaisala
radiation balance	$W\ m^{-2}$	10 Min	9 m	CNR 1	Kipp&Zonen
photosynthetic active radiation	$\mu mol\ m^{-2}\ s^{-1}$	10 Min	9 m	PAR LI-190 QS	Li-Cor
surface radiation temperature	°C	10 Min	7 m	OS 65 (till 20.11.2009)	Omega
		10 Min	7 m	IR 120 (since 20.11.2009)	Campbell
air temperature	°C	10 Min	6 m	WXT 520	Vaisala
relative air humidity	%	10 Min	6 m	WXT 520	Vaisala
precipitation	$mm\ h^{-1}$	10 Min	6 m	WXT 520	Vaisala
wind direction	°	10 Min	6 m	WXT 520	Vaisala
wind speed	$m\ s^{-1}$	10 Min	6 m	WXT 520	Vaisala
air pressure	mbar	10 Min	6 m	WXT 520	Vaisala
2x wind direction	°	10 Min	2.5 m, 0.8 m	WMT 50	Vaisala
2x wind speed	$m\ s^{-1}$	10 Min	2.5 m, 0.8 m	WMT 50	Vaisala
soil temperature	°C	10 Min	4 cm below ground	TCAV-L	Campbell
soil heat flux	$W\ m^{-2}$	10 Min	8 cm below ground	HFP 01 SC	Hukseflux
soil volumetric water content	%	10 Min	4 cm below ground	CS 616 -L	Campbell
time leveling coordinates				GPS 16-HVS	Garmin
data acquisition				CR3000	Campbell

*Full names of companies: Li-Cor, Lincoln, NE, USA. Campbell Scientific, Logan, UT, USA. Vaisala, Helsinki, Finnland. Kipp&Zonen Delft, Netherlands. Omega Engineering inc., Stamford, CT, USA. Hukseflux, Delft, Netherlands. Garmin, Olathe, KS, USA.

Table 7. Setup of the satellite station Lackenberg and the corresponding measured variables.

Parameter	Unit	Temporal Resolution	Sensor Height	Instrument	Company*
air temperature	°C	10 Min	9 m	WXT 510	Vaisala
relative air humidity	%	10 Min	9 m	WXT 510	Vaisala
precipitation	mm h^{-1}	10 Min	9 m	WXT 510	Vaisala
wind direction	°	10 Min	9 m	WXT 510	Vaisala
wind speed	m s^{-1}	10 Min	9 m	WXT 510	Vaisala
air pressure	mbar	10 Min	6 m	WXT 510	Vaisala
time leveling coordinates				GPS 16-HVS	Garmin
data acquisition				CR1000	Campbell

*Full names of companies: Campbell Scientific, Logan, UT, USA. Vaisala, Helsinki, Finnland. Garmin, Olathe, KS, USA.

2.1.5.1. The gradient system

In addition to the micrometeorological data collection setup, a gradient system was installed in May 2010 on the central mast of the Lackenberg site to determine the VOC exchange between biosphere and atmosphere (see section 3.2.1). It consist of two platinum temperature probes (model 41342) in aspired radiation shields (model 43502, both R. M. Young Company, Traverse City, Mi, USA) and a system to measure the concentration of H_2O and CO_2 at the heights 1.4 and 7.2 m (Figure 21). A Li-840 infrared gas analyzer (Li-Cor, Lincoln, NE, USA) monitors continuously the concentration of the two gases, while fast solenoid valves (model 6606, Christian Bürkert GmbH & Co. KG, Ingelfingen, Germany) switch between the two heights every two minutes. A constant gas flow in the measurement and bypass stream of 350 ml/min is ensured by two vacuum pumps (DC12/08, Fürgut GmbH, Tannheim, Germany). Data are collected by a CR 3000 datalogger (Campbell Scientific, Logan, UT, USA) with a two second interval.
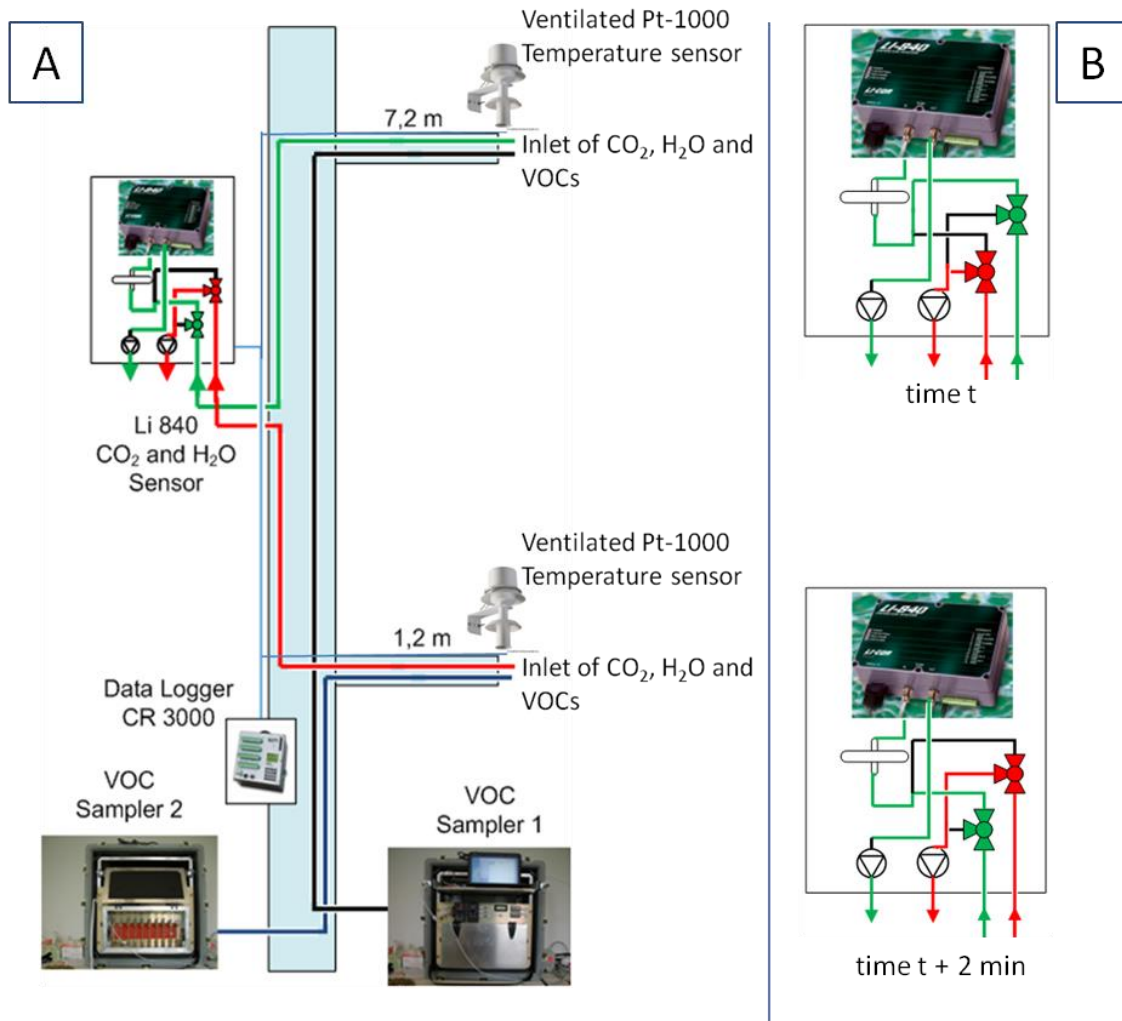
Figure 21. System setup to quantify gradients of CO_2, H_2O and temperature at the central station Lackenberg. A: Instrumentation. B: Gas flow scheme for the carbon dioxide and water vapor analysis. Valve switching was every two minutes. Green color indicates measurement flow, red bypass flow.

2.2.   The National Park Berchtesgaden

The National Park Berchtesgaden with a total area of 208 km^2 is the only German national park located in the Alps. The large altitudinal range of 2110 m between the lake Königssee (603 m a.s.l) and the Watzmann mountain (2713 m a.s.l.) results in a wide diversity of climate, landscapes, flora and fauna in the National Park Berchtesgaden and provides unique research opportunities for a variety of disciplines. The mean annual precipitation of the years 2002 – 2007 was approximately 1600 mm, ranging from 1500 mm in the valleys up to 2600 mm in the peak regions of the Watzmann mountain. About 30% of this total precipitation is typically falling as snow. Together with a mean temperature of -2 °C in the high altitude regions this leads to a long period of snow coverage of 144 days per year.

The annual average temperatures are +7 to -2 °C depending on altitude (Nationalparkverwaltung Berchtesgaden, 2001).

The vegetation consists of forest (44%), grasslands (21%), rocks (19.5%), mountain pine (12.5%), and lakes and glaciers (3%). In the montane level the natural forest is a mixing of Norway spruce (*Picea abies* (L.) Karst.*)*, European beech (*Fagus sylvatica* L.*)*, white fir (*Abies alba* Mill.*)*, and sycamore maple (*Acer pseudoplatanus* L.*)*. The fraction of spruce is increasing with altitude until the subalpine mixed forest is replaced by an almost pure spruce forest (Nationalparkverwaltung Berchtesgaden, 2001).

2.2.1.   The wind-throw situation in the National Park Berchtesgaden

The National Park Berchtesgaden was less affected by the storm Kyrill than the regions further north, so the resulting wind-throws are smaller and more scattered than in the Bavarian Forest National Park. In the lee of the Watzmann mountain ridge, the wind-throw areas show a different pattern than in the Bavarian Forest, with small, isolated patches (typically smaller than 3 ha. (Figure 22)). The biodiversity in these wind-throw areas is higher than in the Bavarian Forest; in addition to the dead spruce, there are still some living Norway spruce, deciduous trees and small shrubs. For these reasons the bark beetle was not spreading out very heavily, so no additional large amounts of dead wood were produced. In contrast to the large beetle-affected areas in the high altitude regions of the Bavarian Forest National Park bark beetle infested areas were small.
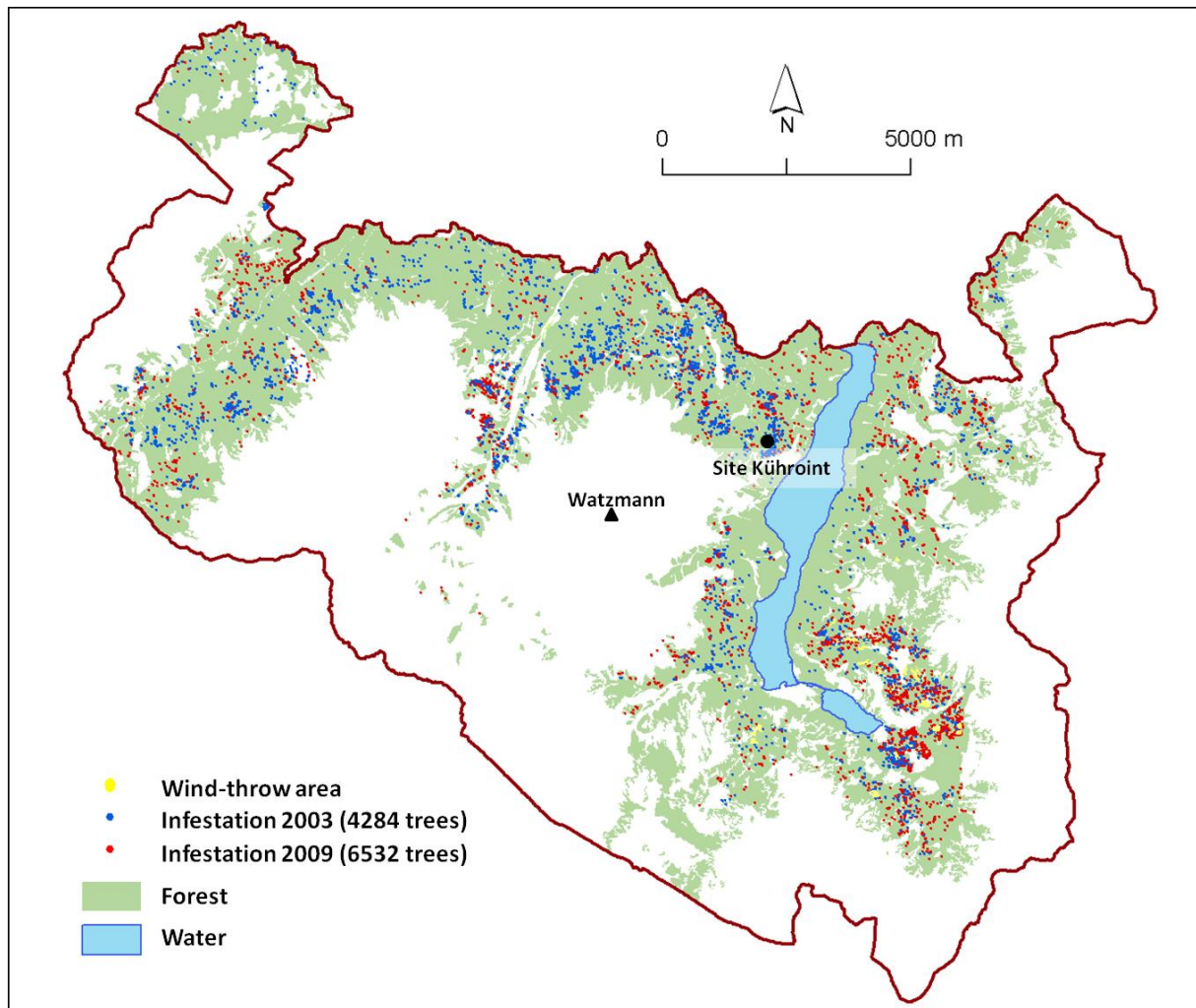
Figure 22: Wind-throw areas caused by the storm Kyrill in January 2007 and bark-beetle infected trees in the National Park Berchtesgaden. (after Kautz and Schopf (submitted) and personal communication M. Kautz)

2.2.2.   Measurement site Kühroint

A wind-throw area of 3.15 ha close to the Kühroint Alm (1420 m a.s.l.) north east of the Small Watzmann peak (2307 m a.s.l.) was chosen to study the air concentration of volatile organic compounds in wind-throw areas of the montane zone of the National Park Berchtesgaden. In winter 2003 some trees were felled by one of the frequently occurring small winter storms (Helmut Franz, National Park Berchtesgaden, personal communication) in the northeastern part of the investigation area (Figure 23, 2003 yellow ovals). So a small area of the wind-throw of 2007 was already affected by a storm 5 years before, but the vegetation already started to recover well since then (Figure 23, 2006).
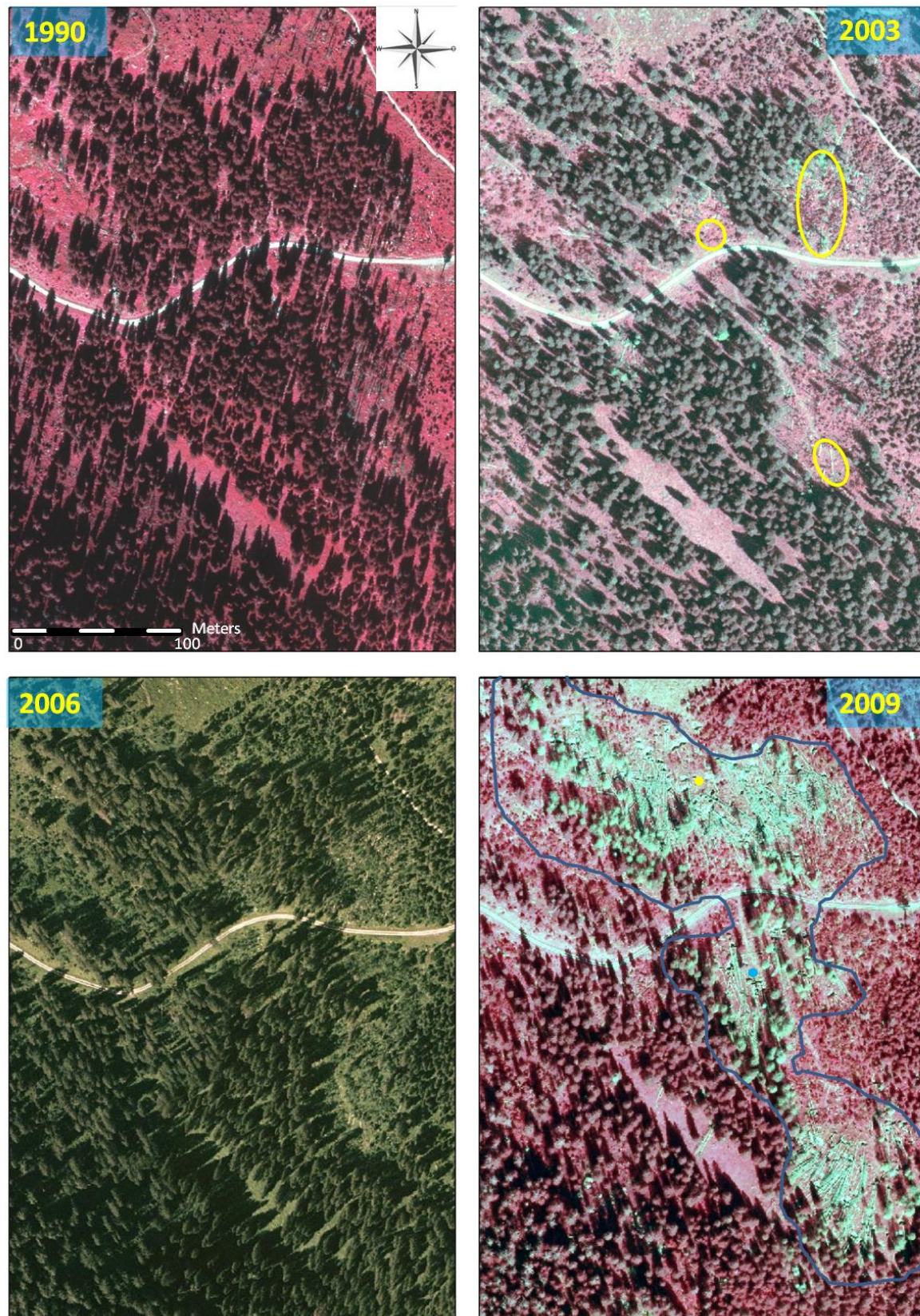
Figure 23: Aerial photos of the Kühroint site in the years 1990, 2003, 2006 and 2009. In the pictures of the year 1990, 2003 and 2009 the red channel of the RGB composite is exchanged by the near infrared. The yellow dot represents the central station; the blue dot the satellite station, both installed in 2009. The blue line represents the area selected for dead wood analysis (see Figure 24 and text), the yellow ovals the wind-throw area of 2003. The aerial photos were kindly provided by the National Park Berchtesgaden.

The aerial photos of the Kühroint site were interpreted in the same way as the ones at the Lackenberg site described in chapter 2.1.2 (Figure 24). The projected area of dead wood material in the wind-throw area in summer of 2009 was determined to be 51% ± 3% or 16.2 ha. This result is not directly comparable to the one at the Lackenberg site, since there are many dead trees still standing at the Kühroint site. Their crowns occupy a considerably larger area in the aerial photo than the ones of lying trees. Due to this, the projected area is much higher than if all trees were already knocked down. A differentiation between the dead wood material on the ground, which was felled by the storm Kyrill and the standing dead trees, most of them killed by bark beetles, was not possible based on the aerial photo analysis alone, because of their very similar spectral properties.
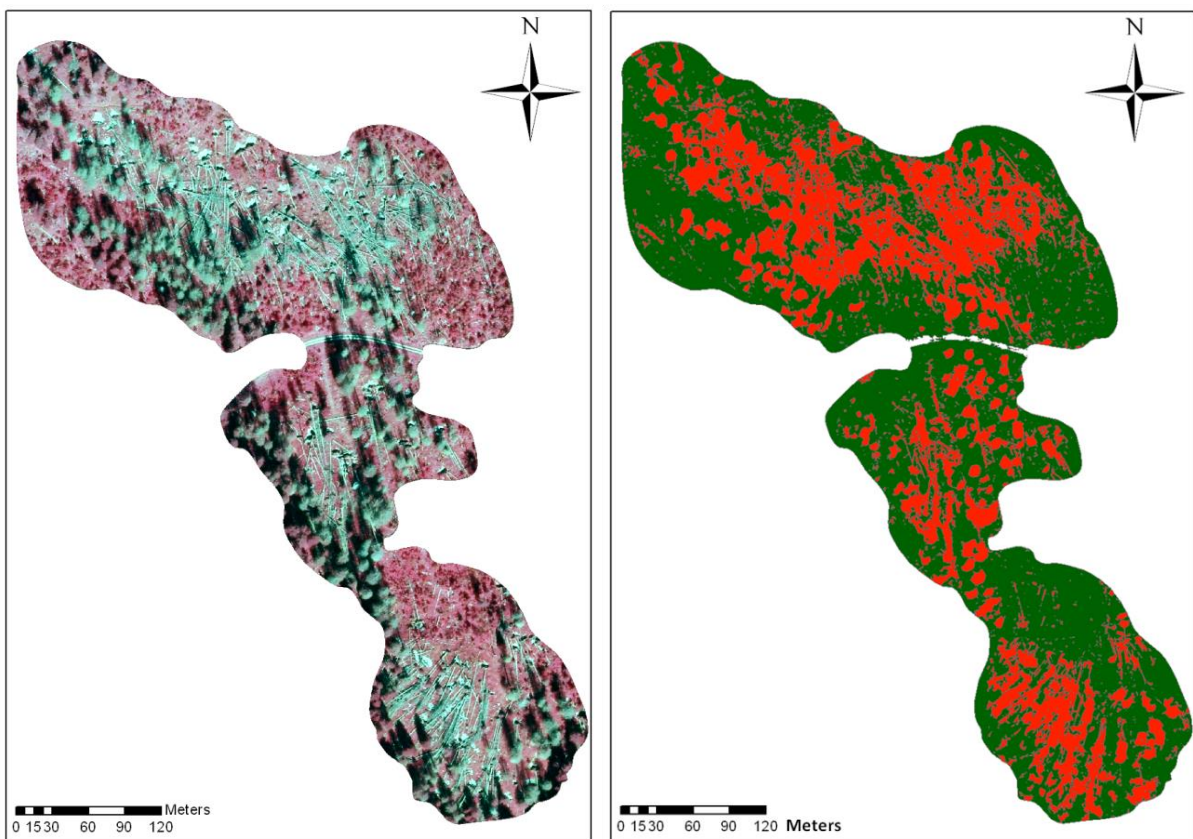
Figure 24. Analysis of the amount of dead wood in the wind-throw area Kühroint. Left: Image section of the aerial photo from 2009 representing the wind-throw area (red is replaced by near infrared). Right: Result of the supervised classification; red color indicates dead wood, green living vegetation or ground material.

2.2.3.   Vegetation at the Kühroint site

The biodiversity at the measurement site Kühroint is considerably higher than the one at the Lackenberg. Besides lying and standing dead spruce, the canopy and

undergrowth consist mainly of living spruce, sycamore maple (*Acer pseudoplatanus* L.), rowan berry (*Sorbus aucuparia* L.), raspberry (*Rubus idaeus* L.), European larch (*Larix decidua* Mill.) and goat willow (*Salix caprea* L.). The ground vegetation is formed by grasses (e.g. great wood-rush (Luzula sylvatica (Huds.) Gaudin)), blue berries (*Vaccinium myrtillus* L.), and St John's wort (*Hypericum perforatum* L.) (Raimund Henneken, TUM, personal communication, 2011). Since living spruce, maple, willow and larch are known to emit monoterpenes (Ruuskanen et al., 2007; Keenan et al., 2009), the composition in the air should be a mixture of emitted volatiles from the dead spruce material and living plants.

2.2.4. Instrumentation of the measurement site Kühroint

To determine meteorological factors, which may influence the VOC concentration in the air above the wind-throw area, the Kühroint site was equipped with two 9 m high towers in its upper (northern) and lower (southern) part, respectively (Figure 23). The satellite station in the southern part was installed in January 2009; the central station in the northern part of the wind-throw in July 2009. Their instrumentation is shown in Table 8, Table 9, Figure 25 and Figure 26. The central station Kühroint has a lower electricity consumption than the one at the Lackenberg site, so it was powered by eight solar panels and one fuel cell and buffered by two 12 V batteries (for details see chapter 2.1.5). The power supply of the satellite station was achieved equally to the Lackenberg site by two solar panels and one battery.

The central station is located north of a gravel road at 47°, 34.05 min N; 12°, 57.74 min E at 1415 m (a.s.l.) and the satellite station south of it at 47°, 33.99 min N; 12° 57.77 min E at 1385 m (a.s.l.). With a distance of 117 m and an altitude difference of 30 m between the towers the mean slope of the area is calculated to be 25%.
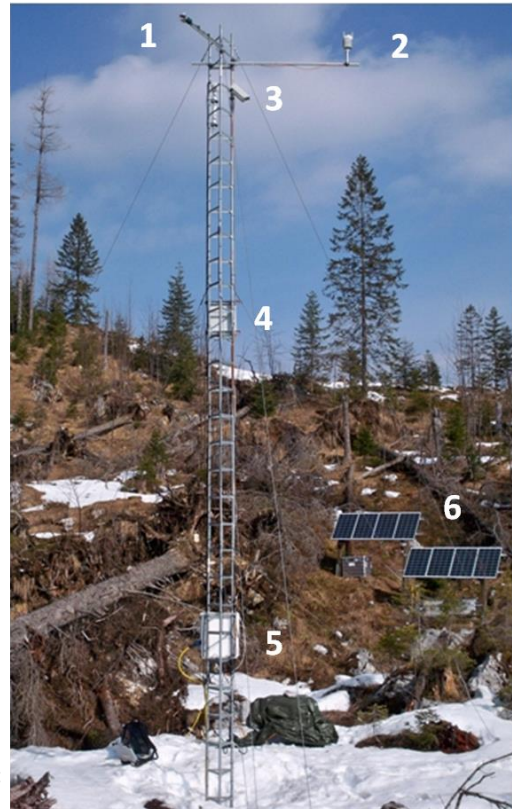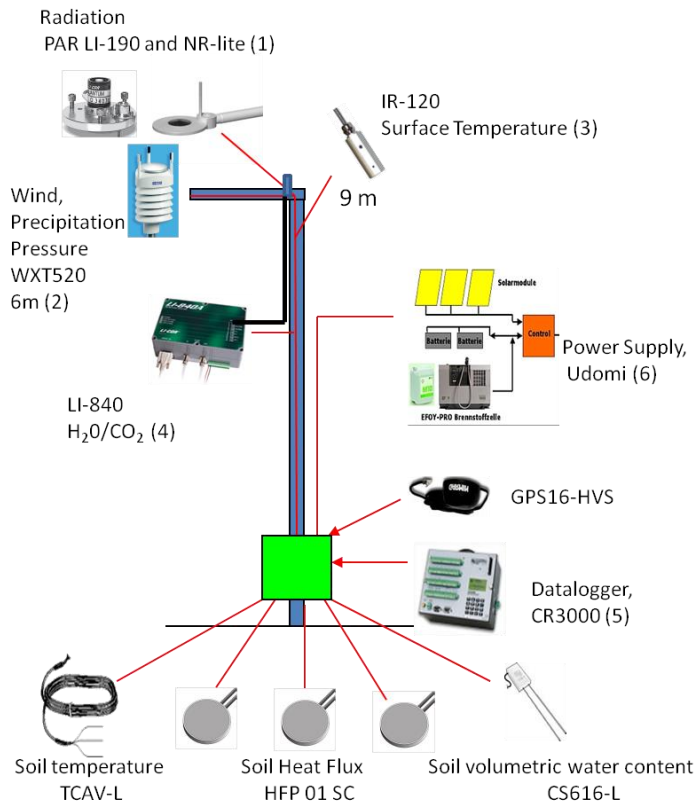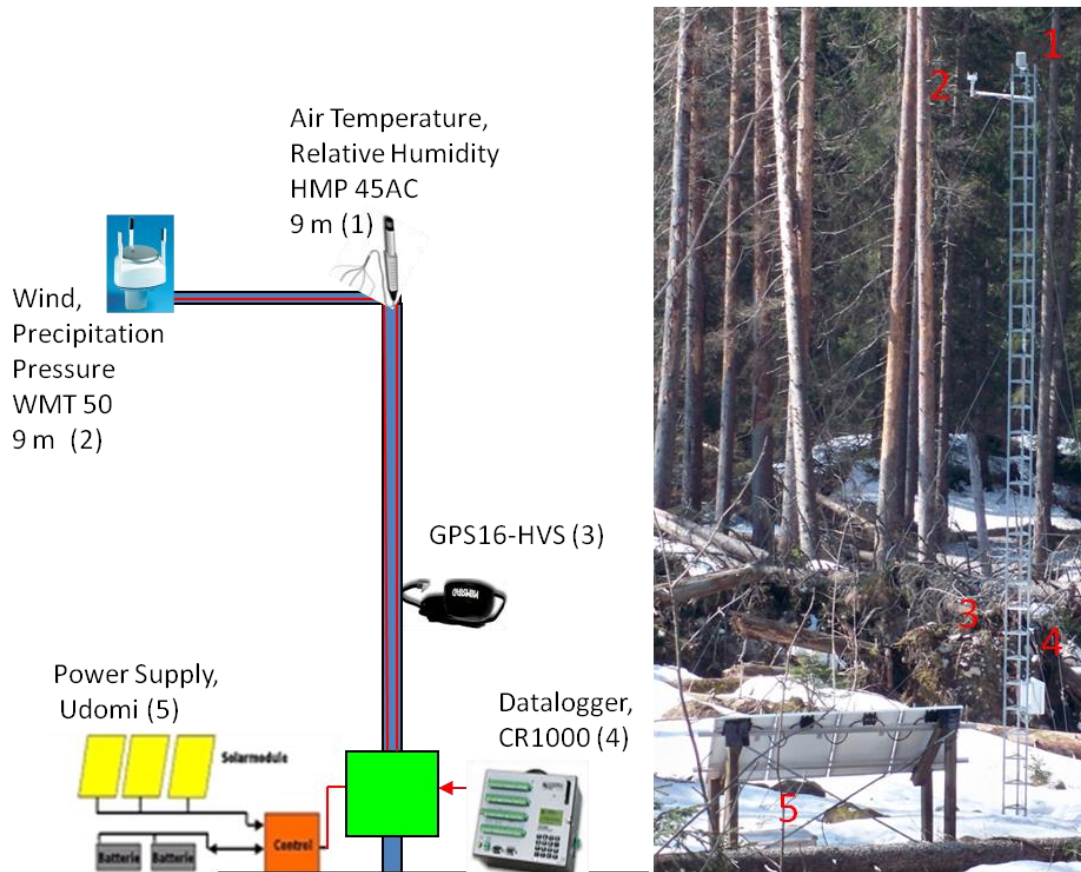
Figure 25: Instrumentation of the central station Kühroint. Photo of the station taken from southern direction. Numbers in the photo correspond to numbers in brackets in the schematic figure.

Table 8. Setup of the central station Kühroint and the corresponding measured variables.

Parameter	Unit	Temporal Resolution	Sensor Height	Instrument	Company*
H_2O	g m^{-3}	10 Min	9 m	Li-840	Li-Cor
CO_2	mmol m^{-3}	10 Min	9 m	Li-840	Li-Cor
radiation balance	W m^{-2}	10 Min	9 m	NR lite	Kipp&Zonen
photosynthetic active radiation	µmol m^{-2} s^{-1}	10 Min	9 m	PAR LI-190 QS	Li-Cor
surface radiation temperature	°C	10 Min	8 m	OS 65 (till 18.11.2009)	Omega
		10 Min	8 m	IR 120 (since 18.11.2009)	Campbell
air temperature	°C	10 Min	9 m	WXT 520	Vaisala
relative air humidity	%	10 Min	9 m	WXT 520	Vaisala
precipitation	mm h^{-1}	10 Min	9 m	WXT 520	Vaisala
wind direction	°	10 Min	9 m	WXT 520	Vaisala
wind speed	m s^{-1}	10 Min	9 m	WXT 520	Vaisala
air pressure	mmbar	10 Min	9 m	WXT 520	Vaisala
soil temperature	°C	10 Min	4 cm below ground	TCAV-L	Campbell
soil heat flux	W m^{-2}	10 Min	8 cm below ground	HFP 01 SC	Hukseflux
soil volumetric water content	%	10 Min	4 cm below ground	CS 616 -L	Campbell
time leveling coordinates				GPS 16-HVS	Garmin
data acquisition				CR3000	Campbell

*Full names of companies: Li-Cor, Lincoln, NE, USA. Campbell Scientific, Logan, UT, USA. Vaisala, Helsinki, Finnland. Kipp&Zonen Delft, Netherlands. Omega Engineering inc., Stamford, CT, USA. Hukseflux, Delft, Netherlands. Garmin, Olathe, KS, USA.

Figure 26: Instrumentation of the satellite station Kühroint. Photo of the station taken from northern direction. Numbers in the photo correspond to numbers in brackets in the schematic figure.

Table 9. Setup of the satellite station Kühroint and the corresponding measured variables.

Parameter	Unit	Temporal Resolution	Sensor Height	Instrument	Company*
air temperature	°C	10 Min	9 m	HMP 45 A	Campbell
relative air humidity	%	10 Min	9 m	HMP 45 A	Campbell
wind direction	°	10 Min	9 m	WMT 50	Vaisala
wind speed	m s^{-1}	10 Min	9 m	WMT 50	Vaisala
time leveling				GPS 16-HVS	Garmin
coordinates				GPS 16-HVS	Garmin
data acquisition				CR1000	Campbell

*Full names of companies: Campbell Scientific, Logan, UT, USA. Vaisala, Helsinki, Finnland. Garmin, Olathe, KS, USA.

2.3.   The climatic situation at the measurement sites Lackenberg and Kühroint

The measurement sites in the two national parks are situated in high altitude regions (1308 /1415m a.s.l.) at a distance of 170 km. Based on the small altitudinal, longitudinal and latitudinal difference of the locations (107 m; 2° 24"; 0° 20"), the climatic situation of the measurement sites should be quite similar.

Figure 27 shows the air temperature of the satellite stations Lackenberg and Kühroint in the years 2009 to 2010. No relevant differences in the seasonal cycle were observed. The annual mean temperatures in 2010 were 4.6°C at the Kühroint site and 3.8 °C at the Lackenberg. Additional meteorological data is presented in the appendix, Figure 91 and Figure 92.
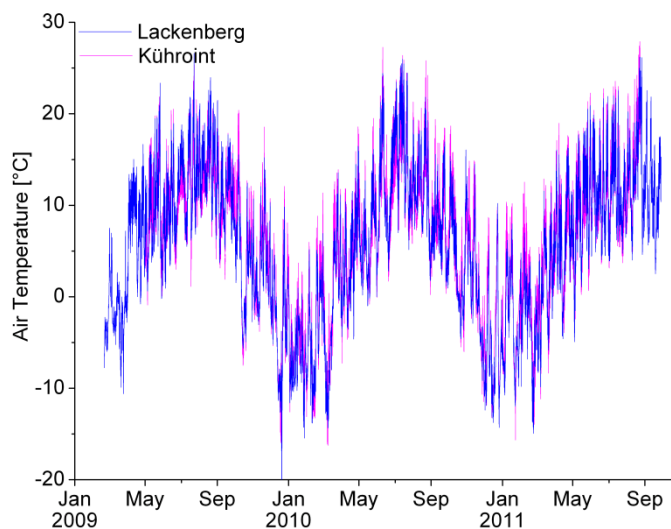
Figure 27: Air temperature in 9 m above ground at the satellite stations Lackenberg (blue) and Kühroint (pink). 10-minute data from 20.2.2009 - 28.9.2011 (Lackenberg) and 1.5.2009 - 31.8.2011 (Kühroint). For gap-filling of missing values at the Kühroint site, see text.

The lowest measured air temperatures in a 10-minute-mean at 9 m above ground were -20.6°C at the Lackenberg and -17.4°C at the Kühroint site, both in winter 2009/2010. Highest temperatures were 26.6°C in summer 2009 at the Lackenberg site and 27.9°C in summer 2011 at the site in the National Park Berchtesgaden. At the satellite station Kühroint data gaps due to problems in the power supply or malfunction of the temperature sensor were filled by air temperatures collected at the central station (23.9.09 - 18.11.09 and 1.2.10 - 19.2.10) and collected at a nearby (370 m northwest, 1420 m a.s.l.) station of the Bavarian Avalanche Warning Service

(AWS) (10.9.09 - 23.9.09). For details of the station of the AWS and a comparison of the air temperatures see chapter 2.4.2, Figure 33 and Figure 29.

Table 10. Air temperature and net radiation of the central stations Lackenberg and Kühroint classified by meteorological seasons. (Averaging time period: Spring: 01.03 - 31.05. Summer: 01.06. - 31.08. Autumn: 01.09. - 30.11. Winter: 01.12. - 28./29.02.; T: average air temperature in 9 m; Max/Min: Maxima- and Minima of the air temperature in the averaging time period; R_{net}: net radiation).

	Lackenberg				Kühroint			
	T [°C]	Max	Min	R_{net} [W/m²]	T [°C]	Max	Min	R_{net} [W/m²]
Spring 2009	5.2	23.4	-10.6	118				
Summer 2009	12.6	26.6	0.9	114	13.4	24.8	0.3	76
Autumn 2009	5.9	21.5	-5.6	29	6.9	21.4	-7.5	30
Winter 09/10	-4.8	9.8	-20.6	-3	-3.9	12.1	-17.4	-14
Spring 2010	2.7	16.5	-14.4	67	3.2	19.5	-16.3	39
Summer 2010	13.1	26.0	1.7	109	12.7	27.3	0.2	83
Autumn 2010	4.3	16.9	-10.7	30	4.6	19.4	-11.5	14
Winter 10/11	-3.8	10.2	-14.9	-15	-1.9	12.5	-15.7	-13
Spring 2011	5.6	20.9	-9.9	66	5.8	22.3	-11.2	60
Summer 2011	12.1	26.2	3.9	112	12.1	27.9	3.1	86

A plot air temperature Kühroint versus air temperature Lackenberg showed a very good agreement of both measurement sites with a slope (0.945) and regression coefficient (0.936) near one (Figure 28). The temperature at the Kühroint site is in general approximately one degree warmer than at the Lackenberg site (Table 10 and Figure 28). The comparison of the meteorological values air temperature and net radiation, which are important for the VOC emission (see section 1.6), showed similar temperatures and slightly lower net radiation at the station Kühroint (Table 10). The temperature at the station Lackenberg is generally slightly lower than at the Kühroint site, although the Kühroint site is approximately 100 m higher. This is presumably because of the more open landscape on the hill top and no influence of the foehn-wind in the Lackenberg area. The more exposed situation at the Lackenberg site is likely also responsible for the higher wind speeds at this site (Figure 30 and Figure 31). The lower net radiation at the Kühroint may be attributed to partial shading of the area by the Watzmann ridge and by some standing trees at the measurement site.
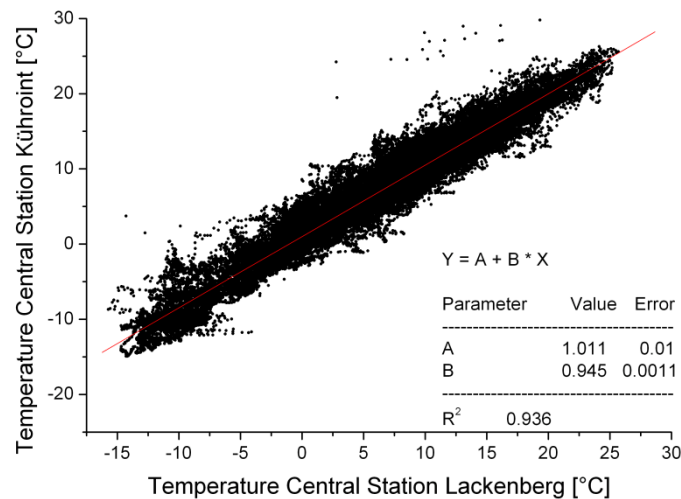
Figure 28: Comparison of the air temperature at the stations Lackenberg and Kühroint in 2009 and 2010.

The measurements of air temperature at the respective central and satellite stations at each site were in very good agreement with each other at both sites, as expected (Figure 29).
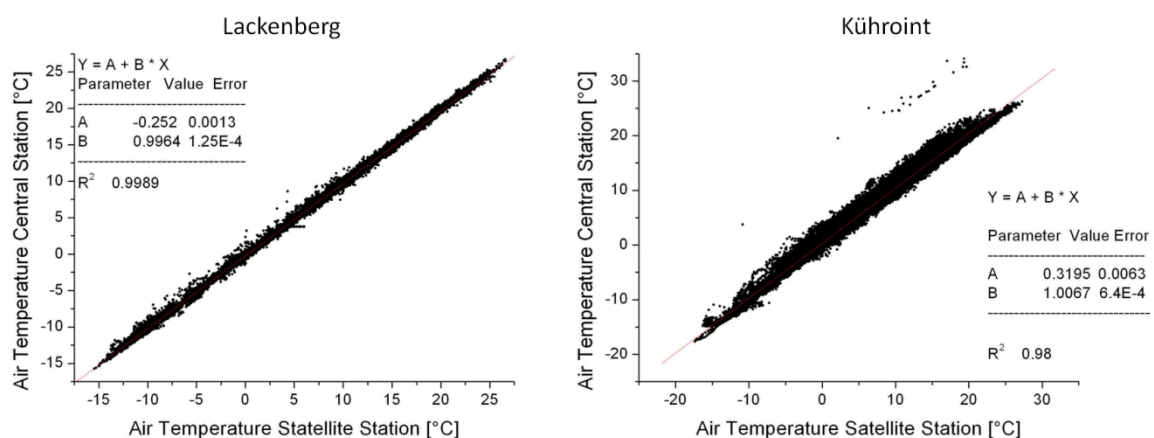

Figure 29: Comparison of the air temperature at the central and satellite station in 2009 and 2010 at the Lackenberg and Kühroint site, respectively.

The wind speed at 9 meter above ground in the period 2009/2010 at the central station Lackenberg was typically between 0.5 - 5.7 m/s (87% of the time) (Figure 30, left). Calm periods were very rare at this height. The wind speed characteristic at the satellite station in 9 meter above ground was quite similar to the measurement at 9 m at the central station with a little shift to lower wind velocities (Figure 30, right).

The predominant wind direction at the two stations was west to south-west (Figure 30). The three dimensional wind sensor (CSAT-3) and the fast CO_2 and H_2O detector

(Li-7500) for the eddy covariance system were mounted in this main wind direction at 210°.
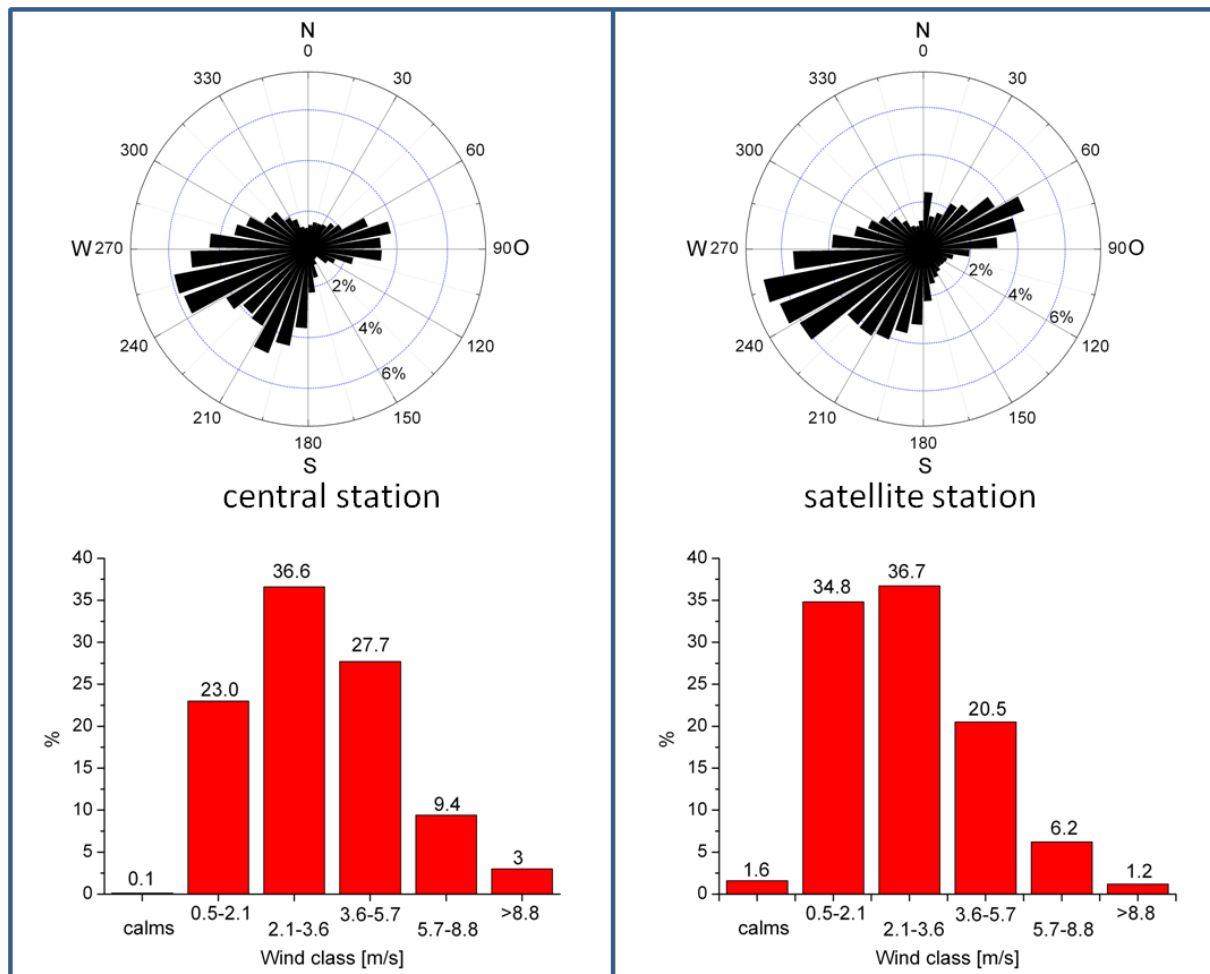
Figure 30: Wind roses and wind speed frequency distribution at the central station (left) and at the satellite station (right) at 9 m above ground at the Lackenberg site in 2009 and 2010.

The wind speed at the Kühroint site in 9 meter above ground is considerably lower than at the Lackenberg with a main wind speed class of 0.5 – 2.1 m/s representing 80% of the total time at both stations. In contrast to the Lackenberg, this site is still sheltered by some trees, especially at the satellite station, where no wind speeds higher than 8 m/s were observed. The wind direction distribution at the central and satellite station are very similar, with the dominant wind direction north-west (Figure 31).
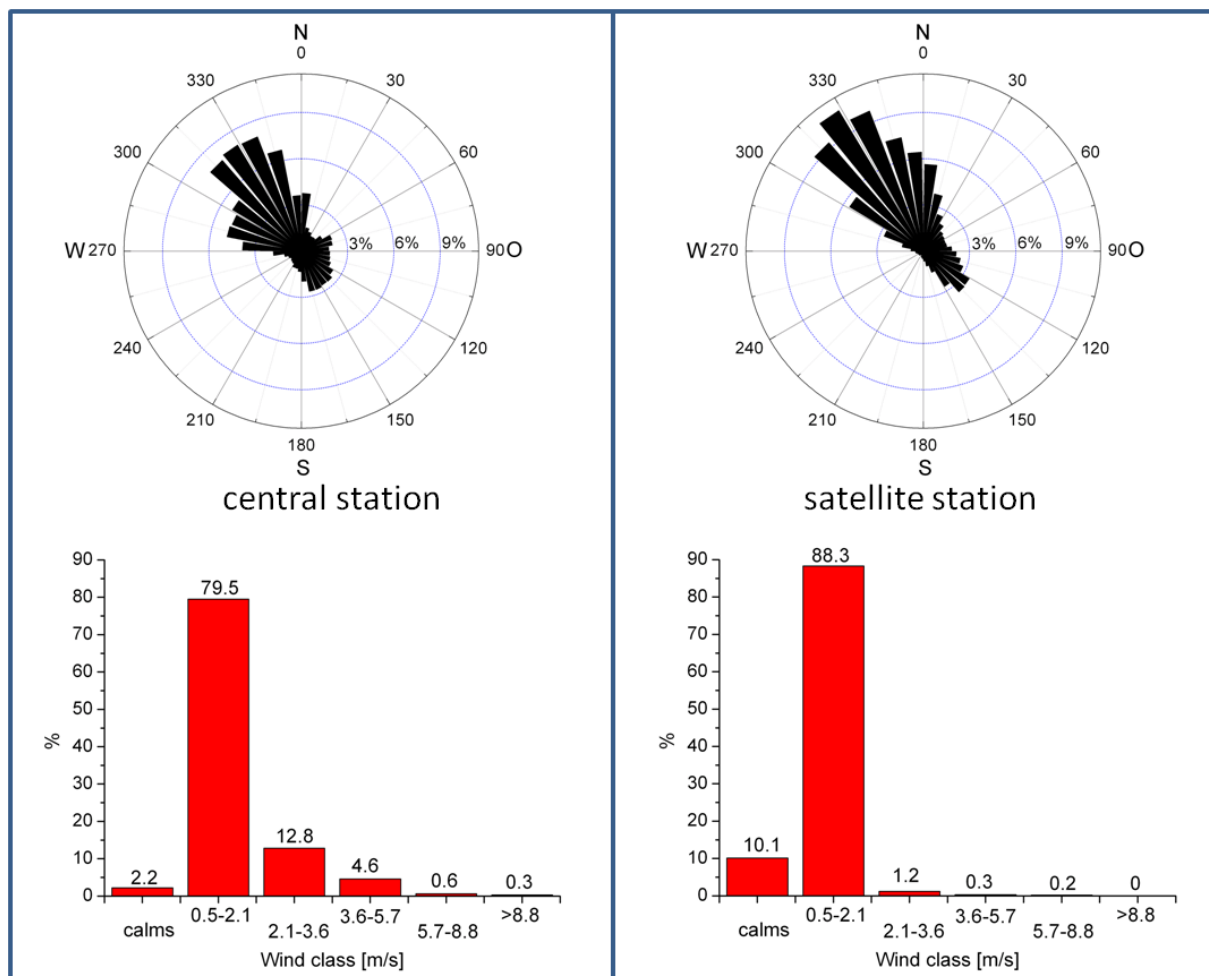
Figure 31: Wind roses and wind speed frequency distribution at the central station (left) and the satellite station (right) at 9 m above ground at the Kühroint site in 2009 and 2010.

It has to be noted that in particular in the case of the air temperature, which is one of the most relevant meteorological controlling factors for the emission of monoterpenes, both Lackenberg and Kühroint sites are very similar and a comparison of the concentration and emission behavior of monoterpenes likely is not much biased by site-specific differences in environmental parameters.

2.4. Comparison of meteorological data collected at the measurement sites to data of nearby weather stations

To embed the meteorological data collected at the sites Lackenberg and Kühroint into a longer timescale and fill possible gaps in our data, it was compared to data kindly provided by the National Parks Bavarian Forest (Claus Bässler) and Berchtesgaden (Helmut Franz), which were recorded at climate stations near to the measurement sites.

2.4.1. Comparison of the station Lackenberg to the Meteomedia station at the Falkenstein

The measurement station at the Falkenstein mountain (49°, 5.005 min N, 13° 16.8 min O) is ideal for a comparison with meteorological data collected at the Lackenberg. It is located only 2.5 km southeast of the central station Lackenberg at almost the same height of 1315 m above sea level. The data were collected at a 30 m high tower (instruments by Adolf Thies GmbH & Co., Göttingen, Germany) above a spruce canopy. The air temperature was recorded at 4 meter above ground. The air temperature in 2009 was very similar with an average of 4.7 °C at the Lackenberg and 4.6 °C at the Falkenstein, respectively.
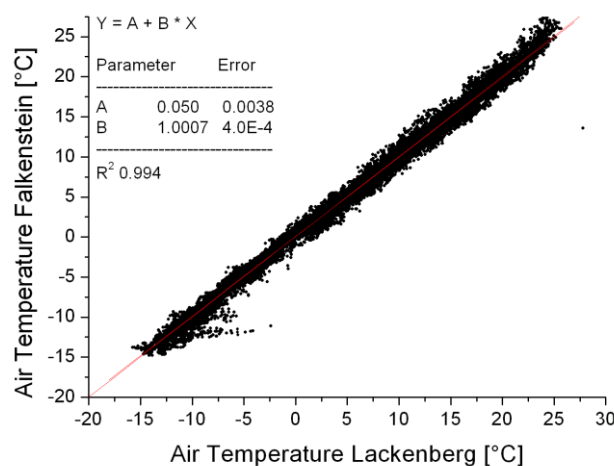
Figure 32: Comparison of the air temperature at the Lackenberg and the Falkenstein in 2009. Air temperature data of the Falkenstein station courtesy of the Bavarian Forest National Park.

The comparison of the Lackenberg versus Falkenstein temperatures showed a slope very close to one and a coefficient of determination of 0.987 (Figure 32). Therefore, the air temperature measured at the Falkenstein station could be used to fill possible data gaps at the Lackenberg site.

2.4.2. Comparison of the station Kühroint to the station of the Bavarian Avalanche Warning Service

At the pasture of the Kühroint Alm at a distance of 370 m northwest of the central station Kühroint is a meteorological station operated by the Bavarian Avalanche

Warning Service (1420 m a.s.l. 47°, 34.21 min N, 12° 57.57 min O) (instruments by Sommer GmbH & Co. KG, Koblach, Austria). This close proximity makes it a very promising candidate for a comparison to our collected data. The recorded air temperatures at both stations were very similar in the year 2009 with no measurable offset and a slope of approximately 1 (Figure 33).
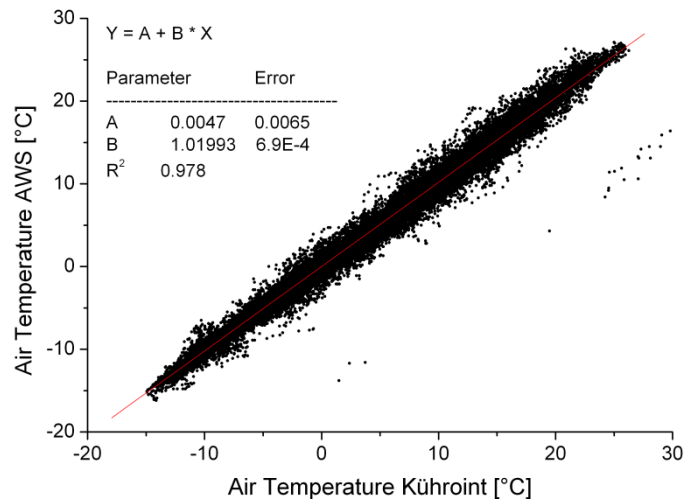
Figure 33: Comparison of the air temperature at the central station Kühroint and the station of the Bavarian Avalanche Warning Service (AWS) in 2009. Air temperature data of the AWS station courtesy of the National Park Berchtesgaden.

The air temperature measured at the station of the Bavarian avalanche warning service showed a good congruence with the one measured at the site Kühroint and were used to fill data gaps in the measured air temperature at the station Kühroint as described in section 2.3.

2.5.   The radiation surface temperature as indication for the dead wood stem temperature

The main emission source of volatile organic compounds in the wind-throw area is supposed to be the dead wood material. The emission of VOCs is usually temperature controlled (see chapter 1.6). A convenient way to get an area averaged temperature is to use the radiation temperature measured by an IR sensor. The sensor (IR-120) used in the present work offered a broad field of view (half angle 20°). The sensor is placed at a height of 7 m above ground with an inclination angle

of 30° to the mast and is directed to northwest. This leads to a field of view of 180 m^2 of wind-throw ground area. The Bavarian Forest National Park conducted temperature measurements directly at stems in the area Lackenberg in summer 2011, which could be used to compare the measured radiation surface temperature to the stem temperature. Temperature loggers (VOLTCRAFT TH logger Conrad Electronic SE, Hirschau, Germany) were installed directly at eight stems in 5 sites in the wind-throw area (5 in the sun, 3 shaded, Figure 34 left). The measured temperatures at the bark of these stems were in very good agreement with the radiation surface temperature determined at the central tower Lackenberg (Figure 34 right).
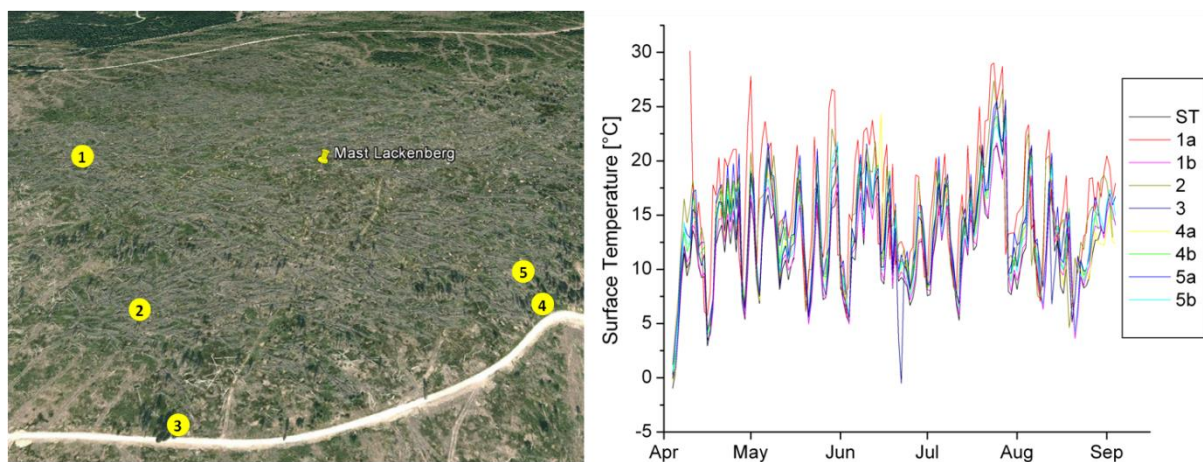
Figure 34. Left: Measurement points of the temperature loggers in the wind-throw area (see also Table 11). Right: Measured mean daily stem temperatures (numbers) and radiation surface temperature at the central mast (ST, black) at the Lackenberg (3.5.- 28.9.2011). Stem temperature data courtesy of Bavarian Forest National Park.

Table 11. Description of the stem temperature measurement points. Data courtesy of the Bavarian Forest National Park.

Measurement point	height above ground [cm]	exposition	sunny
1a	30	W	yes
1b	60	SW	yes
2	160	N	no
3	50	W	yes
4a	50	S	no
4b	170	S	no
5a	10	N	yes
5b	70	W	yes
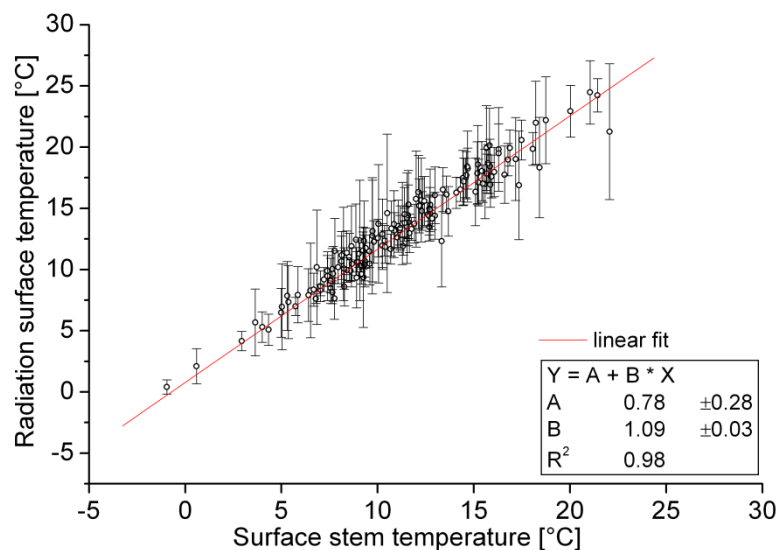
Figure 35. Comparison of the mean value of the 8 stem temperatures with the radiation surface temperature. Mean daily averages 3.5.- 28.9.2011. Error bars represent the standard deviation of the 8 single stem temperatures. N=149. Stem temperature data courtesy of Bavarian Forest National Park.

The mean value of the eight single stem temperatures agreed very well with the measured radiation surface temperature in the vegetation period 2011 (Figure 35). The slope of the linear fit is close to 1 (1.09) and the temperature displayed a small bias towards the radiation temperature (0.78°C). The observed higher radiation surface temperatures are possible due to a higher fraction of sunny parts in the field of view of the sensor, compared to the temperatures measured directly at the stems. Hence, the radiation temperature can be used flawlessly to describe the temperature of the surface of the dead wood material in the wind-throw area.

3.   Methods

3.1.   VOC Analysis

A very versatile and sensitive way of analyzing BioVOCs in real air samples is coupled gas chromatography-mass spectroscopy (GC-MS). The analysis is usually carried out in three steps: sample concentration on adsorption tubes, transfer of the adsorbed compound matrix with subsequent separation on a gas chromatographic (GC) column and detection by mass spectroscopy (MS).

3.1.1.   Pre-concentration on adsorption tubes

Due to the low atmospheric concentration of biogenic organic volatile compounds it is necessary to pre-concentrate them on adsorption tubes before analysis. In this work the sampling was achieved on multi-bed glass cartridges with a length of 90 mm and an inner diameter of 4 mm (PerkinElmer Inc., Waltham, MA, USA). The adsorbent materials were arranged in the tube due to their adsorption strength. The first bed is Tenax TA (60/80 mesh, 70 mg, PerkinElmer Inc., Waltham, MA, USA), a porous polymer based on 2,6-diphenylene-oxide, which is suitable for a sampling of C_5 - C_{26} analytes. According to Gallego et al. (2010), Tenax TA presents high breakthrough values for some VOCs. Therefore, a second bed consisting of the stronger adsorbent Carbopack X (60/80 mesh, 40 mg, SIGMA-ALDRICH, St. Louis, MO, USA) is used as a backup for a potential breakthrough of monoterpenes and an adsorption of lighter analytes (C_3 – C_5). Silanized glass wool (SIGMA-ALDRICH, St. Louis, MO, USA) separates and fixes the two beds.
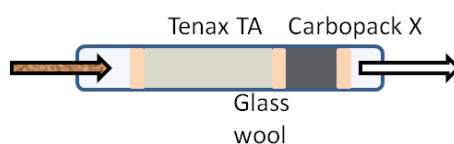
Figure 36: Scheme of an adsorption tube. Loading direction from left to right

On Tenax TA very small amounts of water and carbon dioxide are accumulated during the adsorption (Helmig and Vierling, 1995). Therefore, a special separation of water is not necessary. Both adsorption materials used are very suitable for this application due to their good adsorption and desorption characteristics for monoterpenes (Butler and Burke, 1976; Gallego et al., 2010) and high thermal stability (Tenax TA up to 380°C, Carbopack X more than 400°C).

Previous to each use, the tubes were conditioned at 330°C for 30 min under a flow of helium in an ATD 400 auto-sampler (PerkinElmer Inc., Waltham, MA, USA). The conditioned tubes were sealed with Swagelok caps with Teflon ferrules and stored in the refrigerator at 7°C. They showed no relevant contaminations, even if stored for several weeks. Nevertheless, long time storage of conditioned adsorption tubes previous to the measurements was avoided. Tubes loaded with monoterpenes from field measurements or calibrations were sealed, stored in the refrigerator and analyzed as soon as possible (at least within one week). An additional investigation of the stability showed no decrease of terpene loading within four weeks. Stability studies carried out at the Dutch meteorology institute showed no instability for α-pinene, Δ^3-carene, limonene, eucalyptol and p-cymene trapped on Tenax TA and stored at room temperature for a period of two month (Annarita Baldan, VSL, personal communication). No breakthrough of monoterpenes was found when sampling for 3 hours with a flow rate of 180 ml/min at 35°C. The concentration in this experiment (500 pmol/mol for the single compounds) was higher than the usual ambient air concentration. The collection time in real air samples never exceeded 2 hours and 24 minutes at no more than 30°C, so an incomplete recovery of the VOC level in ambient air due to break-through was avoided.

3.1.2.   VOC sampling during measurement campaigns

VOC samplers built in the Atmospheric Research Lab at the University of Colorado (Hueber, 2009) were used to load adsorption tubes in field measurements and for calibration experiments (Figure 37). They consist of a temperature controlled sampling compartment for ten adsorption tubes. To avoid water condensation in the valves and lines the temperature was set to 35°C. Software control of the sampling valves gives the opportunity to take several samples within 24 hours or even longer time periods. The sampling flow was controlled by precision mass flow controllers to keep flow changes due to different gas flow resistances of individual cartridges as low as possible. The samplers provide the possibility to perform a leak test for every tube, which was done before every measurement cycle. They are enclosed in water tight Hardigg rags, which allowed measurements in bad weather conditions like rain or snowfall.
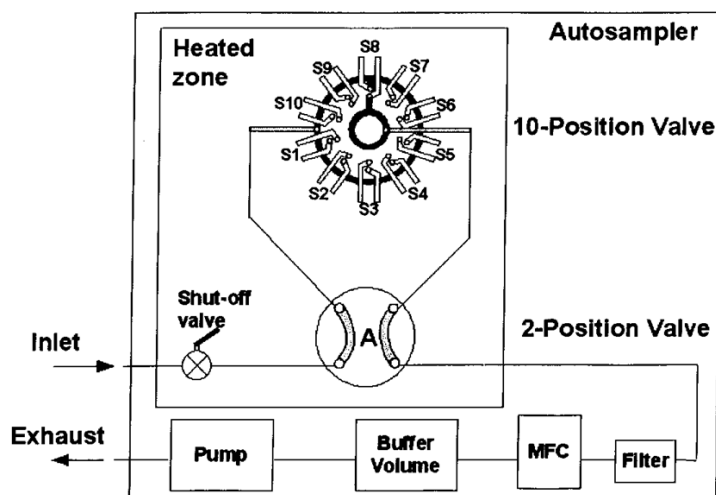
Figure 37. Scheme of the VOC sampler in sample mode.MFC = mass flow control. (Figure from Hueber, 2009).

The atmospheric samples were collected at the central masts at the sites Lackenberg and Kühroint via 12 meter Teflon tubes with an inner diameter of ¼ inch. The tube was protected from direct sunlight by a black insulation cover. In previous studies (Steinbrecher et al., 2000) no tubing effects on VOC air concentrations were observed, even when 60 m long Teflon tubes were used. Stainless steel filter holders with manganese dioxide coated nets at the inlet of the Teflon tubes were used to remove atmospheric ozone during the sampling (Helmig, 1997). The dead volume of the Teflon tubes was calculated from the inner diameter and length to be 730 ml. With the usual flow of 180 ml/min a time delay of 4 minutes results, which was considered as a time shift in the sampling times.

3.1.3.   Preparation of VOC standards for calibrations by a diffusion system

A diffusion system described in Steinbrecher et al. (1994) and Schitzler et al. (2004) was modified to prepare gaseous standards of BioVOCs. Standards in the range of ppt (pmol/mol) are achieved by the controlled evaporation of pure VOCs and subsequent dilution by clean air.
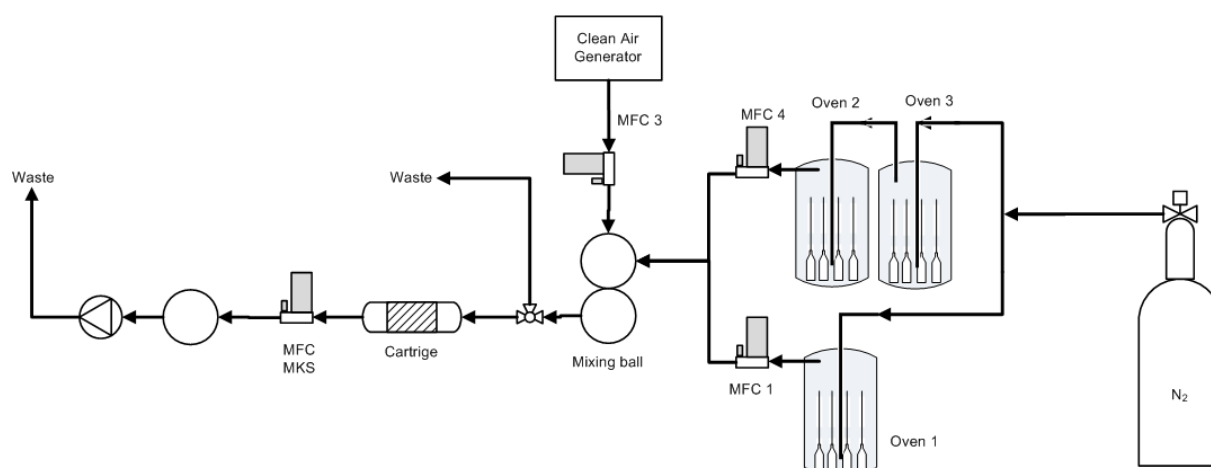
Figure 38: Schematic diagram of the diffusion unit. Temperatures: oven 1 = 35°C, oven 2 = 35°C, oven 3 = 25°C. MFC = mass flow controller.

The diffusion sources are brown glass bottles with a volume of 1.8 ml, filled with approximately 200 mg of the target VOC and sealed by a Teflon coated septum. Depending on the vapor pressure of each substance (Table 2) the septums are punctured by GC transfer lines (Hydroguard Nr. 10076, Restek, Bad Homburg, Germany) or glass tubes with an inner diameter of 1 mm (Table 12) and placed in different thermostatted compartments. Mass flow controllers ensure a constant flow of pure nitrogen (130 ml/min, 99.9999%, AIR LIQUIDE, Düsseldorf, Germany) into the ovens. Purified air (4600 ml/min, generated in an AADCO 737 pure air generator, Randolph, VT, USA) is used to dilute the resulting high concentrated gas flow in electropolished stainless steel mixing balls. Several analyses of adsorption tubes loaded only with air from this clean air generator at different times in the years 2008 to 2011 showed no contaminations.

Samples of the gaseous standards are loaded on adsorption tubes from a bypass. The glass bottles with the target VOCs were weighted in constant time periods and the resulting weight losses converted in diffusion rates. A consistent weighing procedure was used to minimize systematical errors. The weighing was done very thoroughly on a high precision balance in an air conditioned room, in which the diffusion sources were placed 20 minutes before each weighing to adapt to room temperature. Silica gel was used as desiccant in the balance chamber to avoid water adsorption on the glass vessels. An empty glass bottle was used as standard weight to identify potential variations in the weighing due to changes in temperature, air pressure or humidity.

Table 12. Diffusion temperature and purity of the standards used in the diffusion system.

VOC	Diffusion temperature [°C]	minimal purity [%]	Diffusion tube
α-pinene	25	95	GC
Δ^3-carene	25	90	GC
limonene	25	98.5	GC
p-cymene	25	97	GC
camphene	35	95	GC
β-pinene	35	90	GC
1.8-cineol	35	97	GC
cis-verbenol	35	95	Glass
α-terpineol	35	95	Glass
(-)-verbenone	35	99	Glass
2-methyl-3-butene-2-ol	35	97	GC

All standards purchased from Carl Roth except of cis-verbenol and (-)-verbenone from Fluka.
GC = Diffusion through GC transfer line (Hydroguard Nr. 10076), inner diameter 0.1 mm, length 50 mm. Glass = Diffusion through glass tubes, inner diameter 1 mm, length 70 mm.

3.1.4. Permeation rates of the diffusion system

To investigate if the diffusion device for the preparation of reference standards described in chapter 3.1.3. is suitable for the quantitative determination of monoterpenes in ambient air, the diffusion tubes were weighted on a high precision balance at least once a month. The permeation rate is calculated from the weight loss and the time interval between two weightings (Figure 39).
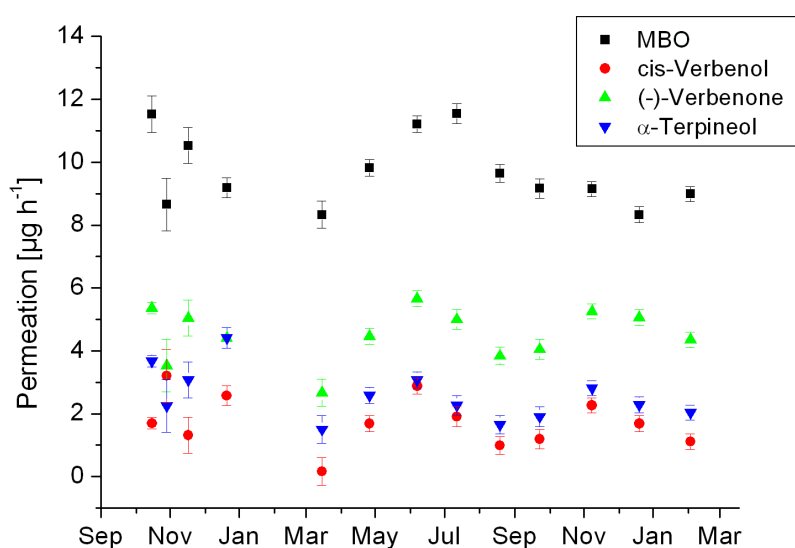
Figure 39: Permeation rates of volatile organic compounds stored at 35 °C from September 2009 to March 2011. Error bars represent the standard deviation of the mean value (n=3) of the weighing error. MBO = 2-methyl-3-butene-2-ol.

The permeation rates showed a high uncertainty of up to 35% (eucalyptol), while for some components (α–pinene, limonene, camphene, β–pinene, verbenone) the deviation is in a lower range (Table 13), which makes the diffusion device prospective for the preparation of gaseous standards of these substances.

Table 13. Permeation rates and resulting concentrations of the VOC standards prepared in the diffusion system. Accuracy is the standard derivation of the permeation rates calculated from 10 consecutive weighting procedures. MBO = 2-methyl-3-butene-2-ol.

VOC	Permeation rate [$\mu g\ min^{-1}$]	Concentration [$pg\ ml^{-1}$]	Accuracy [%]
α-pinene	0.36	75	6.7
Δ^3-carene	0.07	14	26.2
limonene	0.16	33	7.3
p-cymene	0.12	26	16.1
camphene	1.03	217	4.3
β-pinene	0.77	174	6.4
eucalyptol	0.41	86	35
MBO	0.14	30	18.7
cis-verbenol	0.03	6	33.3
(-)-verbenone	0.08	18	12.9
α-terpineol	0.04	8	18.4

With the applied dilution and sample flows, the concentration of volatile organic compounds in the standard is calculated with equation (5) to be substance specific between 6 and 217 $pg\ ml^{-1}$ (Table 13).

$$c_{VOC} = \frac{\frac{\Delta m_{VOC}}{\Delta t}}{F_{VOC} + F_d} \tag{5}$$

c_{VOC} is the concentration of a VOC in pg/ml, Δm_{VOC} the mass difference between two weightings in pg, Δt the time difference between two weightings in minutes, F_{VOC} the gas flow in the diffusion ovens, and F_d the dilution gas flow, each in ml/min.

3.1.5.   Monoterpene gas mixture as calibration standard

Due to the high uncertainties of the diffusion system for some compounds, a high precision 17-component gas standard was purchased from NPL (National Physical Laboratory, Teddington, England). Relevant monoterpenes and their uncertainties are listed in Table 14. The standard was first calibrated in October 2009 and again in January 2011 by NPL. No differences in the concentration and uncertainties were reported between both calibrations.

Table 14. Monoterpene gas standard in nitrogen. Amount fractions listed with standard uncertainties.

Monoterpene	Amount fraction [nmol mol^{-1}]
α-pinene	1.99 ± 0.03
Δ^3-carene	1.98 ± 0.03
limonene	2.00 ± 0.03
p-cymene	2.01 ± 0.03
β-pinene	2.01 ± 0.05
eucalyptol	2.05 ± 0.05

3.1.6.   Analysis of VOCs with gas chromatography–mass spectroscopy (GC-MS)

The adsorption tubes were analyzed by gas chromatography-mass spectroscopy using a Turbo Mass spectrometer - AutoSystem XL chromatograph unit (PerkinElmer, Waltham, MA, USA) (Figure 40). Prior to each analysis the tubes were purged for 60 seconds at 5°C in a flow of oxygen-free, pure helium (99.9999%, AIR LIQUIDE, Düsseldorf, Germany) to remove potential residues of water or very volatile substances which may interfere the analysis. Afterwards, in an ATD 400 auto-sampler (PerkinElmer, Waltham, MA, USA), the terpenes were automatically thermally desorbed at 280°C in a carrier gas flow and cry-focused on a cooled (5°C) low-flow-trap-tube packed with Tenax GR 60/80. The trap was heated to 280°C to transfer the analytes into the GC column (30 m, 0,25 mm ID, 1 µm, crossbond 14% cyanopropylphenyl – 86% dimethylpolysiloxane, Rtx-1701, Restek, Bad Homburg, Germany), where they were separated according to their physio-chemical properties. Therefore, the substances left the column at different retention times, depending on

their mass to charge ratio. The column was connected to the MS source (70 keV, 230°C) via a heated interface (250°C). The m/z range of the mass spectrometer was 33-300.
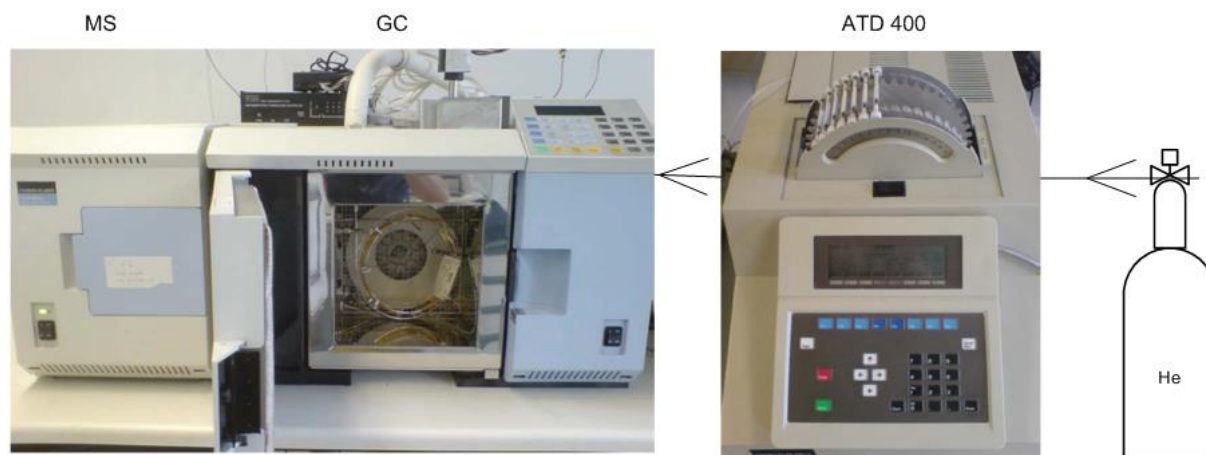
Figure 40: Setup of the GC-MS analysis. VOCs are desorbed in the ATD, separated in the GC (picture with open oven, column viewable) and analyzed in the MS.

In the mass spectrometer the incoming VOCs are ionized by electron impact ionization and fragmented into characteristic patterns (spectrum). So the coupled GC-MS has two possibilities to identify substances: the retention time and the spectrum. Typical system parameters of the GC are listed in Table 15 and Table 16. One sample takes approximately 64 minutes to be analyzed including the heating and cooling process.

Table 15. System parameters of the desorption of sampling tubes in the ATD 400 auto-sampler.

	Time	Temperature tube	Temperature cold trap
Desorption of the tube, Cryo-focusing on the cold trap	10 min	280°C	5°C
Desorption of the cold trap	20 min	/	280°C
Cleaning of the tubes	30 min	330°C	/

Table 16. Temperature program of the gas chromatography. Total time of the GC analysis 47 min. Helium pressure was 70 kPa, flow 0.4 ml min^{-1}.

Ramp	Heat rate [°C min^{-1}]	Temperature [°C]	Time hold [min]
1	0	40	4
2	5	220	0
3	20	260	5

A second analysis of tubes which had already run through the analysis cycle once, showed a almost complete desorption of the analytes (remaining monoterpene loading below 1% of the initial loading).

3.1.7. Identification of VOCs in the GC-MS

Volatile organic compounds were identified in the GC-MS by their retention times and characteristic fragmentation patterns (spectrum) in the mass spectrometer. These two independent ways of determining analytes lead to a very high level of confidence for the analysis of volatile organic compounds in the gas chromatography - mass spectroscopy. The retention times and spectra were determined by loading adsorption tubes with the same pure substances, which were used in the diffusion system described in chapter 3.1.3. A separation of most of the compounds was achieved by using the temperature program and column described above (Table 17). A separation of β-pinene and sabinene was not possible, although different heating rates and temperature ramps were tested.

Table 17. Retention times and main mass fragments of selected volatile organic compounds (VOC). System parameters of the GC-MS described in Table 15 and Table 16. MBO = 2-methyl-3-butene-2-ol.

VOC	Retention time [min]	Main fragment [g/mol]
MBO	6.95	71
α-pinene	15.96	93
camphene	16.88	93
β-pinene	18.04	93
sabinene	18.04	93
Δ^2-carene	18.60	93
Δ^3-carene	19.09	93
limonene	20.00	68
p-cymene	20.64	119
eucalyptol	20.74	43
cis-verbenol	26.56	109
α-terpineol	28.10	107
(-)-verbenone	30.57	107

The identification of the specific mass spectra was done by a comparison of the measured spectrum to a reference library (NIST MS search 2.0, National Institute of Standards and Technology, Gaithersburg, MD, USA). The main fragment in the fragmentation pattern for each VOC is listed in Table 17. An example chromatogram of the most important VOCs of Norway spruces is shown in Figure 41. The elution of the substances occurs in narrow bands, which are suitable for the quantification.
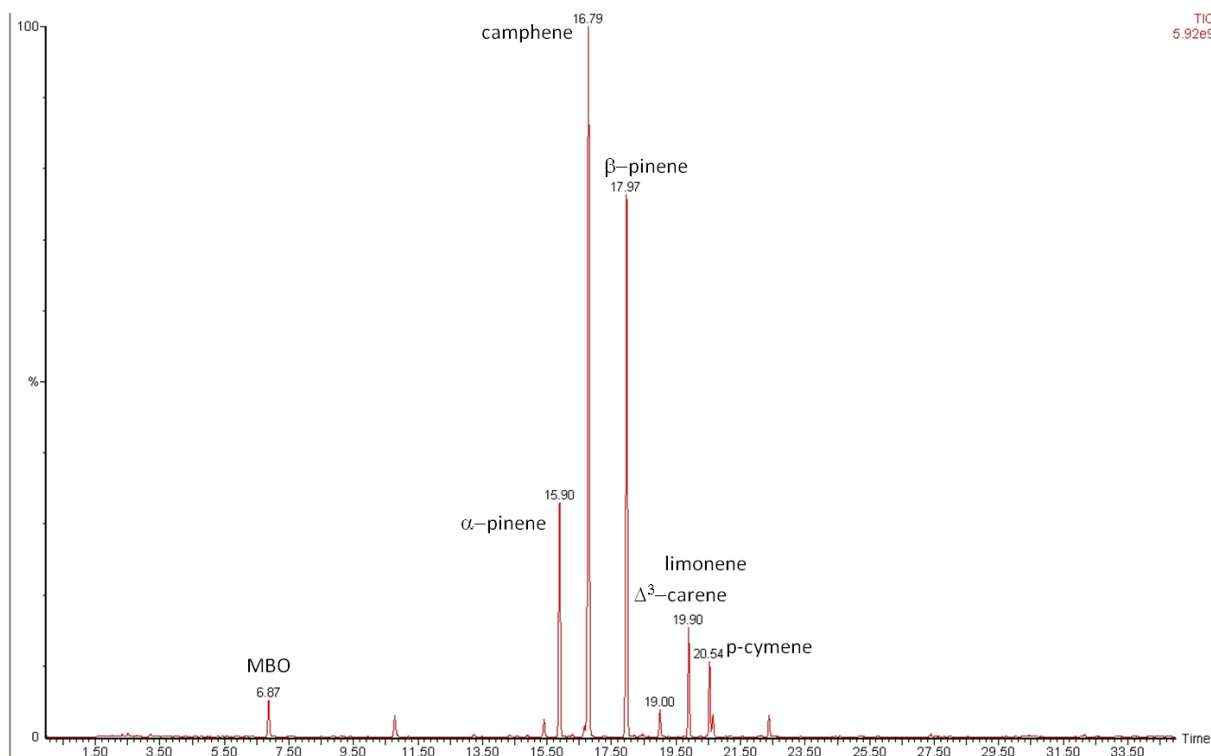
Figure 41: Example chromatogram of standards from the diffusion system recorded in the single ion mode (mass 93) with the system parameters described in Table 15 and Table 16. y-axis is the relative ion current of the highest peak. Masses: 2-methyl-3-butene-2-ol (MBO) 20 ng, α-pinene 50 ng, camphene 150 ng, β-pinene 120 ng, Δ^3-carene 9 ng, limonene 23 ng, p-cymene 18 ng.

3.1.8.   Quantification of VOCs in the GC-MS

The amount of volatile organic compounds loaded on adsorption tubes was calculated by the use of an internal standard. An internal standard is a compound which has to be chemically and physically very similar to the analytes, but must not appear in the real sample. It should be detectable with the same measurement method with a similar sensitivity as the target substances. A substance which meets these requirements for monoterpene analysis is the artificial monoterpene Δ^2-carene, a structural isomer of the naturally occurring Δ^3-carene, but not present in natural samples. The retention time of Δ^2-carene is 18.60 minutes, so none of the peaks of other VOCs of interest is overlapping (Table 17). Due to the chemical and physical similarity of monoterpenes, no relevant difference in the adsorption and desorption behavior of the analytes and the internal standard was found. The mass of the analyte on a tube can be calculated from the known amount of Δ^2-carene on this tube and a substance specific response factor of the analyte, according to

$$m_i = \frac{A_i}{k_i * RF_{carene}} \qquad\qquad RF_{RF_{carene}} = \frac{A_{RF_{carene}}}{m_{RF_{carene}}} \qquad (6)$$

where m_i is the mass of compound i loaded on an adsorption tube, A_i the compound peak area in the chromatogram, k_i a relative correction factor specific for each analyte i, and RF_{carene} is the response factor of the internal standard Δ^2-carene for this tube calculated from the found peak area (A_{carene}) and loaded mass (m_{carene}) of Δ^2-carene on this tube.

The relative correction factor was determined by loading known amounts internal standard and of VOC compounds from the monoterpene standards on adsorption tubes. Correction factors for each compound were calculated according to

$$k_i = \frac{RF_i{}^c}{RF^c{}_{carene}} = \frac{A_i{}^c * m^c{}_{carene}}{A^c{}_{carene} * m_i{}^c} \qquad (7)$$

where $RF_i{}^c$ and $RF^c{}_{carene}$ are response factors of compound i and the internal standard in the calibration, $A_i{}^c$ is the area of compound i in the calibration chromatogram, $A^c{}_{carene}$ is the peak area of Δ^2-carene, $m^c{}_{carene}$ and $m_i{}^c$ are known loaded masses of compound i and internal standard Δ^2-carene in the calibration process.

The use of an internal standard minimizes many errors which may occur if an external standard is employed such as:

- Uncertainties of the volume flow do not affect the results if the internal standard and the sample are loaded onto the adsorption tube with the same device.
- Different adsorption characteristics of tubes are compensated, because the standard shows the same adsorption behavior as the analytes.
- Potential sample losses during desorption or storage do not affect the results as the internal standard behaves similar than the analytes.

Thus, it is recommended to use an internal standard as more accurate results are provided.

Δ^2-carene is loaded directly from the gas flow of the standard cylinder on the adsorption tubes in the bypass mode by the help of the VOC samplers (see Figure

37). A controlled loading was ensured by the temperature and flow control of the automated VOC samplers described above.

The response (area of the chromatogram) of the mass spectrometer should be linear depending on the mass of injected Δ^2-carene to quantify monoterpenes from real samples without large systematical errors. This linearity is given at least in the range of 5-40 ng of internal standard (Figure 42).
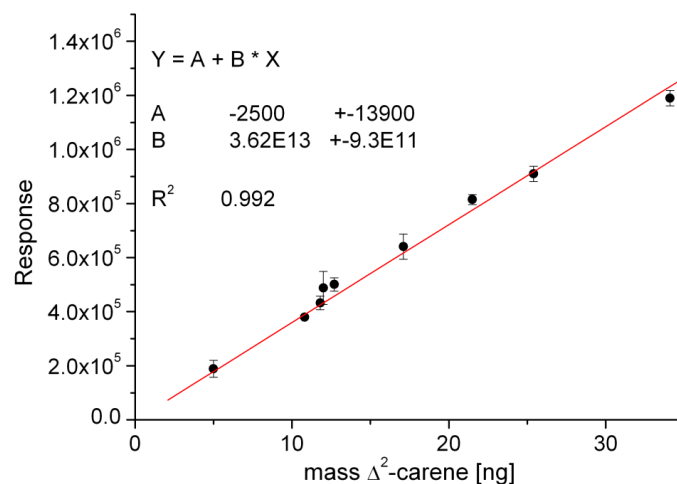
Figure 42: Response of the mass selective detector (MS) per mass Δ^2-carene recorded in the single ion mode (mass 93) with the system parameters described in Table 15 and Table 16. Error bars represent the standard deviation of the mean value (n = 5).

No interference of the internal standard with other volatiles was detected when Δ^2-carene and monoterpenes from the gas mixture where loaded simultaneously on adsorption tubes and analyzed in the GC-MS (Figure 43).
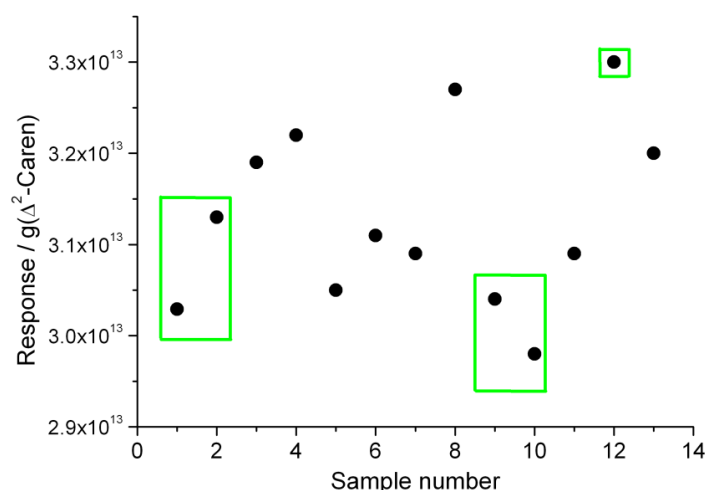
Figure 43. Responses of the MS per gram Δ^2-carene. Sample numbers 1, 2, 9, 10 and 12 loaded with Δ^2-carene only (in green boxes), sample numbers 3 – 8, 11 and 13 adsorption tubes with additional loading of VOC standard. Masses of Δ^2-carene: 10.8 ng (1, 6, 10 – 13); 21.5 ng (2 – 5, 7, 8, 9). Masses of VOC: 8 ng (3, 5, 7, 11); 16 ng (4, 6, 8, 13).

Response factors of the investigated monoterpenes relative to Δ^2-carene, their precision and accuracy and the limit of detection of each analyte are reported in Table 18. For differential measurements, which are used to determine the source strength by the method of the micrometeorological gradient approach (see section 3.2), the precision of the analysis is relevant.

Table 18: Response factor of volatile organic compounds relative to Δ^2-carene calculated with standards from the monoterpene gas cylinder (NPL) and the diffusion system (DS). Precision results from the standard deviation of the mean (n=9) of the areas in the GC-MS; accuracy from the error propagation of the precision and the uncertainties of the used standards. Δ (NPL/DS) is the difference between the response factors of a substance calculated by standards of the gas cylinder and the diffusion system. Limit of detection (LOD) is three times the noise in the GC-MS spectrum.

VOC	Response factor relative to Δ^2-carene (NPL)	Precision [%] (NPL)	Accuracy [%] (NPL)	Response factor relative to Δ^2-carene (DS)	Precision [%] (DS)	Accuracy [%] (DS)	Δ (NPL/DS) [%]	LOD [pg]
eucalyptol	1.27	5.6	10.6	1.91	3	37	34	33.2
β-pinene	1.50	1.5	8.7	2.04	1.8	12	26	4.8
Δ^3-carene	1.38	2.2	8.8	1.54	2.3	28	10	5.8
limonene	1.064	2.1	8.8	1.01	2.6	13	5	8.8
p-cymene	2.42	2.7	9.4	3.73	11.1	22	35	3.7
α-pinene	1.59	1.5	8.7	2.28	1.9	12	30	4.8
camphene				0.93	4.3	12		4.0
verbenol				0.49	31	47		120
α-terpineol				0.37	26	33		102
verbenone				0.53	27	32		69
MBO				1.16	5	22		3.5

The relative response factors to Δ^2-carene were stable within the analytical error during the measurement period (Figure 44). Maintenance work on the analysis system (chances of the cold trap, valves, etc.) can slightly change the response factors of the target components. Therefore, it is necessary to review the calibration factors periodically, especially after system changes.
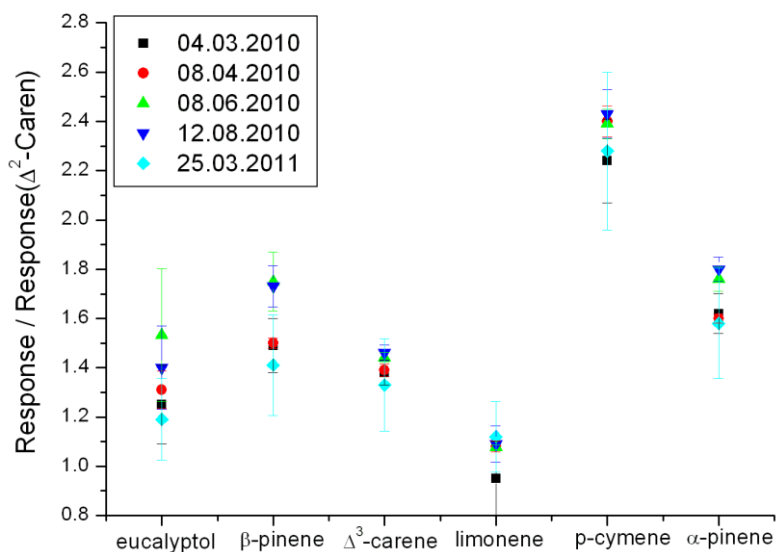
Figure 44: Response factors of monoterpenes relative to Δ^2-carene in 2010 and 2011. Error bars represent the standard deviation of the mean value (N=8).

The signal-to-noise ratio of the mass spectrometer can be considerably enhanced if not the total ion current (TIC) but the response of the main fragments (Table 17) after ionization of the monoterpenes are used for quantification. Very low detection limits of a few picograms can be realized in this single ion mode (SIM) (Table 18). Due to the different fragmentation patterns of the analytes (i.e. Figure 45) the response factors can vary strongly for different components, particularly if the usual main fragment 93 is not used for the analysis (e.g. 119 for p-cymene, Table 18).
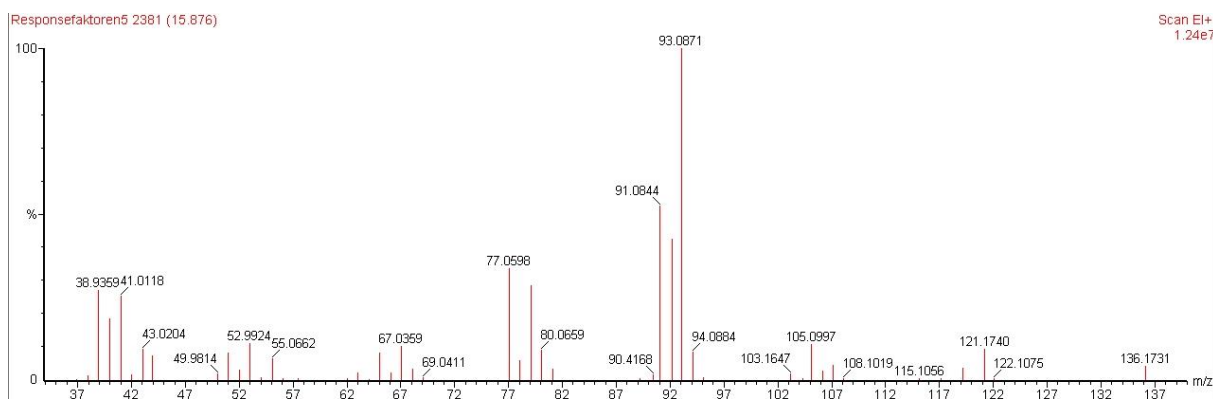
Figure 45: Typical spectrum of α-pinene recorded with the system parameters described in Table 15 and Table 16.

A further advantage of the SIM is that interfering substances with the same retention time as the analytes do not impact the quantification, as long as their fragmentation patterns show no identical masses to the compounds of interest in this work.

3.1.9. Determination of the monoterpene pool in the dead wood at the Lackenberg

To quantify the amount of monoterpenes in the dead wood at the Lackenberg site, 26 samples of stem wood, including bark, were taken on the 15th of June and 12th of July 2011 (Figure 46). The dead wood was sampled by cutting out pieces with a diameter of 2 cm and a thickness of 1.5 cm by a round chisel. Additionally, 20 branches with a diameter below 3 cm and three samples of needles found in sheltered areas between lying stems were collected at the same days. The samples were immediately put in air-tight plastic bags, stored in ice cooled boxes, and processed the next day.
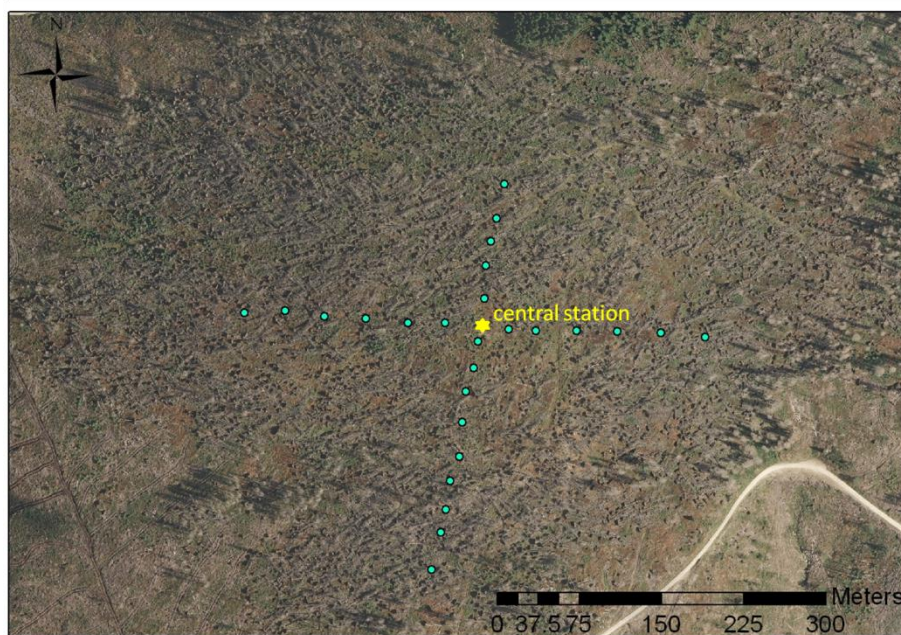
Figure 46. Sample points of dead wood in the wind-throw area Lackenberg.

Frozen samples were cut into pieces with an approximately thickness and width of 1 mm and a length of 5 mm. Approximately 150 mg of this material was put into 1 ml of hexane at 6°C for 4 days under constant shaking. After this extraction 1 μl of the solution was analysed in a GC-MS, the samples thoroughly washed 3 times with hexane, and the extraction process repeated. The second analys of the solution showed a monoterpene concentration of less than 3% of the first one, which means the first extraction was almost complete. After the analysis, the wood samples were dried for 24 hours at 80°C and for 12 hours at room temperature in a vacuum-desiccator and weighted on a high precision balance.

Analysis of the monoterpenes was done by the gaschromatography-mass spectrosopy system Saturn® 2200 (Agilent Technologies, Santa Clara, CA, USA) at the Institute of Animal Ecology of the Technical University Munich. The solvent

hexane was spiked with 0.1 nmol/µl of nonane, which was used as internal standard in the quantification. Specifications of the GC-MS are listed in Table 19. A CP-cyclodextrin column (Cat.Nr. 7501, 50 m, diameter 0.25 mm, film thickness 0.25 µm, Agilent Technologies, Santa Clara, CA, USA) was used to separate the monoterpenes.

Table 19. Specifications of the Saturn[®] 2200 GC-MS

trap temperature	200°C
manifold	70°C
transfer line	240°C
photomultiplier	2050 V
ratio m/z	40-200

3.2.   Flux measurements

Two main approaches are commonly used to quantify fluxes of biogenic volatile organic compounds from the biosphere into the atmosphere. The first one is the cuvette technique where parts of the ecosystem, whole plants, or plant parts are enclosed in chambers or bags and the emission is determined from concentration chances over time in the known volume of the cuvette system (Guenther et al., 1996; Grabmer et al., 2006; Bouvier-Brown et al., 2009). The enclosure methods are inherently limited since the conditions in the cuvettes can differ strongly from the ambient air conditions, likely impacting the observed VOC fluxes. In addition, every plant is an individual, and even between different leaves of the same age and species the emissions factors can vary strongly (Bäck et al., 2011). Furthermore, VOC emission factors of leaves can be influenced by the light environment the leaves have been exposed to throughout their development, so that shade leaves and sun leaves can have different VOC emission characteristics, even at the same light exposure (Kesselmeier and Staudt, 1999). For these reasons, it is challenging to derive ecosystem scale flux estimates on the basis of enclosure measurements. Further, due to logistical problems in VOC sampling and system maintenance, cuvette measurements are hard to operate for continuous long term flux observations and statistically sound ecosystem scale fluxes can usually only be achieved if a large number of chambers are used (Davidson et al., 2002).

A more direct way to estimate ecosystem scale trace gas fluxes is to use micrometeorological techniques (for a summary see e.g., Baldocchi et al., 1988; Foken, 2006). These are *in-situ* techniques, which do not alter the observed environment, provide information about area integrated fluxes between biosphere and atmosphere, and are relatively easy to employ for continuous measurements. With these methods the atmospheric concentration above an ecosystem is measured and area-averaged fluxes are calculated from this value. If fast gas sensors are available (i.e. frequency response > 1 Hz), the eddy covariance technique (Kaimal and Finnigan, 1994; Foken, 2006; Aubinet et al., 2012) can be used.

This method has been successfully applied for measurements of vertical fluxes of a variety of scalar species, including water, CO_2, methane, ozone, NO_x, energy (e.g., Baldocchi et al., 2001; Rinne et al., 2007), and BioVOCs like isoprene (e.g., Guenther and Hills, 1998).

If no fast sensors are available to fully capture small eddies of the turbulent transport, micrometeorological methods derived from the eddy covariance technique, e.g. relaxed eddy accumulation (Graus et al., 2006) and disjunct eddy covariance (Grabmer et al., 2004) combined with proton transfer reaction-mass spectrometry (PTR-MS) can also be applied for measuring the flux of the sum of monoterpenes (e.g. Grabmer et al., 2004; Ruuskanen et al., 2005; Langford et al., 2010). In the present work the air concentrations and the emissions of individual monoterpenes are of great interest, which are not distinguishable in the PTR-MS method. Furthermore, the remote site with its limitations in power supply and strict nature protection guidelines of the Bavarian Forest National Park does not allow employing this extensive technique.

A common, low power approach to quantify fluxes of individual volatile organic compounds on ecosystem scales is based on the assumed proportionality of gradients and fluxes, explained in the following section.

3.2.1.   Gradient technique

The micrometeorological gradient technique derives from the well understood theories of diffusive transport. In molecular diffusion the flux is proportional to the gradient of a substance (Fick´s first law of diffusion, see e.g. Atkins, 1986):

$$J = -D \frac{\delta c}{\delta x} \tag{8}$$

where J is the diffusive flux of a substance c (e.g. in mol m^{-2} s^{-1}), c the concentration (e.g. in mol m^{-3}), x the position (in meter), and D the diffusion coefficient (m^2 s^{-1}).

With the assumption that the turbulent transport in the atmosphere follows similar laws (not valid in all cases, see e.g. Kaimal and Finnigan, 1994), a proportionality of the turbulent flux (F) and a corresponding variable (ξ) can be proposed:

$$F = -K_S \frac{\delta \xi}{\delta z} \tag{9}$$

In this case K is called eddy diffusivity or turbulent transfer coefficient and z is the measurement height. K was determined in this work by two different ways explained in the following chapters.

3.2.1.1.   The surface layer gradient technique (SLG)

Andrei Monin and Alexander Obukhov generalized a relationship between the vertical mean gradient and turbulence properties within the atmospheric surface layer (Monin and Obukhov, 1954). Their similarity theory predicts that the atmospheric flux gradient relationship can be described as dimensionless universal stability functions φ of the four fundamental scaling variables (u_*, friction velocity; H, kinematic virtual heat flux at the surface; g/T, buoyancy parameter, where g is gravitational acceleration and T is virtual temperature; z, effective height over ground) (e.g., Fuentes et al., 1996):

$$F = \frac{\kappa z u_*}{\varphi(\frac{z}{L})} \frac{\delta \xi}{\delta z} = -K_S \frac{\delta \xi}{\delta z} \tag{10}$$

where F is the flux, ξ the corresponding scalar and κ the von Kármán constant (0.4). The so called universal functions φ characterize the stratification depending on the stability parameter z/L, where L is the Obukhov length:

$$L = -\frac{u_*^3}{\kappa \frac{g}{T} H} \tag{11}$$

The ratio z/L is negative for unstable conditions, positive for stable conditions and near zero in the neutral case.

In this work the universal functions based on Businger (1971) in the modification of Högström (1988) were used to quantify turbulence exchange:

$$\varphi_{(H)} = 0.95(1 - 11.6(\frac{z}{L}))^{-0.5}$$

in unstable conditions (z/L < 0)   (12)

$$\varphi_{(H)} = 0.95 + 7.8(\frac{z}{L})$$

in stable conditions (z/L ≥ 0)   (13)

These functions have a value near 1 for neutral stratification and vary above and below 1 for stable and unstable conditions, respectively. For very strong stability (*z/L* >> 1) the universal functions are nearly constant and the exchange is usually underestimated (Foken, 2006). Therefore, the VOC flux is calculated only for a range of -2<z/L<2.

To describe the turbulence close to the surface properly, the so called zero-plane displacement (d) is introduced, which allows an upward shift of the exchange plane by surface roughness elements. The measurement height z is replaced by (z-d) for a better characterization of the flow close to the surface (see section 3.2.1.2 for a method to determine d).

Measuring the scalar ξ at two heights z_1 and z_2, the integration of equation 9, including the zero-plane displacement, leads to:

$$F = \frac{\kappa u_*(\xi_2 - \xi_1)}{\ln(\frac{z_2 - d}{z_1 - d}) - \Phi_2 + \Phi_1} = \lambda(\xi_2 - \xi_1) \qquad (14)$$

where λ is the atmospheric bulk conductance, ξ_1 and ξ_2 are the scalars, and Φ_1 and Φ_2 the integrated forms of the universal function at height z_1-d and z_2-d, respectively. The integrated universal functions have to be analyzed case-by-case according to the stability:

$$\Phi = 2\ln\left| \frac{1 + 0.95[1 - 11.6(\frac{z}{L})]^{0.5}}{2} \right|$$

in unstable conditions (z/L < 0)   (15)

$$\Phi = -7.8(\frac{z}{L})$$

in stable conditions (z/L ≥ 0)   (16)

With equations 14, 15 and 16 and the hypothesis that fluxes in the surface layer are uniform with height, the exchange rate of a scalar can be calculated from its gradient measured by available slow sensors and micrometeorological parameters determined by fast eddy covariance measurements. This approach has been used successfully to quantify fluxes of volatile organic compounds on ecosystem scales (e.g., Fuentes et al., 1996; Steinbrecher et al., 2000; Rinne et al., 2000; Simon et al., 2005; Kuhn et al., 2007).

3.2.1.2. Determination of the zero plane displacement from logarithmic wind profiles

The roughness of a surface has a strong influence on the atmospheric turbulent exchange above the area. Obstacles on the ground lead to an upward shifting of the zero-level to a new, "effective" level of the momentum sink. The horizontal wind speed becomes zero not directly at the surface but displaced at a certain height above ground. This height is characterized by the roughness length (z_0) and the zero-plane displacement height (d) (Figure 47).
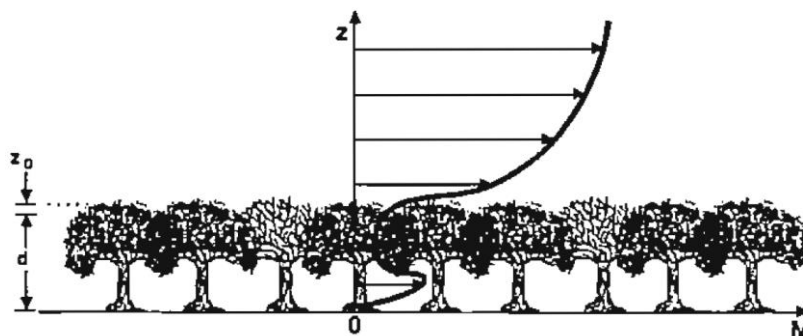
Figure 47: Air flow over a forest canopy showing wind speed M, as a function of height z. The canopy layer acts as a surface displaced a distance d above the true surface. z_0 = roughness length. (Picture from Stull, 1988, p.381).

Where the vegetation is dense, the zero-plane displacement height d is not the true surface, but somewhere in the vegetation canopy, because the wind flow is displaced upward. The displacement height is typically about two-thirds of the average height of the top of the canopy (Foken, 2006). This common approximation cannot be used in the case of a wind-throw area. Here the obstacles are very inhomogeneously distributed in the area, with wide gaps in between and the parameters d and z_0 must be determined from the logarithmic wind profile (Figure 48). In this case, the

y−intercept of the curve is the sum of the roughness length z_0 and the displacement height d.
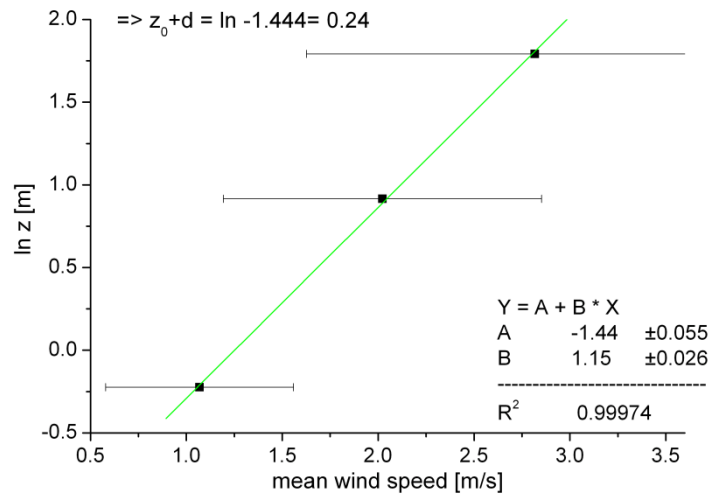
Figure 48: Logarithmic wind profile at the station Lackenberg (Data from 30.04.2009 – 21. 10 2009). Wind speed measurements at 0.8, 2.5 and 6 m above ground. Horizontal bars represent the range of wind speed during this period.

The value for the sum of z_0 + d is slightly decreasing with increasing turbulence (0.26 m for u^* = 0.2-0.3 m/s, 0.25 m for u^* = 0.3-0.35 m/s, 0.23 m for u^* = 0.35-0.45 m/s, 0.22 m for u^* = 0.45-0.65 m/s) and shows a small seasonal behavior due to the growing of the grass at the site and the so changed surface roughness. The sum of the displacement height and the roughness length is highest in the summer and considerably lower before and after the growing season (0.18; 0.23; 0.27; 0.26; 0.24 m for May, June, July, August, September). The lowest wind sensor (0.8 m) had to be removed in winter, due to the high snow cover.

The roughness length z_0 at the measurement site Lackenberg can be assumed to be similar to those from bush land, as the root plates are approximately equally high and distributed as isolated bushes. Typical values of z_0 over bush land are about 25 cm (Stull, 1988; Foken, 2006). As the sum of roughness length and zero-plane displacement (z_0+d) determined from the logarithmic wind profile is approximately 24 cm (Figure 48), the value of the zero-plane displacement d appears to be close to zero and was disregarded in this work.

3.2.1.3.   The modified Bowen Ratio Method (MBR)

Another indirect way to determine the transfer coefficient is the modified Bowen-ratio method (e.g., Businger, 1986; Goldstein et al., 1995; Meyers et al., 1996; Schween et

al., 1997; Helmig et al., 1998; Plaza et al., 2005; Fritsche et al., 2008). In this method it is assumed, that the exchange coefficients K of different scalars (e.g. for CO_2, H_2O, sensible heat and BioVOC) are equal in the atmospheric surface layer. Integration of equation (9) over a discrete layer for two scalars and the assumption of equal turbulent transfer coefficients leads to:

$$F_{\xi_y} = F_{\xi_x} \frac{\Delta \xi_y}{\Delta \xi_x} = \lambda_{\xi_x} \Delta \xi_y \tag{17}$$

In this case the vertical flux of the scalar of interest $F\xi_y$ is calculated from the measured flux of another scalar $F\xi_x$ (e.g. the flux of water, CO_2 and temperature measured by eddy covariance technique) and the concentration differences of these scalars $\Delta\xi_y$ and $\Delta\xi_x$ measured simultaneously over the same height interval. The height interval Δz is included in the bulk conductance λ.

An advantage of this technique is that different scalars and fluxes, providing the same information about atmospheric mixing processes, can be used to determine the flux of the target scalars, e.g. monoterpenes. For example, sensors of temperature usually have lower uncertainties than the ones of CO_2 and water, but under certain circumstances, e.g. in periods with neutral or slightly stable atmospheric stability conditions, measurement of temperature gradients can become very challenging. In this case, sometimes reliable gradients of other scalars are easier available. However, differences in concentrations between two heights have to be resolvable and must be determined very accurately. If these gradients are small, a large error can be introduced in the calculation of the flux. Application of the MBR method requires that the gradient of monoterpenes and at least one other scalar can be measured accurately enough. The modified Bowen ratio method to determine atmosphere-biosphere exchange rates has the advantage that potential uncertainties which can appear in the surface layer gradient approach introduced by surface parameters (e.g. roughness length, zero-plane displacement), are compensated in the calculation, because of cancellation

3.2.2. Uncertainties in the flux measurements

There are various sources of uncertainty in the quantification of the biosphere-atmosphere exchange rates of volatile organic compounds by micrometeorological

techniques. Errors in measured fluxes can result from uncertainties of gas and temperature sensors, air samplers, GC analysis, and from violating the required micrometeorological assumptions. The second type of uncertainty includes errors caused by changes of the concentration of a scalar in the measurement volume over time, advection and horizontal inhomogeneity leading to horizontal gradients, and artificial vertical gradients produced by non-stationarity. These fake vertical gradients are caused by temporal trends in the scalar concentration and can particularly affect the results if the gradient is not measured simultaneously at both heights (Walker et al., 2006). In this work the concentrations of CO_2 and H_2O were measured intermittently (in a time switching mode between the two heights, measured with one sensor) and the monoterpene concentrations and air temperatures were concurrently sampled (simultaneously measured at the two heights with two instruments).

Errors related to concentration changes over time (storage in the volume) should not influence the flux measurement strongly in this work, since the canopy is not closed and a generally high turbulence (average u* of 0.38 m/s and 0.37 m/s in the years 2009 and 2010) leads to a good mixing of the air volume down to the ground.

While advection is very difficult to estimate (e.g., Aubinet et al., 2010), there is some evidence that the problem of horizontal gradients is likely of minor importance at the Lackenberg site. The wind-throw area exhibits a good homogeneity at the footprint scale (Figure 17), so vertical fluxes from different parts of the site should be approximately the same. Another indication for the fulfillment of micrometeorological requirements is the closure of the energy balance. If this closure is 100%, the sum of the turbulent fluxes of latent (LvE) and sensible heat (HTs) equals the sum of available energy, i.e. the net radiation (R_{net}) minus the soil heat flux (G).

$$R_{net} = HTs + LvE + G \qquad\qquad (18)$$

Typically, a closure of the energy balance of approximately 80% is found over land surfaces (Foken, 2008). At the site Lackenberg the closure was 85% in the year 2009 and 2010 (Figure 49). The values of the sensible and latent heat fluxes are measured by the eddy covariance system which detects only turbulent fluxes while the radiation and soil heat flux is determined by slow sensors. The good agreement of these two independent ways to calculate the energy balance indicates an excellent suitability of the site for micrometeorological flux measurements.
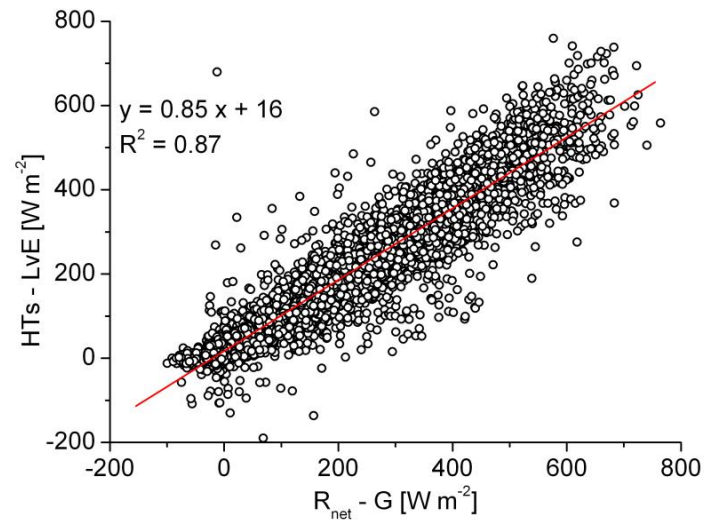
Figure 49. Energy balance at the site Lackenberg in the years 2009 and 2010. R_{net} = net radiation, G = soil heat flux, HTs = sensible heat, LvE = latent heat. The red line is the orthogonal regression.

Another way to asses if the sensor technology at the Lackenberg site is applied correctly, is to plot the wind direction against the Bowen ratio (ratio of sensible heat (HTs) to latent heat (LvE)).
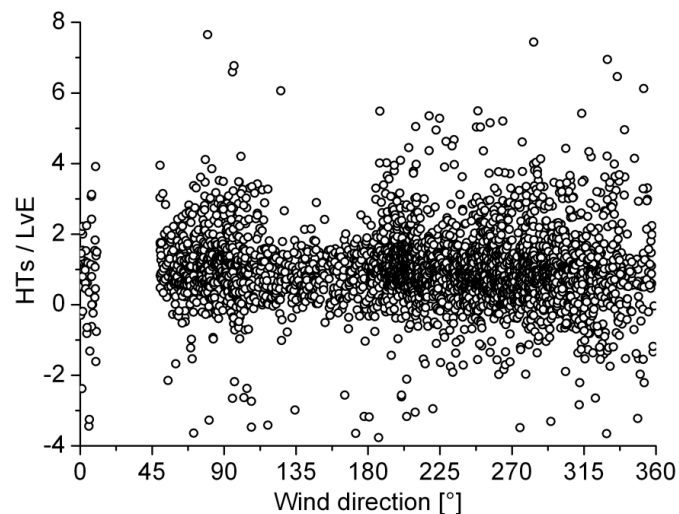
Figure 50. Wind direction dependent Bowen ratio. Data is selected according to wind disturbances by the mast (wind direction 10 - 50 °) and micrometeorological criteria (u* > 0.2 m/s).

The Bowen ratio is independent of the wind direction (Figure 50), which means the sources of water vapor and sensible heat are approximately uniformly distributed in the measurement area, and the terrain is homogeneous; thus micrometeorological techniques can be employed to calculate gas exchanges.

The errors caused by intermittent sampling of the ambient concentrations of H_2O and CO_2 are quantified by placing the inlets of the sensor at the same height for two days (Figure 51). Any differences in the measured concentration of the two inlets are then

due to analytical and systematical errors of the sensor plus an artificial gradient caused by temporal trends. In the present work the time specification is general in Coordinated Universal Time (UTC). The small shift to the Central European Time (CET), which is valid at the measurement stations, of one hour has to be kept in mind for daily variations particularly of the radiation.
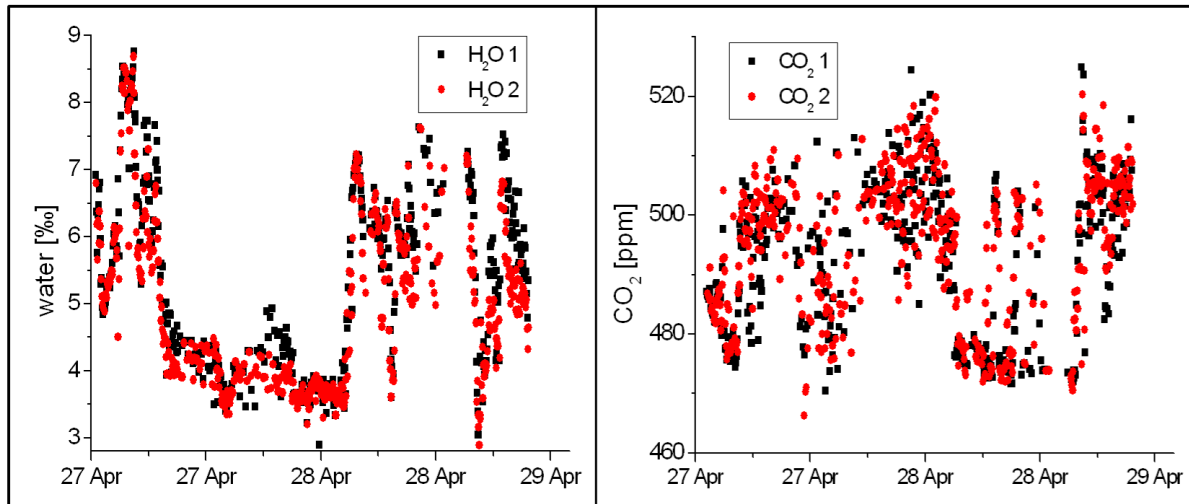
Figure 51. H_2O (left) and CO_2 (right) mixing ratios at the Lackenberg site. Both inlets at 1.4 m above ground. Data collected in two-minute-steps and averaged to two minutes each from 27.4.2011 12:00 h - 29.4.2011 7:30 h (UTC).

The relative analytical precision of the sensor (Li-840) was determined to be 1% for CO_2 and 4% for H_2O. The total uncertainty of the intermittent sampling at two minute intervals was calculated from the difference of the measurements of the two inlets at the same height to be 0.4 mmol/mol for H_2O and 5 µmol/mol for CO_2.

Plots of the measured mixing ratios of the two inlets against each other (Figure 52) showed no bias towards one of the sample heights. The measurement values of inlet 1 and inlet 2 were combined in 60 minute means, as used in the data processing to quantify fluxes.
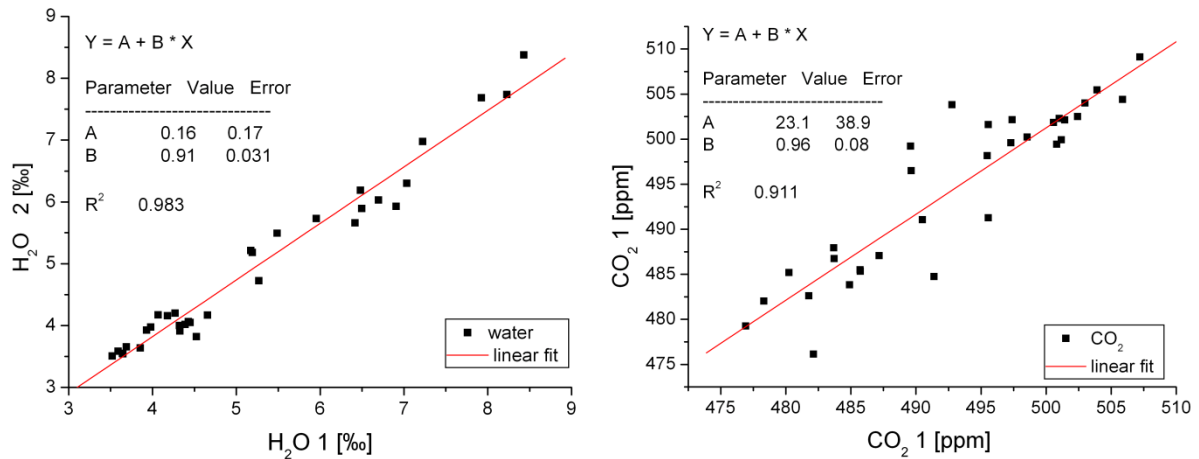
Figure 52. 60 minutes mean value of the mixing ratios of water (left) and CO_2 (right) at the inlet 1 and inlet 2 at the Lackenberg 27.4.2011 12:00 h - 29.4.2011 7:00 h (UTC). Both inlets at 1.4 m above ground.

Temperatures and VOC mixing ratios were determined in a concurrent sampling at the two heights, thus the error of these gradients is not influenced by intermittent sampling and only depending on the precision of the sensors. The temperature sensors and inlets of the VOC auto-samplers were placed at the same heights of 1.4 meter above ground and the uncertainty assessed by comparing the resulting values.
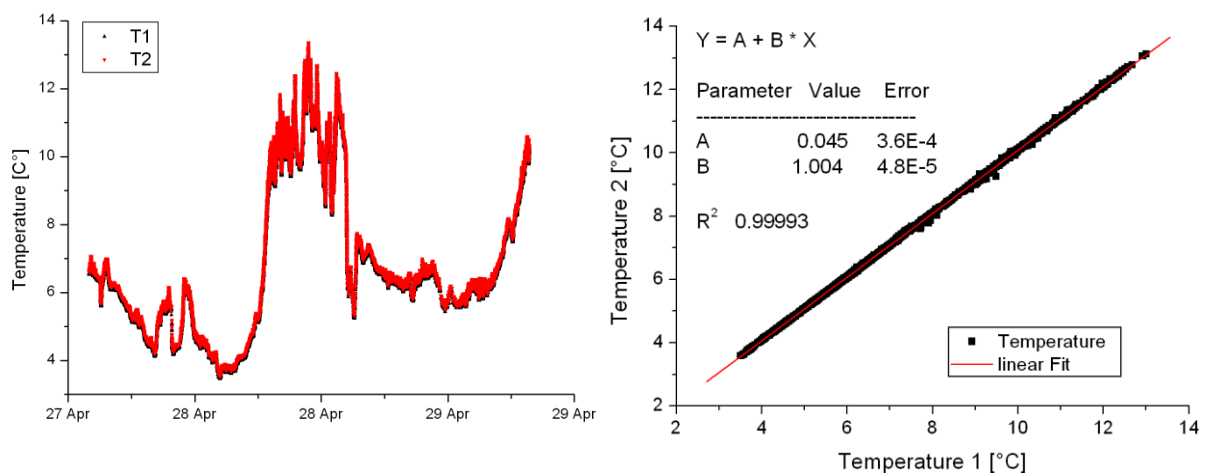
Figure 53. Temperature at the Lackenberg site. Data of both sensors (1 and 2) at 1.4 m above ground (left) and plotted against each other (right). Data collected in two-seconds-steps from 27.4.2011 14:00 h - 29.4.2011 7:30 h (UTC).

The temperature curves of both sensors match almost perfectly (Figure 53 left) and the uncertainty was calculated to 0.05°C. There seems to be a little bias of 0.045°C towards sensor 2 (Figure 53 right).

The VOC air concentrations collected with two auto-samplers at the same heights and analyzed with Δ^2-carene as internal standard showed a good agreement with almost no bias towards one sampler (e.g., α-pinene in Figure 54). The total error of the gradient determination of α-pinene results from the difference of the concentration between both heights to be 0.025 ng/l or 5% at average concentrations. Measurement in the laboratory under controlled conditions validated the results and showed a slightly better agreement between both samplers in a concentration range of 40 - 300 ng/l (30 sample pairs, B=0.997).
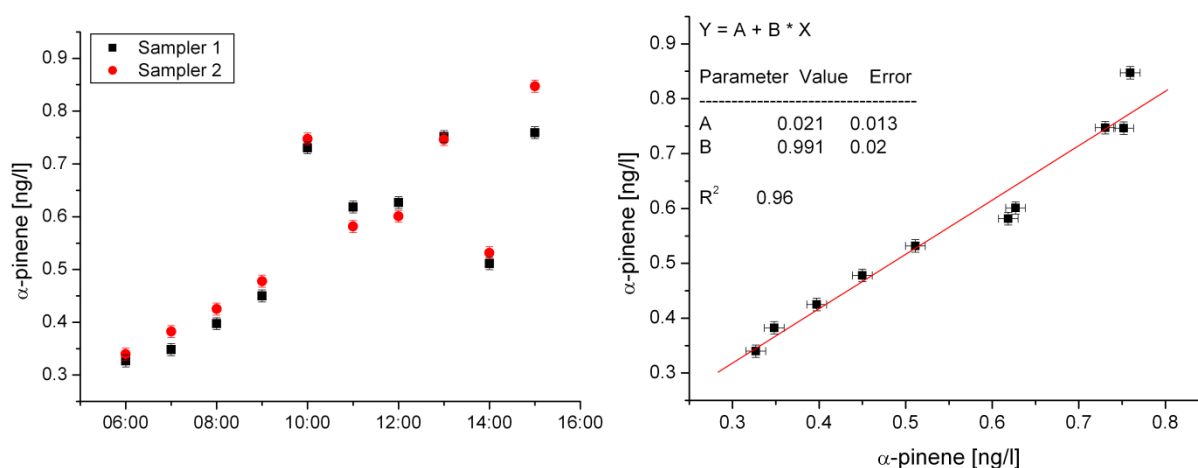
Figure 54. Air concentrations of α-pinene at the Lackenberg collected with two samplers at the same height of 1.4 m above ground (left) and plotted against each other (right). Data from 08.06.2010. Sampling time 60 minutes, sampling flow 180 ml/min.

All uncertainties of the variables used to determine monoterpene fluxes by the modified Bowen ratio method are listed in Table 20 and Table 21. The confidence interval used in this work is in general 68.3% (1σ).

Table 20. Precision of monoterpene gradients determined from 20 sample pairs at the 08.06.2010 and 27.04.2011 at the Lackenberg. Inlet height 1.4 m, loading 60 min, flow 180 ml/min.

	eucalyptol	β-pinene	camphene	Δ^3-carene	limonene	p-cymene	α-pinene
absolute error [ng/l]	0.09	0.030	0.0017	0.006	0.024	0.005	0.025
relative error [%]	34	8	5	10	68	14	4
mean value [ng/l]	0.26	0.37	0.033	0.06	0.035	0.037	0.57

Table 21. Precision of the gradients of H_2O, CO_2 and temperature at the Lackenberg. Measurement height 1.4 m. Data from 27.04.2011. * Precision of fluxes (HTs = sensible heat, LvE = latent heat) taken from Mauder et al. 2006.

	ΔH_2O	ΔCO_2	ΔT	LvE *	HTs *
absolute error	0.4 [mmol/mol]	5 [µmol/mol]	0.05 [K]	30 [W/m²]	20 [W/m²]
relative error [%]	6.9	1.0	0.5	15	10
mean value	5.8 [mmol/mol]	500 [µmol/mol]	10 [K]		

To determine valid bulk gradients, the differences at the two heights of all variables must be larger than the absolute errors listed in Table 20 and Table 20, which is difficult particularly in the case of water, CO_2 and some of the monoterpenes (eucalyptol and limonene).

The error of the measured monoterpene flux (δF_{MT}) is calculated by Gaussian error propagation of equation (17).

$$\delta F_{MT} = \left[\left(\frac{\Delta MT}{\Delta x} \delta F_x \right)^2 + \left(\frac{F_x}{\Delta x} \delta \Delta MT \right)^2 + \left(\frac{F_x \Delta MT}{(\Delta x)^2} \delta \Delta x \right)^2 \right]^{1/2} \tag{19}$$

where F_{MT} is the flux and ΔMT the gradient of a monoterpene and F_x and Δx the flux and gradient of another scalar (CO_2, H_2O, temperature). In addition to this uncertainty caused by measurement errors, systematic errors due to the implicit assumptions of the eddy covariance technique and K-theory are possible; but these are very hard to quantify (e.g., Moncrieff et al., 1996; Schmid et al., 2003).

3.2.3. Transport times and reactivities of the investigated volatile organic compounds

The methods for the quantification of vertical fluxes described in the chapters above are in general valid only for inert gases. To investigate whether the reactivity of the VOCs in the atmosphere has to be taken into account, the maximum transport time of the volatiles in the wind-throw has to be compared to their atmospheric lifetimes. If the ratio of the characteristic chemical reaction time to the transport time (Damköhler number) is much smaller than one, the influence of degradation of the reactive

volatiles on the flux measurement is negligible. The transport time can be calculated by integrating the logarithmic horizontal wind profile $u_{(z)}$ over the heights z_0 to z_1:

$$\int_{z_0}^{z_1} u(z)\, dz = \int_{z_0}^{z_1} \frac{u*}{k} \ln\left(\frac{z}{z_0}\right) dz = \frac{u*}{k}\left(\frac{z_1}{z_1 - z_0}\left(\ln\left(\frac{z_1}{z_0}\right) - 1\right)\right) \tag{20}$$

Inserting the average friction velocity (u*=0.35 m/s) and the two heights (z_0 = 0.25 m, z_1 = 7.2 m) leads to a mean transport speed of 2.14 m/s. The maximum transport length is the distance from the main tower to the boundary of the wind-throw (420 m), since this is the maximal fetch area allowed for the calculation of fluxes. This is a very conservative consideration, since the maximal transport time (transport time from the boundary of the wind-throw to the EC sensors) is calculated. The resulting transport time of approximately 3.3 minutes (including vertical and horizontal transport) is considerably smaller than the atmospheric lifetimes of the VOC (Table 3). Damköhler numbers (τ_T/τ_R) are between 0.09 (terpinolene) and 0.002 (eucalyptol) if the reaction rates for monoterpenes with OH are considered. The reaction times of VOCs with ozone in the atmosphere are generally even slower than those with OH. Therefore, it is justified to treat the investigated biogenic volatile organic compounds as non-reactive compounds in the calculation of their ecosystem exchange rates.

3.2.4. Data processing

3.2.4.1. Data processing of the eddy covariance measurements

The raw data of the eddy covariance sensors described in section 2.1.5 were stored to a CR3000 data logger, automatically copied to an embedded industrial PC and there split into hourly files (split program provided by Danilo Dragoni, Indiana University). These data are processed with the software package TK3 (modified according to Mauder et al., 2006). An overview of the processing scheme is given in Figure 55.
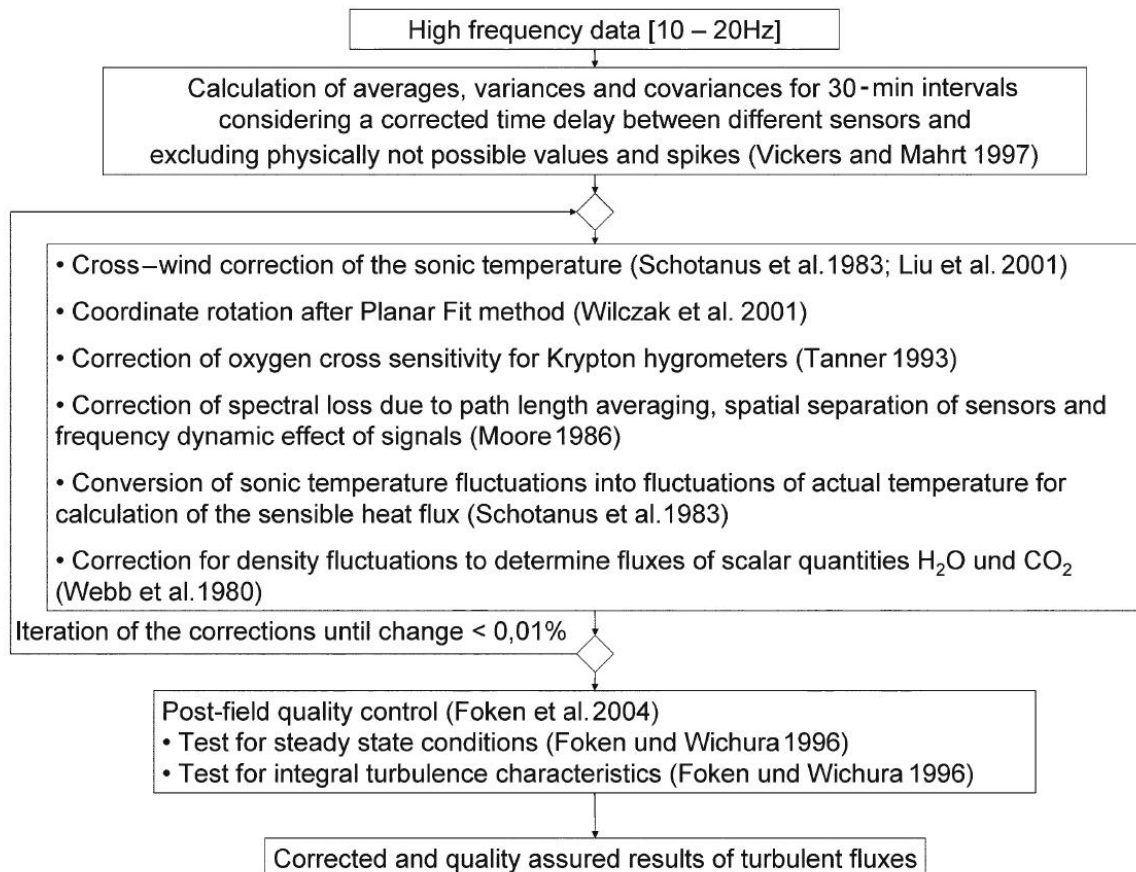
Figure 55. Processing scheme of the software package TK (Mauder et al., 2006).

3.2.4.2.   Data processing of the modified Bowen ratio

Raw data of the gradient system are collected at time intervals of two seconds by a second CR3000 data logger. The data are processed according to Figure 56. Values outside of a range of two minute averages plus/minus 2.5 times the standard deviation are excluded (despiking). The average hourly difference in the temperature between 1.4 m and 7.2 m is directly used in the modified Bowen ratio method. Since the mixing ratios of CO_2 and water are determined by one sensor for both heights with a switching between the inlets every two minutes, no consistent time series for these variables is available. The gradient is therefore calculated by the difference of these two-minute-means averaged over one hour. The first value in each two-minute-interval is discarded due to the time needed to flush the dead volume (ca. 0.5 s at a flow rate of 350 ml/min and a dead volume of approximately 3 ml) inside the experimental set-up after a switching of the valves.

| CO$_2$ and H$_2$O [2s] | Temperature [2s] | Monoterpene [1h] |

Despiking

Calculating gradients from the hourly averages between the two heights

Determination of monoterpene flux from the hourly gradients of a monoterpene and another scalar (CO$_2$, H$_2$O, T) and its corresponding flux

Data rejected if:
• Footprint of the eddy fluxes < 75 % in the windthrow area (Kormann and Meixner, 2001)
• flags of the eddy fluxes > 6 (Foken and Wichura, 1996)
• gradients above detection limit

Figure 56. Data processing scheme used in the modified Bowen ratio approach for calculating ecosystem monoterpene fluxes. See text for details.

Fluxes of monoterpenes are calculated according to equation 17 if the data meet the quality criteria (Figure 55 and Figure 56), the stability parameter z/L is between -2 and 2 indicating not too strong stability or free convection, and the friction velocity is higher than 0.2 m/s to ensure turbulent conditions.

4. Results and discussion

In the first section the results of the analysis of monoterpene levels in ambient air above the wind-throw areas at the sites Lackenberg and Kühroint are presented in relation to the diurnal and seasonal cycle of meteorological data. The second part focuses on investigations at the site Lackenberg with monoterpene fluxes determined by the modified Bowen ration method and surface layer gradient technique and their dependence on meteorological parameters. Finally an empirical model for estimating the wind-throw specific monoterpene emission was derived and employed to calculate annual emission budgets of monoterpenes at the wind-throw area Lackenberg.

4.1. Monoterpene levels in ambient air at the Lackenberg site

Between 20.07.2009 and 28.09.2011 a total of 281 ambient air samples from 21 measurement days were collected on adsorption tubes and analyzed in the laboratory by GC-MS regarding their monoterpene content. Fifteen of these samples were discarded from further processing due to sampling or analysis errors (e.g. leaking of tubes).

Table 22. Maxima of measured mol fractions per measurement day of the most abundant monoterpenes and surface temperatures at the Lackenberg site. Limits of detection of individual monoterpenes are listed in Table 18.

	maximum mol fraction [pmol/mol]							number of samples	maximum surface temperature
	eucalyptol	β-pinene	camphene	Δ^3-carene	limonene	p-cymene	α-pinene		
22.07.2009	20.0	250.0	30.0	25.0	8.0	5.0	320.0	10	31.4
18.08.2009	9.0	/	9.5	16.0	4.7	2.5	81.0	10	28.4
19.11.2009	6.0	13.5	/	/	10.4	0.8	18.4	10	17.5
26.02.2010	1.0	2.2	0.0	0.0	0.0	0.0	1.2	1	0
25.03.2010	12.7	24.5	3.0	2.5	10.0	3.1	28.4	10	5
09.06.2010	64.7	87.0	6.8	11.8	12.6	8.6	125.0	10	29.2
10.06.2010	88.6	221.6	12.3	24.2	25.4	11.2	281.0	10	30.0
07.07.2010	12.9	30.2	2.2	5.2	4.0	2.9	46.8	20	21.8
08.07.2010	22.4	103.1	7.1	15.9	3.9	8.0	112.8	20	20.6
09.07.2010	28.4	85.9	5.9	12.3	6.8	9.7	103.7	10	29.3
22.07.2010	38.1	178.2	17.7	37.1	4.8	4.8	192.1	10	28.5
18.09.2010	7.5	7.8	1.4	1.3	1.9	2.2	15.5	16	12.2
19.09.2010	5.7	16.0	1.5	1.6	1.2	3.9	15.3	16	14.5
20.09.2010	7.3	17.9	2.0	3.1	2.4	1.6	26.4	16	17.6
15.02.2011	4.0	2.5	0.7	1.8	0.0	6.0	6.2	4	0.5
28.04.2011	28.1	13.2	2.3	4.0	5.2	11.1	27.9	20	14.7
15.06.2011	37.2	57.9	0.0	10.3	2.1	6.2	62.7	20	20.6
16.06.2011	29.0	50.0	0.0	5.5	3.8	9.0	43.4	20	22.6
12.07.2011	62.3	170.2	0.0	34.2	2.0	8.4	147.0	20	23.7
03.08.2011	42.1	66.4	0.0	14.4	5.8	29.5	51.8	20	25.5
28.09.2011	16.4	36.8	0.0	7.3	0.0	19.4	41.5	8	21.2

Major substances in the investigation period were α- and β-pinene and eucalyptol with a mean fraction of 35.1%, 30.0% and 21.6% of the total monoterpene load in air (Figure 57). Limonene, p-cymene, camphene and Δ^3-carene were present in most samples, but usually in lower concentrations. The highest monoterpene level was found at the 10th of June in 2009 with a mol fraction of 320 pmol/mol of α-pinene in the air. The highest total monoterpene burden was 655 pmol/mol at the same day between 17:30 h and 18:30 h (UTC). Other monoterpenes which occurred very rarely in ambient air were β-phellandrene, β-terpinene and α-thujene.
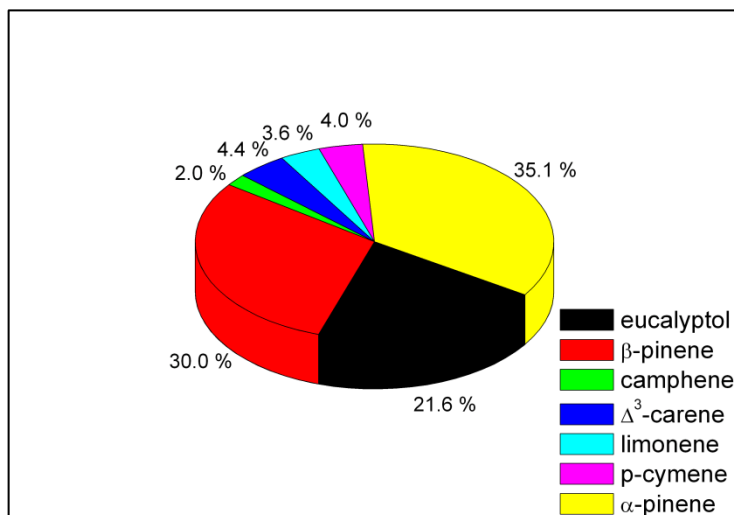
Figure 57. Monoterpene composition of ambient air at the station Lackenberg. Average from all data collected 2009-2011 (see Table 22).

The monoterpene air composition above the wind-throw area was quite similar in the years 2010 and 2011 (Figure 58). The standard deviations of each value were in any case higher than the observed differences. A Student´s t-test showed no significant differences in the means of the years 2010 and 2011 for any monoterpene with a confidence level of 99%.
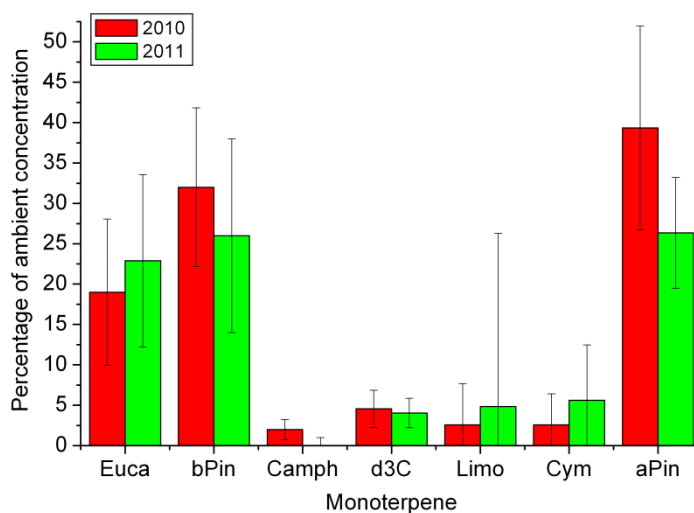
Figure 58. Mean percentages and standard deviations of the average monoterpene concentrations at the Lackenberg in 2010 and 2011. 85 concentration measurements in 2010; 58 in 2011. Euca = eucalyptol; bPin = β-pinene; Camph = camphene; d3C = Δ^3-carene; Limo = limonene; Cym = p-cymene; aPin = α-pinene.

4.1.1. The daily variation of the monoterpene air concentration at the Lackenberg

The levels of monoterpenes in ambient air at the Lackenberg generally showed a maximum around noon or afternoon and a minimum during the night. Night-time minima are usually below 10 pmol/mol. A typical daily cycle of the mol fraction of monoterpenes on a warm summer day (mean air temperature: 14.8 °C; max. 18.5°C; min. 12.2°C) is shown in Figure 59.
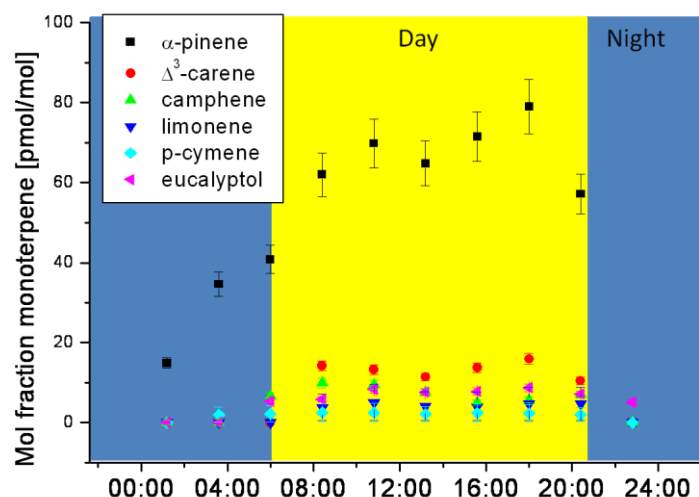
Figure 59. Mol fractions of different monoterpenes at the Lackenberg site 18.08.2009. Sampling flow 184 ml/min; sampling time 143 min. Time is UTC.

The wind direction at the measurement day was constantly from westerly direction (90% of the total wind directions between 240° and 320°, Figure 60 left). The wind speed displayed a higher variability, but was relatively constant during the daytime (03:00-19:30: mean 2.1 m/s; max. 3.5 m/s; min. 1.2m/s; 73% of the wind speed between 1.5 m/s and 2.5 m/s; Figure 60 right). Influences of a changing source area of monoterpenes on the observed air concentrations due to different wind characteristics should not be very high in this time period of the day. Furthermore, the terrain is very homogeneous on a footprint scale (see chapter 3.2.2 and pictures in chapter 2.1.2). The wind characteristic during the day was very typical for the central station at the Lackenberg (see Figure 30).
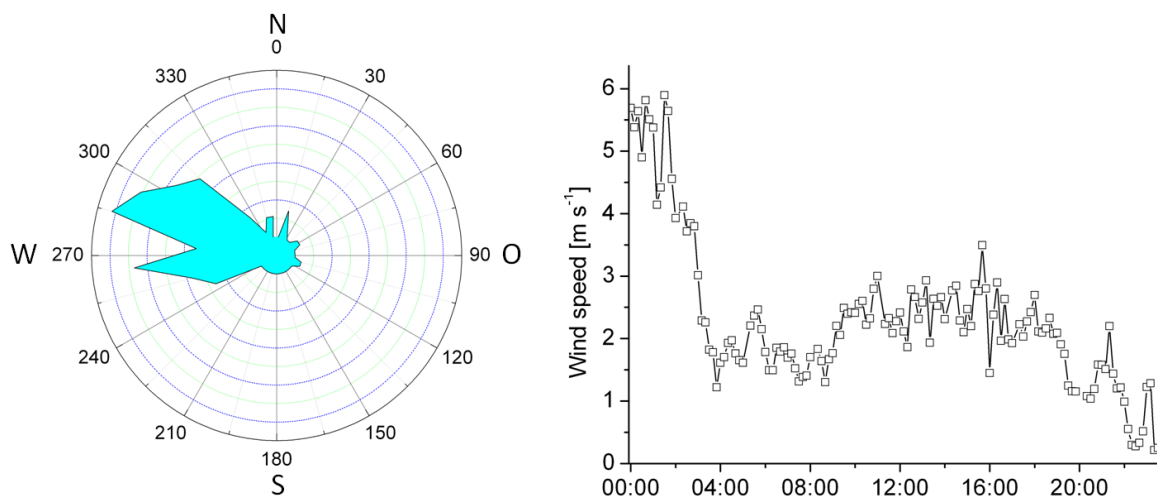
Figure 60. Wind characteristic at the Lackenberg 18.08.2009. Time is UTC.

The diurnal behavior suggests a comparison of monoterpene air concentrations and micrometeorological parameters following a similar daily cycle. These are mainly the air temperature, the surface temperature, the soil temperature and the incoming radiations (photosynthetic active radiation, short and long wave radiation) (Figure 61). The highest surface temperatures were observed between 10 a.m. and 17 p.m (UTC), while the soil and the air temperature was very stable during this day, reaching a small maximum in the evening (ca. 18 p.m.). The incoming shortwave radiation showed a daily cycle very similar to that of the radiation surface temperature. The incoming long wave radiation displayed an unusual behavior, with a pronounced maximum during the night/early morning and a scattered course during the day. This is an indication of dense clouds reflecting the long wave radiation in the night.

Figure 61. Meteorology at the Lackenberg 18.08.2009. Time scale (x-axis) is UTC. Upper left: Air (black), surface (red) and soil temperature (green); Soil temperature was measured at 4 cm below ground, air temperature at 6 m above ground. Upper right: Photosynthetic active radiation (PAR). Down: Long (black) and short wave (blue) incoming radiation.
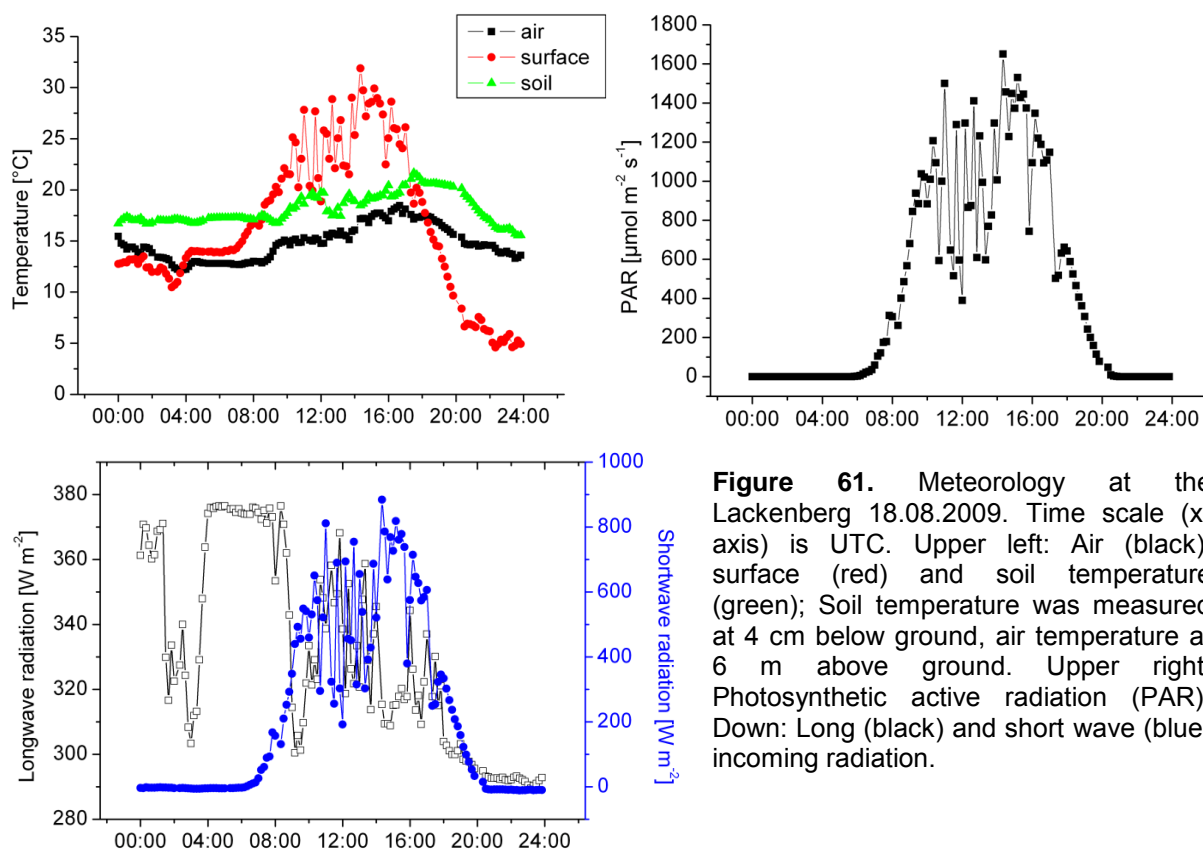
All these selected meteorological parameters provide an energy input in the observed ecosystem (long and short wave radiation, PAR) or are an indication for its energy content (air, surface and soil temperature). The level of the most abundant monoterpene α-pinene correlates best with the surface temperature when using an exponential fit (Figure 62).
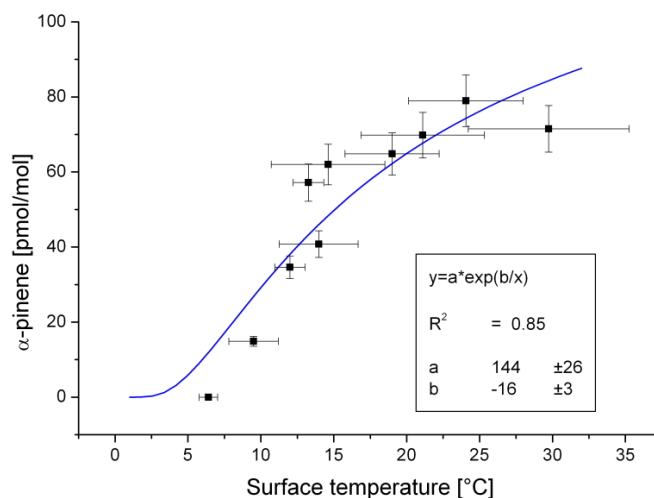
Figure 62. Relation of the mol fraction of α-pinene in ambient air and the surface temperature at the Lackenberg 18.08.2009.

85% of the observed variation of the α-pinene mol fractions in the air at this day can be explained by a simple exponential fit using the surface temperature as the determining parameter (Figure 62). The comparison with other prospective meteorological parameters results in a lower fit of the data (Table 23). These meteorological parameters are obviously not independent from each other, particularly the surface temperature not from the air temperature and the incoming radiations (Table 23). So a correlation of the levels of monoterpene in the air with most parameters is explicable. Especially the photosynthetic active radiation (PCC = 0.925) and the short wave radiation (PCC = 0.926), which are highly correlated to the surface temperature at this day, can also explain a large part of the variation in the measured α-pinene level (R^2 = 0.72 (PAR) and R^2 = 0.82 (R_G)). Divergences of the measured air concentrations from the theoretical exponential fit exist because mechanistically it is not the concentration that is depending on the surface temperature, but the emission. Transport, accumulation, or degradation processes of the monoterpenes in the boundary layer can decrease the correlation between radiation temperature and monoterpene levels.

Suppressed transport processes under stable atmospheric conditions combined with a low boundary layer height can lead to an enrichment of the monoterpenes in the measured air volume. At days with instable stratification and high turbulence the VOCs are rapidly transported to higher layers, so the measured monoterpene concentrations are lower than under average atmospheric conditions.

Table 23. Coefficient of determination of exponential fittings of the relation of mol fractions of α-pinene to meteorological parameters and correlation coefficients between these parameters at the Lackenberg 18.08.2009. ST = surface temperature; AT = air temperature; SoilT = soil temperature; PAR = photosynthetic active radiation; R_G = short wave incoming radiation; LIR = long wave incoming radiation. Pearson correlation coefficients were calculated by the statistics program SPSS (1 is perfect correlation, 0 is no correlation).

Parameter	ST	AT	SoilT	PAR	R_G	LIR
R^2	0.85	0.13	0.57	0.72	0.82	no correlation
Pearrson correlation coefficient to ST	1	0.58	0.46	0.925	0.926	0.175

Since no other relevant sources of monoterpenes were identified in the wind-throw area, the release of monoterpenes is expected to derive mainly from the dead wood. So contributions from living vegetation to monoterpene air levels should be negligible. The emission should take place directly from the dead wood on the ground, so the surface temperature (i.e. radiation temperature which integrates a large area of ground) represents this process best (see also chapter 2.5 for a comparison of stem temperature and radiation surface temperature). The observed exponential dependence of the α-pinene air concentration can be explained by the diffusion limited emission from the inner side of the stem through the bark into the atmosphere (Figure 63).
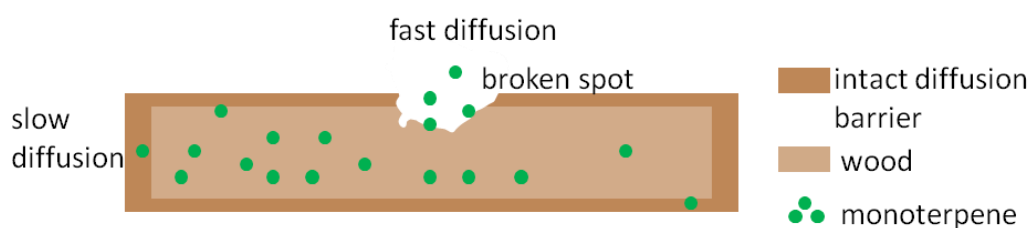
Figure 63. Scheme of the diffusion of monoterpenes from the dead wood into the atmosphere.

During the day the fallen trees are heated by the increasing radiation (surface temperature increases). In consequence, the vapor pressure of the monoterpenes in the resin vessels or resin ducts increases and the VOCs are easily released. The monoterpenes are supposed to be emitted through intact diffusion barriers (cell wall, bark), which represents a high diffusion resistance and also through damaged spots in the wood, in which the diffusion barrier is drastically reduced and the emission is enhanced. On a short term, these diffusion resistances can be assumed to be constant for the whole area, but might change considerably if large parts of the dead wood break, e.g. because of snow break or the own weight of the rotten stems.

In the night the trees are cooling down, the vapor pressure of the VOCs is reduced and almost no emission happens. The remaining monoterpenes in the air, which were emitted during the day are slowly transported into higher layers of the atmosphere (dilution) and are degraded by oxidants, so their level in the air decreases.

To analyze the effect of the surface temperature on the air concentration of α-pinene a graphic linearization can be employed (Figure 64). In this Arrhenius plot the natural logarithm of the mol fraction of α-pinene is plotted against the inverse of the surface temperature (in Kelvin). In the case of a perfect single rate-limited thermally activated

process the Arrhenius plot should give a straight line. The deviation of the measured air levels from the theoretical straight line indicates a non-first-order reaction kinetics. This deviation can be explained by the processes mentioned above (transport, accumulation, degradation), which cause a highly complex dependence of the air concentration of α-pinene on the surface temperature, which is only in the first approximation modeled by an empirical exponential equation.
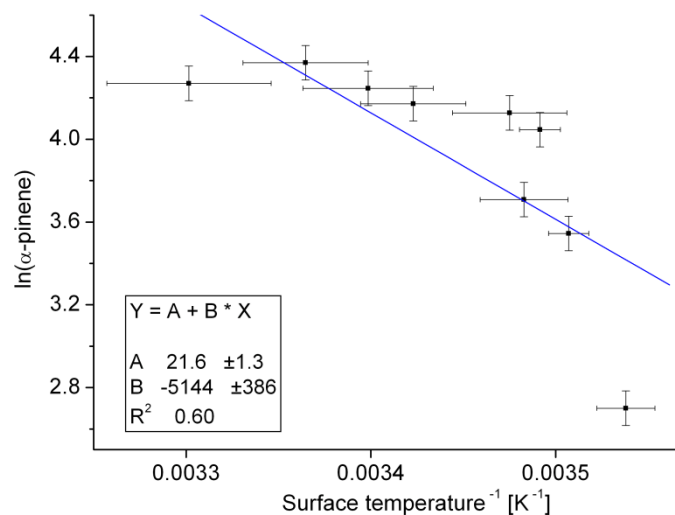
Figure 64. Arrhenius plot of the mol fraction of α-pinene and the surface temperature at the Lackenberg 18.08.2009. Error bars represent the uncertainty (1s) in the mol fraction of α-pinene (y-axis) and the range of the surface temperature during each measurement period (x-axis).

4.1.2. The variability of the monoterpene air concentration at the Lackenberg during the year

The annual variation of the measured volatile organic compounds showed a maximum in summer and almost no measurable amount of monoterpenes in the air during the cold season as expected (Figure 65). Highest measured daily monoterpene content was 372 ppt (pmol/mol) at the 10th of June in 2010. At nighttime the concentration of volatile organics in the air were very low even in summer. Measurements in the winter were especially challenging, because of the extreme weather conditions and the remote location of the station. A complete snow cover starts usually in the end of October and lasts until the beginning of April. This cover should further decrease the monoterpene concentration in the air, due to a suppressed emission from the dead wood material into the atmosphere. A possible emission peak of concentrated monoterpenes below and in the snow cover during snow melting periods (Starokozhev et al., 2009) could not be detected due to the

campaign based measurement approach. Because of the very low air concentrations at temperatures below 5 °C, this potential snow melting peak is not assumed to be considerably high.
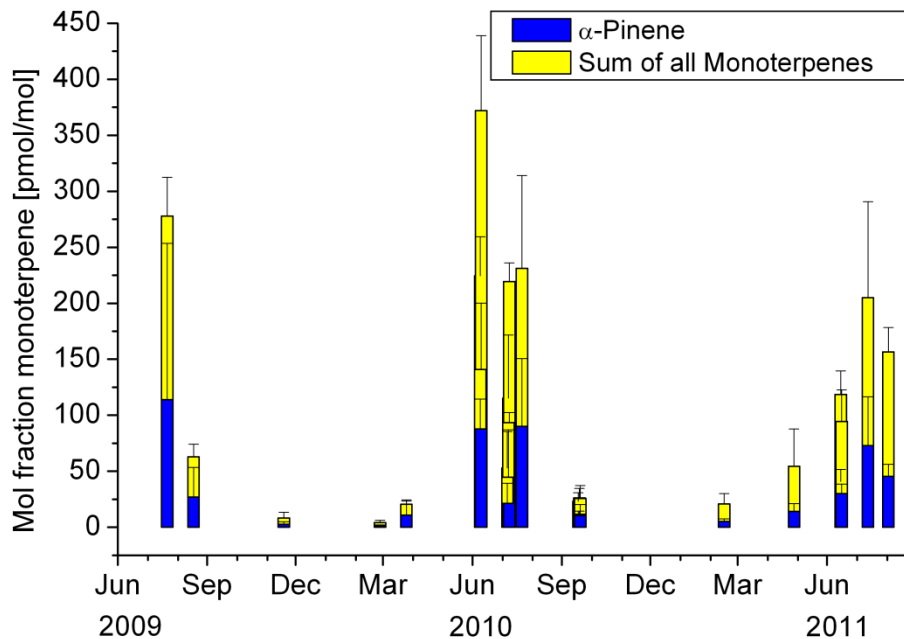
Figure 65. Measured daily mean monoterpene levels in ambient air at the Lackenberg in the years 2009 - 2011. Error bars represent the standard deviation at each day.

The terpenes stored inside the dead wood are not replenished, so their pool in the wind-throw area should slowly decrease over time, starting from the storm event. The overall air concentration measured above the wind-throw is thus supposed to decrease in the same period too. Monoterpene levels in the air above the wind-throw area were exponentially depending on the surface temperature. The slope of this dependence should decrease over the years because of this depletion of the monoterpene pool in the fallen trees. The measurements at the Lackenberg show this expected behavior in the years 2009 and 2010 (Figure 66). The mol fraction of α-pinene in ambient air was higher in 2009 than in 2010 at comparable measurement temperatures. In the years 2010 to 2011 this trend seems to continue, but high uncertainty in the data does not allow to make robust statements.
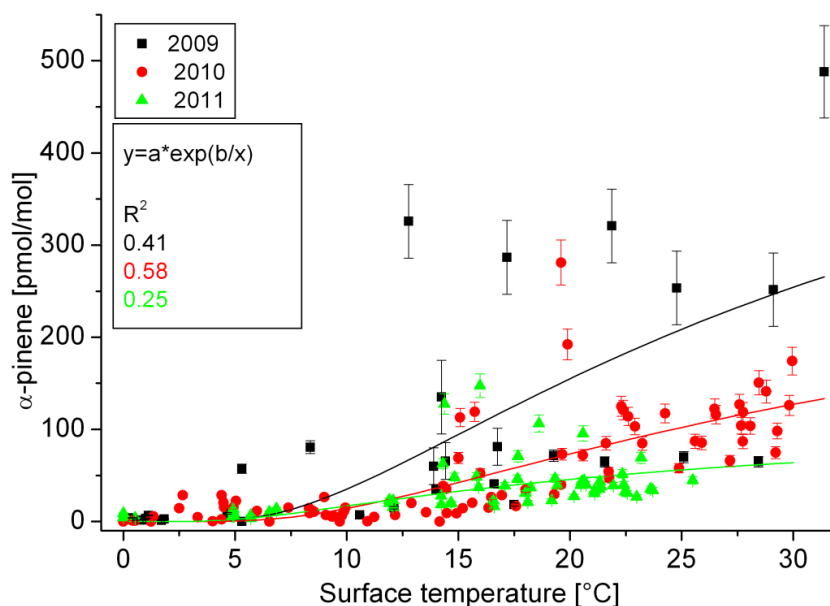
Figure 66. Relation of the mol fraction of α-pinene and the surface temperature at the Lackenberg in the years 2009 (black), 2010 (red) and 2011 (green). Solid lines represent a best fit of each of the measured data using exponential functions.

Other imaginable sources of monoterpenes in the wind-throw area (e.g. living vegetation) cannot explain the observed yearly decrease in the ambient air monoterpene loading. The VOC emission of the sparse vegetation, if any has to be considered, should show an opposite behavior. The spruces were newly emerging and growing in the measurement period, so their contribution to the monoterpene air concentration should increase from 2009 to 2011. This yearly decrease in the mol fraction of monoterpenes in the air above the wind-throw area Lackenberg is therefore another strong indication for the dead wood as the main source of monoterpenes.

4.2.   Monoterpene levels in ambient air at the Kühroint site

A total of 119 monoterpene samples at 16 days were collected at the site Kühroint in the National Park Berchtesgaden in the years 2009 to 2011. Thirteen of them cannot be used due to an incorrect loading.

Table 24. Maxima of measured mol fractions of the most abundant monoterpenes and surface temperatures during the measurement period at the Kühroint site. (AT) means at this day no surface temperature data was available from the central station or the station of the avalanche service station, so the air temperature is reported. Limits of detection of individual monoterpenes are listed in Table 18.

	maximum mol fraction [pmol/mol]							number of samples	maximum surface temperature
	eucalyptol	β-pinene	camphene	Δ^3-carene	limonene	p-cymene	α-pinene		
20.07.2009	12.9	197.0	15.4	19.2	7.4	3.3	252.1	10	30.3
17.11.2009	2.3	49.3	/	/	3.4	3.5	60.5	5	9.3 (AT)
18.11.2009	9.6	105.0	/	/	7.8	7.9	95.4	5	3.2 (AT)
18.02.2010	10.5	10.5	/	0.6	0.6	2.3	9.0	10	2.0
30.03.2010	7.7	10.9	0.6	0.0	4.3	1.3	15.8	2	11.5
22.04.2010	17.9	28.3	7.0	1.8	0.7	4.7	21.6	10	12.9
01.07.2010	18.5	250.7	7.2	46.2	3.3	8.4	187.4	10	24.0
04.08.2010	12.9	124.1	4.5	29.4	18.6	5.4	105.8	10	15.8
25.08.2010	24.5	247.7	13.2	92.5	/	9.8	271.2	2	13.3
26.08.2010	22.7	218.2	7.4	123.3	18.1	8.6	251.0	10	28.4
24.09.2010	7.1	63.8	3.0	51.0	7.6	3.3	80.9	10	24.0
02.02.2011	1.5	5.0	0.3	1.0	/	3.4	1.2	3	1.0
24.03.2011	4.3	14.9	0.0	13.5	0.0	2.1	30.0	2	12.9
07.06.2011	22.2	43.1	9.2	11.9	6.9	5.4	43.3	10	22.5
03.07.2011	11.9	34.3	0.0	8.6	0.0	2.6	30.4	10	26.9
23.08.2011	32.3	136.8	0.0	74.9	15.8	9.5	173.0	10	32.9

Similar to the Lackenberg station in the Bavarian Forest, the air composition at the station Kühroint was dominated by the pinenes (37.3% for α-pinene, 36.2% for β-pinene) (Figure 67). Other important compounds were Δ^3-carene, eucalyptol, limonene, p-cymene and camphene. Their average fractions of the monoterpene composition in the air were 11.5%, 6.4%, 4.8%, 2.1%, and 1.6%, respectively. The highest total loading of monoterpene in the air was measured at the 26.8.2010 between 16:30 h and 18:00 h (UTC) with 649.3 pmol/mol. In few samples the monoterpenes β-phellandrene, β-terpinene and α-thujene were found in marginal amounts.
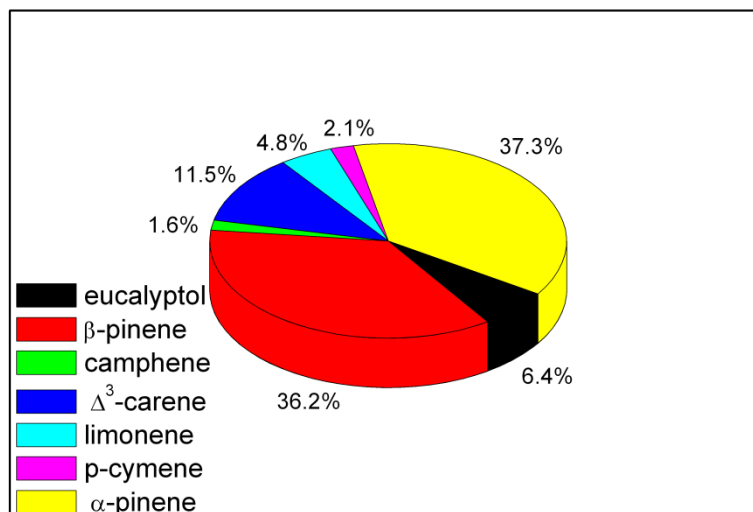
Figure 67. Monoterpene composition of ambient air at the station Kühroint. Average from all data collected 2009-2011 (see Table 24).

The composition of the total monoterpene levels in the air was nearly identical in the two years 2010 and 2011 at the Kühroint site (Figure 68). Student´s t-test proofed no significant differences in the means of the years 2010 and 2011 for any of the measured monoterpenes with a confidence level of 99%.
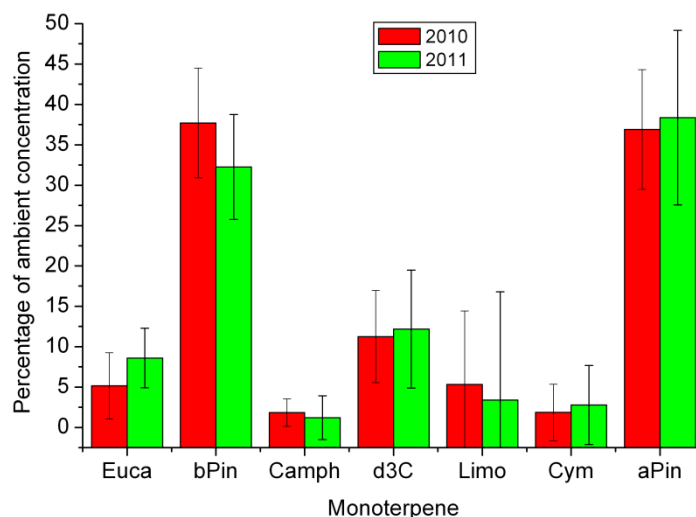
Figure 68. Mean percentages and standard deviations of the average monoterpene concentrations at the Kühroint site in 2010 and 2011. 60 concentration measurements in 2010; 27 in 2011. Euca = eucalyptol; bPin = β-pinene; Camph = camphene; d3C = Δ^3-carene; Limo = limonene; Cym = p-cymene; aPin = α-pinene.

The monoterpene air composition patterns at the measurement sites Kühroint and Lackenberg are very similar, but show one remarkable difference: The proportion of eucalyptol is clearly higher (confidence level 99%, T-test) at the Lackenberg station (21.6% vs. 6.4% at the Kühroint). There are several possible explanations for that:

The first one is natural variability between the monoterpene characteristics at different sites. Even trees of the same age at the same site can show a completely different emission pattern. The variation of monoterpenes in spruce needles ranges between 50% and 70% in mountainous regions in southern Germany (Schoenwitz et al., 1990). Chamber measurements of branches of 40 pine trees in a homogeneous stand in Finland showed 40 very variable emissions patterns, where the fraction of Δ^3-carene as the main component varies from 0-90% (Bäck et al., 2011).

A second explanation may be that due to different temperatures between the two sides at the sampling days the air composition is biased towards less or more volatile compounds. But the boiling points of the six most important monoterpenes are quite similar, varying between 155°C and 173°C (Table 2). Thus the vapor pressures of these VOCs at ambient air temperatures is very similar, too (S.Dev et al., 1982). The mean air temperature during all samplings at the Lackenberg was 13.6°C (minimum -0.3°C, maximum 24.2°C); at the Kühroint site 11.6°C (minimum -3.2°C, maximum 26.7°C). Variability in the air composition pattern due to different vapor pressures caused by different temperatures is therefore expected to be very low. Furthermore, no clear correlation between the surface temperature and the fraction of the single monoterpene components in the air composition at each measurement site was found (Coefficient of determination: eucalyptol 0.02; β-pinene 0.009; camphene 0.006; Δ^3-carene 0.05; limonene 0.006; p-cymene 0.02; α-pinene 0.07).

A third possible explanation is based on the different wind-throw characteristics of the sites: Whereas almost no living vegetation emitting monoterpenes is present at the Lackenberg (see chapter 2.1.4), there are several living spruces and other sources of volatile organic compounds at the Kühroint site (see section 2.2.3). Assuming that the dead wood material at the two sites shows exactly the same emission patterns, differences in the observed air composition can be related to these additional sources. It can be assumed, that compounds showing a high stability in the atmosphere exhibit a high chemical stability in the plant, too. The fraction of very long-living monoterpenes (e.g. eucalyptol, see Table 3) should be enriched in the dead wood compared to that in living wood. In living vegetation the monoterpenes are produced continuously and the fractions should remain quite constant. In dead wood the monoterpenes with a longer lifetime are destroyed slower and their pool size might remain more stable over a long time period. This could be a reason for the observed higher fraction of the most stable monoterpene eucalyptol (Table 3) at the

Lackenberg than at the Kühroint site. The stability of the compounds is also important for a direct degradation of the monoterpenes in the air, so a possibly higher oxidation capacity at the Lackenberg site can result in a higher proportion of eucalyptol. Since the oxidation capacity of the atmosphere was not determined at the sites and natural variability cannot be excluded too, no single explanation for the observed geographic differences in the monoterpene air composition can be found.

4.2.1. The daily variation of the monoterpene air concentration at the Kühroint site

The diurnal behavior of the levels of monoterpenes in the air at the Kühroint site was generally also obvious. The concentrations at night were usually not below 10-20 pmol/mol for the most abundant compounds α-pinene, β-pinene and eucalyptol. In general, the highest levels of volatile organic compounds were reached in the late afternoon/early night. A typical example of the monoterpene levels in the air above the wind-throw area is shown in Figure 69.
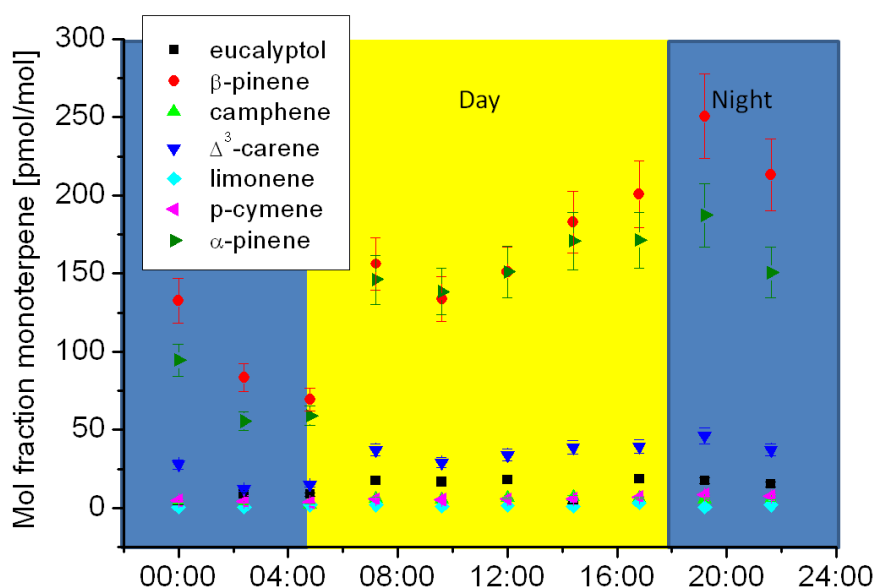
Figure 69. Mol fractions of different monoterpenes at the Kühroint site. 01.07.2010. Sampling flow 190 ml/min; sampling time 143 min. Mean air temperature 17.1°C; minimum 13.5°C; maximum 20.5°C. Time is UTC.

The wind direction during this measurement day was very constant in the sector west to north-west (75 % in the sector 270-345°) at wind speeds of approximately 1.2 m/s (min. 0.3 m/s, max. 2.3 m/s) (Figure 70). These are very common wind characteristics at the site Kühroint, where 80% of all recorded wind speeds are

between 0.5 m/s and 2.1 m/s and the main wind direction is north-west (see Figure 31 in chapter 2.3). Due to the fact that the wind speed and wind direction are quite constant at the measurement day, changes in the monoterpene concentration during this day should not be caused by wind characteristics.
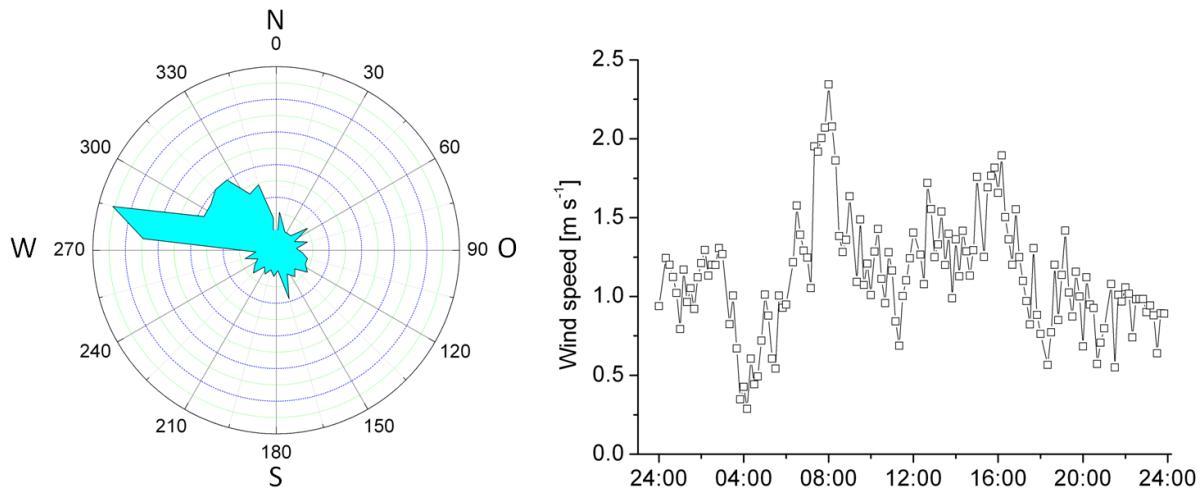
Figure 70. Wind characteristic at the Kühroint site 01.07.2010. Time is UTC.

The peak of the meteorological data of interest at the same measurement day is midday in the case of air-, surface-, and soil-temperatures and 10:00 h with a very sharp decrease for photosynthetic active radiation and net radiation (Figure 71). This time-shift between the meteorological parameters which trigger the monoterpene emission and the measured monoterpene levels above the wind-throw is observed at all measurement days. The delay is not constant at all days, but ranging between 1 and 8 hours. A meaningful determination of micrometeorological parameters (stability, turbulence characteristics) and flux calculations based on micrometeorological techniques is not possible at the Kühroint site. The orographic situation there does not meet the criteria for eddy covariance measurements (e.g., Burba and Anderson, 2010). The terrain is very inhomogeneous, presents many edges (e.g. between standing trees and wind-throw) and has a very hilly structure. This makes the interpretation of the daily cycle of the monoterpene air levels and the observed shift between the maxima in the driving meteorological parameters and the VOC concentrations difficult.
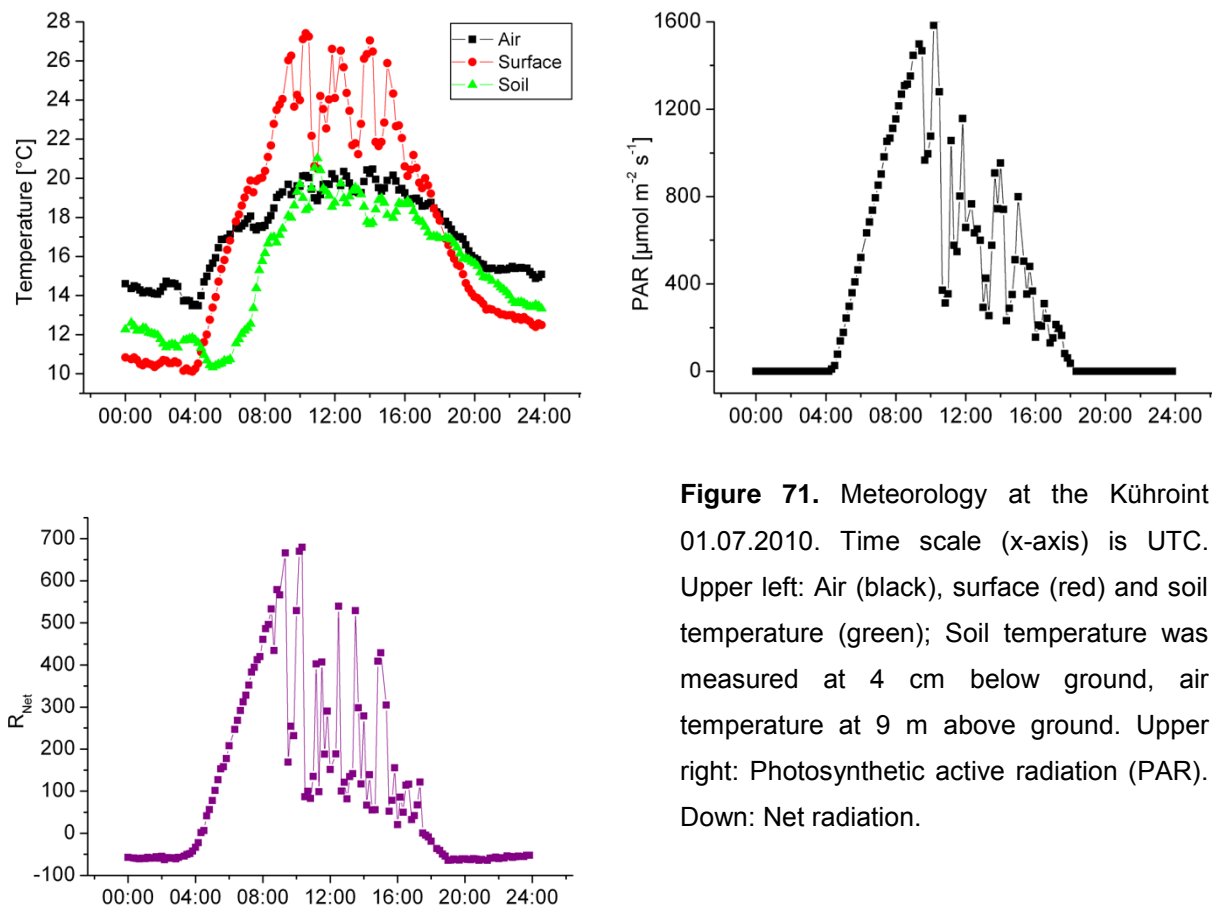
Figure 71. Meteorology at the Kühroint 01.07.2010. Time scale (x-axis) is UTC. Upper left: Air (black), surface (red) and soil temperature (green); Soil temperature was measured at 4 cm below ground, air temperature at 9 m above ground. Upper right: Photosynthetic active radiation (PAR). Down: Net radiation.

Two explanations for the observed time shift are discussed: The first one is based on storage and release of monoterpenes in the canopy. The maximum of the emission should be almost simultaneously with the maximum of the energy input (surface temperature), without a measurable time-shift. But storage during the day and a slow release in the late afternoon would lead to a time shift between the emission at the ground and the time where the monoterpene levels are measured at 9 meter above ground. To reach a better release from the storage, the turbulence causing the transport from the source to the sensors must increase in the afternoon. What argues against this hypothesis is the origin of turbulence: Mechanical turbulence is mainly caused by air moving across obstacles on the ground. In a short time period an increase in mechanical turbulence can therefore only be caused by an increase in wind speed. As discussed above, this is not observed during the measurement day. An increase in thermal turbulence is caused by a higher surface temperature. Since the surface temperature is lower in the evening the influence on the thermal turbulence should be opposite to the assumption needed to explain the shift.

Another explanation is the living vegetation at the site. A release of monoterpenes from the living spruces might be delayed to the meteorological factors triggering the emission. If some parts of the monoterpene levels in the air arise from the dead wood material and others from living vegetation showing different emission kinetics, a broadening and time shift of the monoterpene maximum or even two peaks could be observable. Nevertheless, it is very hard to confirm this hypothesis and a mixture of different influences could lead to the measured daily cycle.

No very marked correlation (R^2 of 0.29 if a linear regression is used) between the surface temperature and the measured levels of α-pinene can be found (Figure 72 left). If a time shift is considered, a better correlation (R^2 of 0.66 if a linear regression is used, R^2 of 0.74 if an exponential regression is used) between the measured levels of monoterpenes and the surface temperature is found (Figure 72 right). Since the reasons for this time delay is not totally clear and the time shift might not be constant during the day, this time shifting between the surface temperature and the monoterpene level has to be treated very cautiously and should serve as a first hint only.
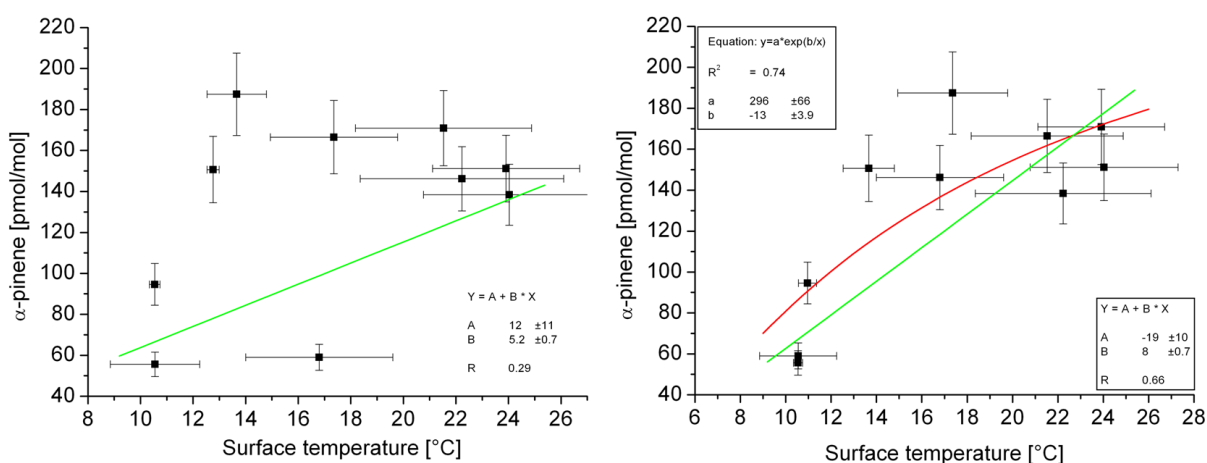
Figure 72. Relation of the mol fraction of α-pinene in ambient air and the surface temperature at the Kühroint site 01.07.2010. Left panel: Using data as measured. Right panel: Using a time shift of two hours.

4.2.2. The variability of the monoterpene air concentration at the Kühroint site during the year

The measured air levels on a daily basis were highest in the summer, with up to 435 pmol/mol for the total sum of monoterpenes. The monoterpene content in the air was low in the wintertime and no values above 10 pmol/mol were observed on the measurement days. The site is usually covered by snow between the end of October and the beginning of April.
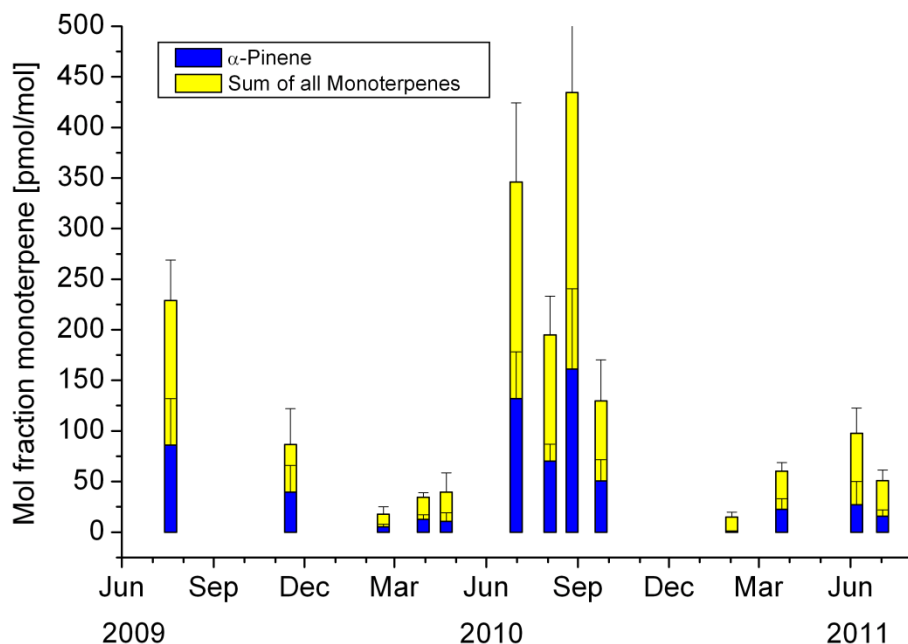
Figure 73. Measured monoterpene levels in ambient air at the Kühroint site in the years 2009 - 2011. Error bars represent the standard deviation at each day.

4.3. Monoterpene fluxes

An experimental characterization of the emissions of monoterpenes in the wind-throw area Lackenberg was carried out in summer and autumn 2010 and 2011. Flux measurement days were selected on short term weather forecast, looking for sunny days. The emission of monoterpenes was expected to be high at elevated temperatures and loading of adsorption tubes is less error prone. Flux calculations based on the eddy covariance system used in this work are not possible during rainy days, because the fast wind sensors and the open path analyzer are not working properly under these conditions. A total of 104 sample pairs of adsorption tubes loaded with monoterpenes at the measurement heights 1.4 and 7.2 meters above ground were collected on twelve days. For the dominant monoterpene α-pinene, 54

sample pairs fulfilled the requirements in terms of accuracy of the measured gradients and meteorological conditions (Table 25). Highest emission determined by the gradient techniques described in chapter 3.2 was measured at the 12th of July 2011 with a value of $5.9 * 10^{-8} \pm 9.2 * 10^{-8}$ g/(m^{2}s).

Table 25. Number of sample pairs of adsorption tubes collected at 7.2 m and 1.4 m at the Lackenberg. Above uncertainty = number of samples in which the differences of the α-pinene concentration between both heights were higher than its uncertainty (see Table 20); Emission calculated = number of samples in which the gradients were resolvable (see Table 21) and the flux measurements met the requirements (see Figure 56).

	sample pairs	above uncertainty	emission calculated
07.07.2010	10	0	0
08.07.2010	10	9	4
09.07.2010	4	1	2
22.07.2010	10	4	2
18.09.2010	10	6	5
19.09.2010	8	6	2
20.09.2010	8	6	5
15.06.2011	10	10	8
16.06.2011	10	8	8
12.07.2011	10	10	9
03.08.2011	10	9	6
27.09.2011	4	4	3
sum	104	73	54

The differences between the measured concentrations at both heights were more difficult to resolve for the less abundant monoterpenes. The numbers of sample pairs which can be used to calculate fluxes are listed in Table 26. The gradient of eucalyptol was hardly resolvable because of the high uncertainty in the quantification (Table 20). Only approximately 10% (10 of 104 sample pairs) of the measured concentration differences of eucalyptol between 1.4 and 7.2 meters were above the uncertainty. The gradients of α-pinene, β-pinene, camphene, Δ^3-carene and p-cymene could be quantified more precisely. In the case of the most abundant monoterpene α-pinene more than 50 % (54 out of 104) of the measured samples could be used to determine the α-pinene emission in the wind-throw area.

Table 26. Number of sample pairs of each monoterpene which fulfill the requirements to calculate fluxes by the gradient methods and maxima of measured emissions.

Monoterpene	eucalyptol	β-pinene	camphene	Δ^3-carene	p-cymene	α-pinene
number	10	31	18	45	32	54
E_{max} $*10^{-8}$ [g m^{-2} s^{-1}]	2.9	3.9	0.44	0.81	1.8	5.9

Measured monoterpene fluxes were always positive, which indicates that the flux was always oriented from the surface towards the atmosphere and a deposition of monoterpenes in the area was not observed.

4.3.1. Determination of the bulk conductance by the modified Bowen ratio method (example day: 08.07.2010)

To quantify monoterpene fluxes by the modified Bowen ratio method a second gradient and its corresponding flux is needed (equation 17). The fluxes of water, temperature and CO_2 were measured at the Lackenberg with an eddy covariance system (see Figure 19 and Table 6). The gradients of the same scalars were determined by sensors which measured at the same heights as the monoterpene samplers (see Figure 21). A typical daily cycle (in this example case: 08.07.2010) of the sensible heat, water and CO_2 flux and their gradients is given in Figure 74.
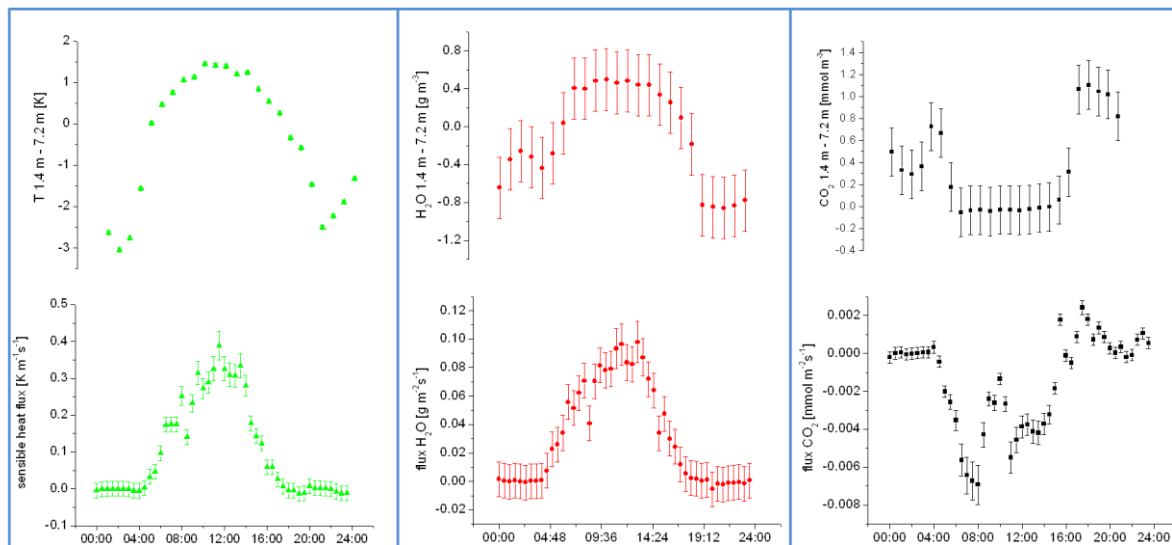
Figure 74. Differences between 1.4 and 7.2 meter above ground (above) and fluxes (below) of temperature (green), water (red) and CO_2 (black) at the 08.07.2010 at the Lackenberg. Time is UTC.

All gradients used in the MBR method were resolvable on this example day with the sensible heat flux and gradient of temperature showing the highest accuracy (Figure 74). CO_2, water vapor and temperature are transported by the same air parcels, so all atmospheric conductances should be equal. In the diurnal cycle this assumption was verified by the measurements (Figure 75).
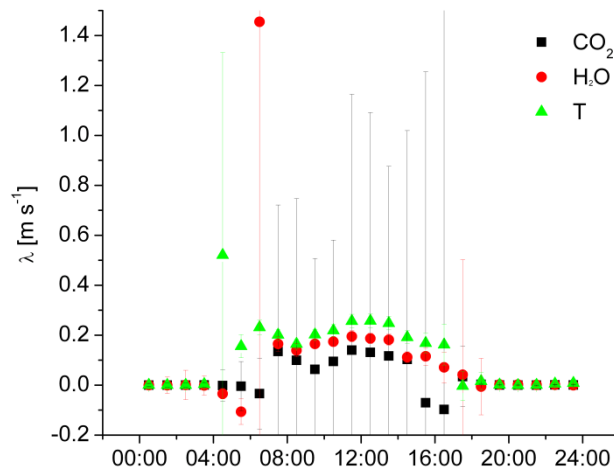
Figure 75. Atmospheric bulk conductance determined by the modified Bowen ratio method with the gradients of CO_2 (black), H_2O (red) and air temperature (red). Measured at the 08.07.2010 at the Lackenberg site. Time is UTC. Error bars represent the uncertainty calculated by error propagation.

Deviances were found during sunrise and sunset, where the conditions of the atmosphere are in general more complex. Fast changes in the fluxes and in the differences of the scalars between the two heights made a correct calculation of atmospheric conductance challeging during these times. The bulk conductance calculated by using the flux and gradient of CO_2 showed a high uncertainty even during the daytime and was generally not reliable. The atmospheric conductance of water vapour was more robust. High uncertainties were observed only in the morning and the evening, where differences between the water vapor content of the air at 1.4 meter and 7.2 meter were very small. The conductance calculated with the help of the sensible heat flux and the temperature difference was in general the most reliable. The heat flux and the temperature gradient could be determined very accurate and the resulting conductance was very precisely at most times of the day (on average 12 % error in the daytime (5:30 - 17:00)). This result met the expectation since the precision of the temperature gradient and heat flux was the highest of the three used scalars (see Table 21). The air temperature was determined continously at both measurement heights, which makes the temperature gradient less error prone to fast changes in scalar differences in the morning and in the evening.

4.3.2. Determination of the bulk conductance by the surface layer gradient technique (example day: 08.07.2010)

The bulk conductance λ can be calculated by micrometeorological parameters without the use of a second gradient (see equations (14), (15) and (16)). These parameters are the friction velocity u_* and the stability parameter z/L (Figure 76). During the night and the morning until 8:00 h, values of u_* below 0.2 m/s indicated prevalence of low turbulence. Strongest unstable stratification was found in the morning, strong stable conditions were not observed during this day. In the daytime atmospheric conditions were turbulent ($u_* = 0.27$ m/s) and slightly unstable ($z/L = -1$). Around 20:00 h the friction velocity decreased and the atmosphere became more unstable again.
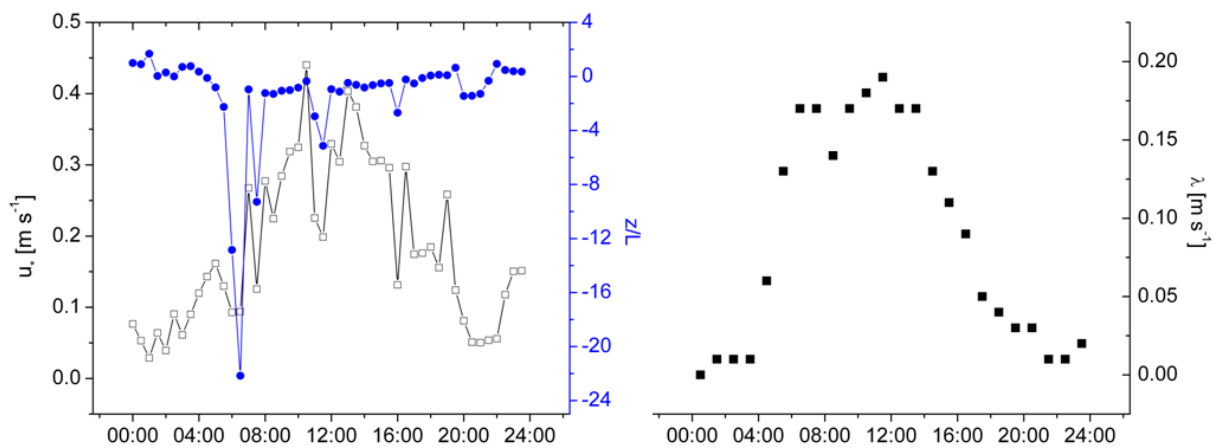
Figure 76. Left: Friction velocity (u_*) and stability parameter (z/L). Right: Bulk conductance determined by the surface layer gradient technique. Measured at the 08.07.2010 at the Lackenberg site. Time is UTC.

The bulk conductance calculated with the universal functions and the friction velocity (Figure 76 right) on this day showed a very similar daily cycle and a similar magnitude than the one calculated by the MBR method (see Figure 75). During the night the conductance was close to zero and the maximum was reached around noon. The similarity of these quite independent methods shows the potential to calculate monoterpene fluxes with the modified Bowen ratio method and the surface layer gradient technique.

4.3.3. Determination of the emission of α-pinene by the MBR and SLG (example day: 08.07.2010)

The emission of the most abundant monoterpene α-pinene was calculated from the concentration differences of α-pinene between 1.2 and 7.4 meter above ground and the mean of the bulk conductance of temperature, water vapor and the one calculated by the use of universal functions. The atmospheric conductance of CO_2 was not used, due to its high uncertainty.

An example of the process of the quantification of the α-pinene emission is shown below. The concentration of the monoterpene is measured at both heights simultaneously 10 times a day for two hours and 24 minutes. The concentration at both levels showed a very similar daily cycle with a maximum in the morning and a minimum at night (Figure 77).
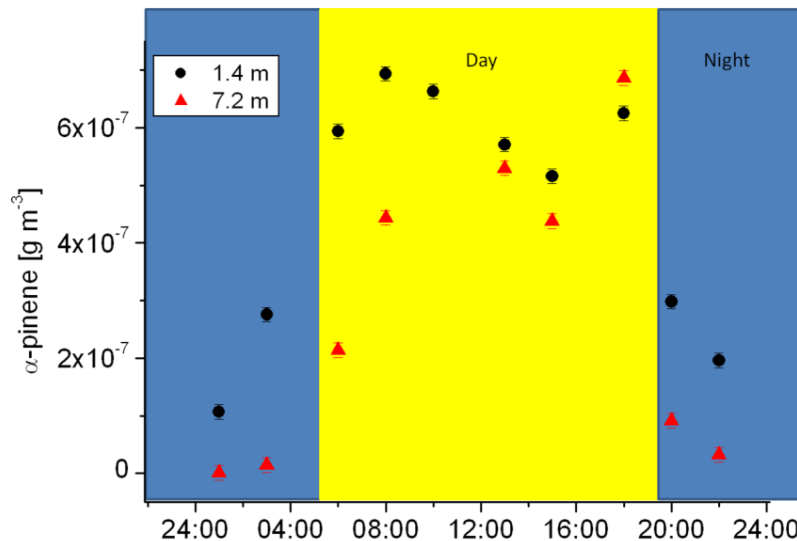
Figure 77. Concentration of α-pinene measured at 1.4 m (black) and 7.2 m (red) above ground at the Lackenberg site 08.07.2010. Sampling flow 194 ml/min; sampling time 144 min. Time is UTC. Error bars represent the precision of the analysis (see chapter 3.1.8).

The adsorption tube loaded between 09:36 h and 12:00 h at 7.2 meter leaked and was not used for further analysis. The sample pair at 16:48 h -19:12 h showed a higher concentration of the upper level, indicating a negative flux of α-pinene, which is difficult to explain in this area. Analysis of the wind characteristics showed a change of the wind direction during this time from South to the unusual wind direction North and an increase in the wind speed from 1.5 m/s to 2.5 m/s (10 minute averages). Combined with relatively stable stratification (z/L = 0.2) this leads to an exceptional large source area of the inlet at 7.2 meter during this time. A large

fraction of the measured air parcel might have originated from a nearby spruce forest north of the central station. The source strength of this living trees or the potential to store emitted monoterpenes in the canopy of the forest can lead to the observed high air concentration during this time.

The emission calculation of α-pinene in the night was not reliable, because the turbulence was not sufficient at this time (u_* below 0.2 m/s, see Figure 76). In the morning and evening the atmospheric stability was too low (z/L below -2), so micrometeorological requirements were not fulfilled. The measurement in the late evening was discarded due to the large footprint area of the eddy covariance system (only 70 % of the source area was within the wind-throw, see Figure 78 right). This large source area further confirms the hypothesis to explain the unexpected high α-pinene concentration at 16:48 h -19:12 h. The three calculated emissions during the daytime and the one at night met all requirements and were implemented in further calculations.
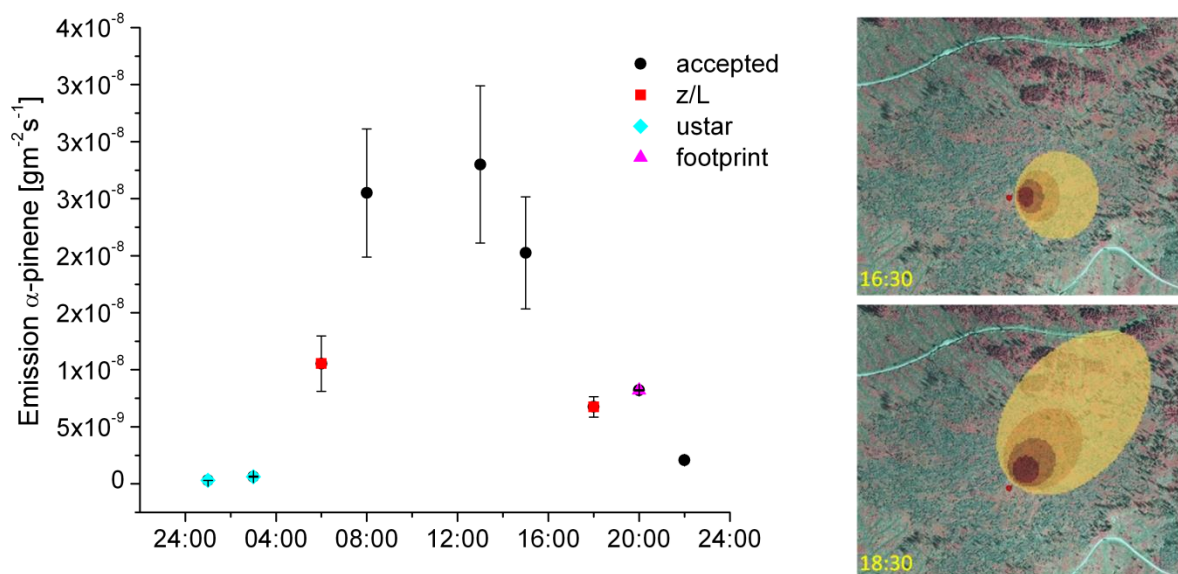
Figure 78. Left: Emission of α-pinene calculated by the mean of the bulk conductance determined from the MBR method with the gradients of H_2O and air temperature and the SLG technique at the Lackenberg 08.07.2010. Black dots represent emissions, where all requirements are met. Colored dots are discarded due to different reasons (see legend and text). Error bars represent uncertainty calculated by error propagation.
Right: Half hourly footprint of the EC system calculated according to Kormann and Meixner, (2001). Dark brown color marks 20 %, light brown 40%, orange 60% and yellow 80 % of the source area. The red dot is the position of the central station,

The emission calculated by the mean of the atmospheric bulk conductance showed the expected diurnal cycle at this measurement day, especially if the emissions, which were discarded for quality reasons, are considered. This suggests that the

criteria to reject data are very conservative. Since the error due to a fail of the micrometeorological assumption is hard to quantify and can be high at different conditions, these rejection criteria are further used.

4.3.4. Comparison of emissions calculated by MBR and SLG technique

The example results in chapters 4.3.1 and 4.3.2 point out that the bulk conductance calculated by the surface layer gradient technique and the modified Bowen ratio method were very similar. The atmospheric conductance of carbon dioxide shows a very high uncertainty due to difficulties in the exact quantification of its gradient. Therefore, the emissions of monoterpenes are calculated with bulk conductance derived from the gradients of temperature, water vapor and determined by the universal functions as mentioned above. All emissions of α-pinene measured during this work match fairly well to each other (Figure 79). Particularly the emissions calculated by the MBR method with the bulk conductance of temperature and the one determined by the SLG technique were in very good agreement (slope of 1.13, low bias of 4.4 $*10^{-10}$ g/(m²s), R^2 0.94).
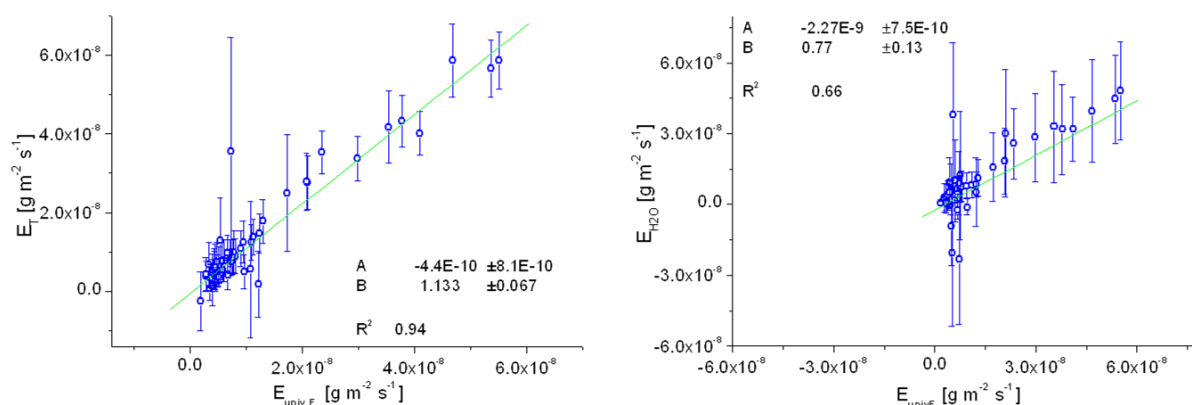
Figure 79. Left: Emission of α-pinene calculated by the bulk conductance of temperature vs. the emission of α-pinene determined by the SLG technique. Right: Emission of α-pinene calculated by the bulk conductance of water vapor vs. the emission of α-pinene determined by the SLG technique. Presented are 54 emissions measured in 2010 and 2011. Error bars represent uncertainty calculated by error propagation.

4.3.5. Relation between the emission of α-pinene and micrometeorological parameters (example day:12.07.2011)

The concentration of α-pinene in the air above the wind-throw area Lackenberg was exponentially depending on the surface temperature (see chapter 4.1.1). This was explained by the emission of α-pinene which is likewise depending on the surface temperature and a fast distribution of the monoterpene which makes storage processes in the canopy negligible. This relation of the monoterpene emission to selected micrometeorological parameters is investigated in this chapter.

An example of the monoterpene emission during the daytime is depicted in Figure 80. The emission of α-pinene calculated by the modified Bowen ratio method and the surface layer gradient technique shows a very good agreement with a maximum around noon.
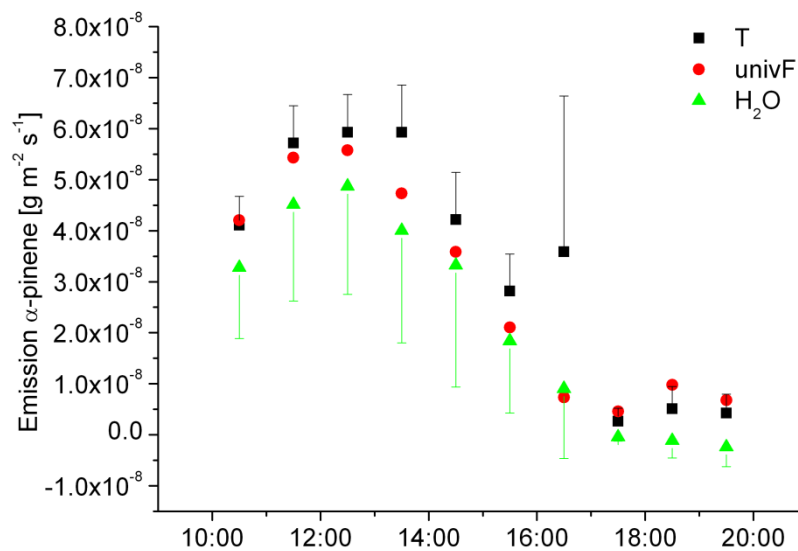
Figure 80. Emission of α-pinene calculated by the bulk conductance determined from the MBR method with the gradients of H_2O and air temperature and the SLG technique at the Lackenberg 12.07.2011. Error bars represent the uncertainty calculated by error propagation. Time is UTC.

The turbulence and atmospheric stability was suitable for flux calculations during the whole measurement period at this day (u*>0.2 m/s, -2<z/L<2, see Figure 81, lower panel). Atmospheric stratification was slightly unstable before noon and almost neutral in the afternoon. The only meteorological quantity which showed a course similar to the emission of α-pinene was the surface temperature (Figure 81). The maxima of the other possible determining parameters, air temperature, soil

temperature and radiation were considerably later and the curves showed a different shape.
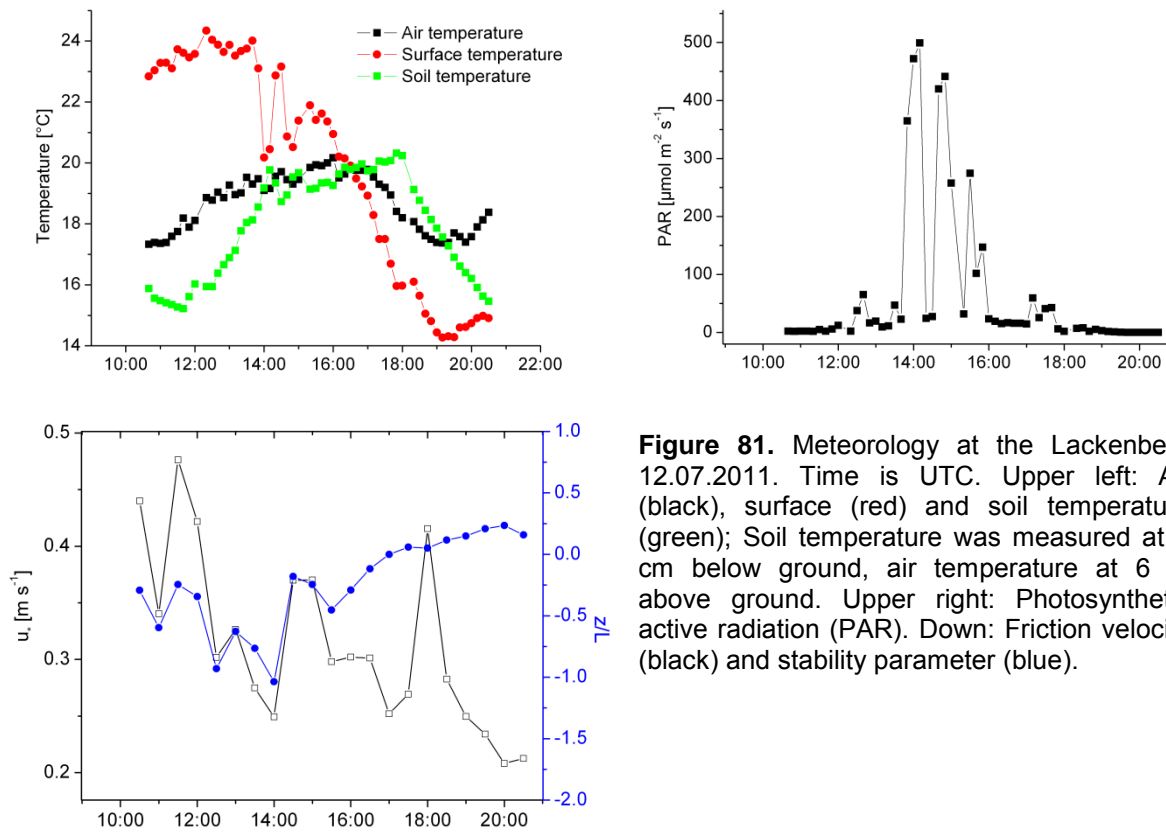
Figure 81. Meteorology at the Lackenberg 12.07.2011. Time is UTC. Upper left: Air (black), surface (red) and soil temperature (green); Soil temperature was measured at 4 cm below ground, air temperature at 6 m above ground. Upper right: Photosynthetic active radiation (PAR). Down: Friction velocity (black) and stability parameter (blue).

To analyze the response of the emission of α-pinene on the surface temperature, an algorithm based on the one proposed by Guenther et al., 1993 (see equation (1) and (2)) was used:

$$E_{\alpha-\text{pinene}} = E_S \, exp(\beta(T - T_S)) \tag{21}$$

Since no data was available at 30°C surface temperature at this day, the standard emission potential of α-pinene was set to 23°C. The empirical factor β was modified from 0.09 to 0.25 to achieve a better fit. With this exponential equation it is possible to explain 95% of the observed variation in the emission at this day only with changes in the surface temperature (Figure 82).

A correlation of the emission of α-pinene with the air temperature, soil temperature or photosynthetic active radiation was not evident ($R^2 < 0.15$) (see Figure 93 in the appendix). The emission, that is strongly depending on the surface temperature, is another indication of the dead wood material as the dominant source of α-pinene in the wind-throw area and supports the previous hypothesis.
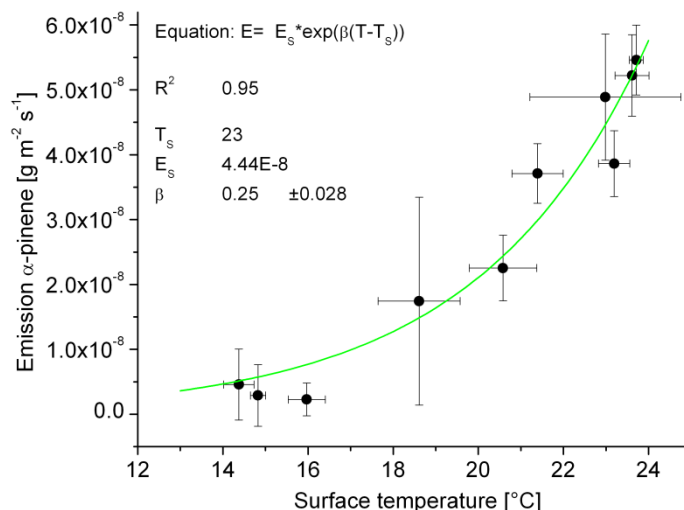
Figure 82. Relation of the surface temperature and the emission of α-pinene calculated by the mean bulk conductance at the Lackenberg 12.07.2011. Green line is the G95 fit of the data (β=0.25). Error bars of the emission represent the uncertainty calculated by error propagation. Error bars of the surface temperature represent the range of surface temperature in the 60 minute measurement interval.

4.3.6. The diurnal course of the monoterpene emission at the Lackenberg (example day:12.07.2011)

The emissions of the other prominent monoterpenes, namely β-pinene, eucalyptol, Δ^3-carene, and p-cymene showed a very similar daily course as the one of α-pinene (Figure 83). The emission of camphene and limonene, which are other frequently occurring monoterpenes, could not be quantified at this day, because their concentration differences were below the limit of detection (camphene below $1.7*10^{-9}$ g/m^3; limonene below $2.4*10^{-8}$ g/m^3, see Table 20).
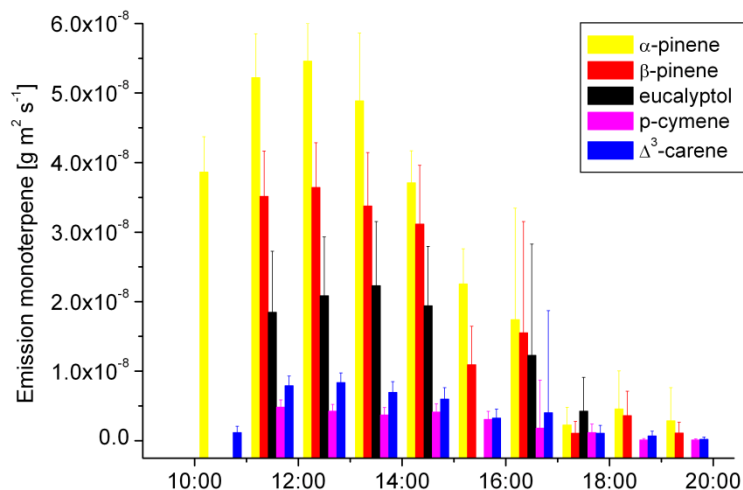
Figure 83. Emission of monoterpenes calculated by the mean bulk conductance determined by the MBR method with the gradients of H_2O and air temperature, and by the SLG technique at the Lackenberg 12.07.2011. Time is UTC. If no data is presented, the difference in the concentration between both heights was below the LOD. Error bars of the emission represent the uncertainty calculated by error propagation.

4.3.7. Development of a model describing the monoterpene emissions by the surface temperature

The exponential relation between the surface temperature and the emission of monoterpenes is also found by using all data collected in the years 2010 and 2011 (Figure 84). The coefficient of determination of the theoretical fitting of the measured emissions is lower in this case (e.g., of α-pinene, $R^2 = 0.52$ for all data) compared to a one day model exercise (e.g., of α-pinene 12.07.11, $R^2 = 0.95$). Due to this relatively high variance in the data, no significant difference (confidence level 99%) of the emissions between the years 2010 and 2011 could be observed. Particularly the emissions measured at the 12th of July 2011 (marked by a pink circle in Figure 84) could not be explained by measured meteorology parameters like temperature, humidity, stratification or turbulence.
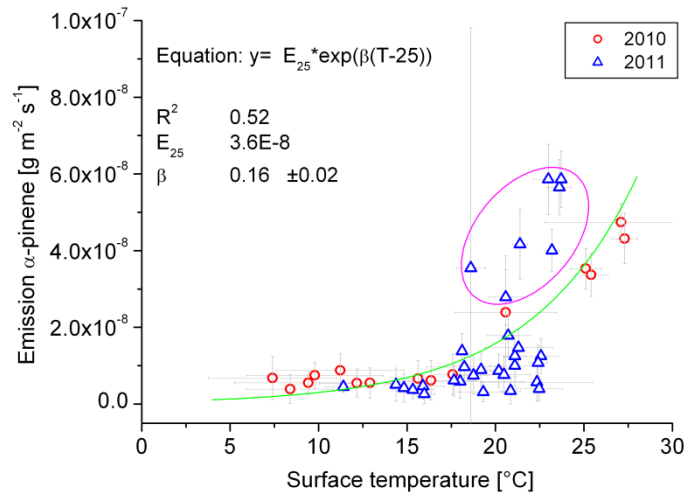
Figure 84. Relation of the surface temperature and the emission of α-pinene calculated by the mean bulk conductance at the Lackenberg in the years 2010 and 2011. Data selected according to quality criteria (see chapter 3.2.4). Error bars of the emission represent the uncertainty calculated by error propagation. Horizontal bars of the surface temperature represent the range of surface temperature in the measurement interval. The pink circle marks the high emission measured at the 12.07.2011.

To investigate if the emission is influenced by any second parameter besides the surface temperature, the emission of α-pinene was normalized. Normalized emission rates were derived by dividing the measured emission by the modeled one to get a dimensionless value, which describes the residual variance which is not explained by the surface temperature. This value (ideally 1) was plotted against possible determining parameters: air temperature, soil temperature, friction velocity, stability, wind speed, incoming radiation, relative humidity, and soil water content (Figure 94 in the appendix). All these factors can possibly influence the emission by directly changing the vapor pressure of monoterpenes (air temperature, soil temperature, radiation), by changing the diffusion resistance of the monoterpenes into the atmosphere (soil water content, humidity) or by modifying atmospheric conditions (u_*, wind speed, z/L). No correlation of any of these parameters with the normalized emission was found, so a different explanation of the high variation of the emission based on the origin of the monoterpenes at this site is proposed.

The dead wood is most likely a relatively variable emission source. The release of the volatile compounds from this dead wood into the atmosphere is depending on the vapor pressure inside the resign duct and the transport resistance into the atmosphere. The vapor pressure is exponential depending on the temperature in the dead wood and explained best by the surface temperature. The transport resistance is influence by various factors: Decomposition of the dead wood is supposed to

happen mainly through microbes, fungi and mechanical damage. These factors could vary strongly with time, particularly the mechanical damage. Breaking of the dead stems, which are lying chaotically in the wind-throw area (Figure 85 left) can happen easily and randomly by wind, by animals or by the own weight of the dead stems. The breaking of the stems can decrease the resistance of the emission of monoterpenes drastically because resin ducts are destroyed and the bark barrier between the monoterpene containing resin and the atmosphere is removed (Figure 85 right).
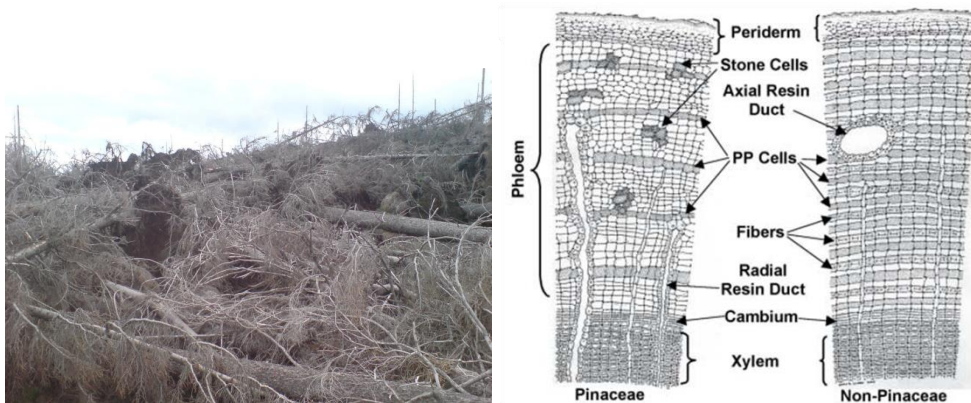
Figure 85. Left: Photo of dead wood material in the wind-throw area Lackenberg. Right: Drawings of two different basic types of conifer bark and their resin-producing structures, PP = polyphenolic parenchyma. Figure from Franceschi et al. 2005.

On days where freshly wounded trees are in the source area of the inlet, the measured emission would be unexpected high. This damage-induced increase in the emission could be an explanation for the observed high variability between measurement days, while the emissions at single days were described very accurately by the exponential surface temperature model.

The emissions of β-pinene, eucalyptol, p-cymene, Δ^3-carene and camphene showed a very similar correlation with the surface temperature (Figure 86) and could be modeled by the same exponential algorithm.
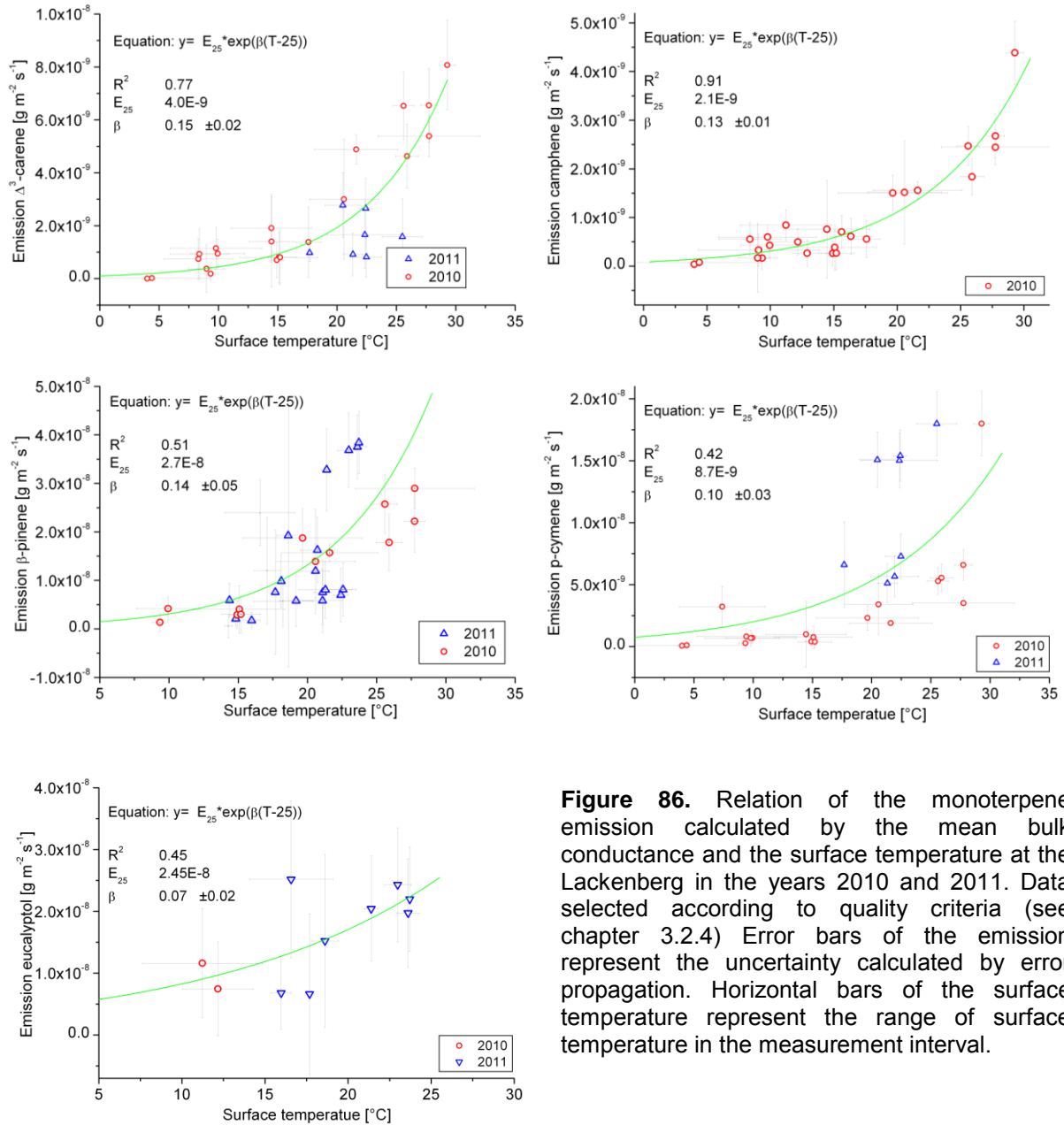
Figure 86. Relation of the monoterpene emission calculated by the mean bulk conductance and the surface temperature at the Lackenberg in the years 2010 and 2011. Data selected according to quality criteria (see chapter 3.2.4) Error bars of the emission represent the uncertainty calculated by error propagation. Horizontal bars of the surface temperature represent the range of surface temperature in the measurement interval.

Standard emission factors (25°C) and β-values are listed in Table 27. The empirical factor β varies between 0.07 (eucalyptol) and 0.16 (α-pinene), but is close to the originally suggested value of 0.09 for all monoterpenes.

Table 27. Standard emission factors at 25°C (surface temperature), β-values and coefficients of determination of the exponential model for the measured monoterpene emissions in 2010 and 2011.

Monoterpene	eucalyptol	β-pinene	camphene	Δ^3-carene	p-cymene	α-pinene
E_{25} $*10^{-8}$ [g m^{-2} s^{-1}]	2.45	2.7	0.21	0.40	0.87	3.6
β	0.07	0.14	0.13	0.15	0.10	0.16
R^2	0.36	0.51	0.91	0.77	0.42	0.52

4.3.8.   The monoterpene emission pattern at the Lackenberg site

Major compounds emitted in the measurement period were α-pinene, β-pinene, and eucalyptol, responsible for more than 85% of the measured monoterpene emission (Figure 87).

p-cymene, Δ^3-carene and camphene were emitted in lower quantities. It was not possible to quantify the emission of limonene, because the gradient could not be resolved. If the low average air concentration of limonene (maximum in the measurement period 2009-2011: 25.4 pmol/mol) is considered, the emission of limonene is expected to be low. The high chemical reactivity of limonene in the atmosphere (see Table 3) can also contribute to the problems of resolving limonene gradients, but as explained in chapter 3.2.3, the VOCs can be treated as relatively inert in the flux calculations at this site.
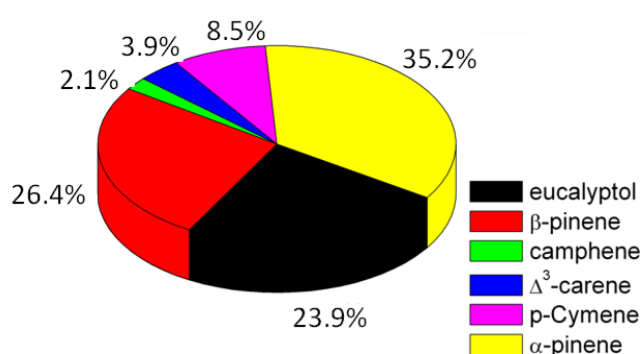
Figure 87. Emission pattern at the Lackenberg site derived from the standard emission factors.

The averaged emission pattern of monoterpenes depicted a similar picture than the mean monoterpene composition of the air at the station Lackenberg (Figure 57). Small changes can be explained by different measurement periods (concentration measurements 2009-2011; emission measurements 2010-2011), by a higher number

of data points in the concentration pattern and by the additional substance limonene in the concentration pattern, which is responsible for 3.7 % of the monoterpene loading in ambient air.

4.3.9. The annual monoterpene emission

The algorithm developed in chapter 4.3.7 was used to estimate the emission of monoterpenes in the years 2010 and 2011 (Figure 88). The source strength of α-pinene was modeled by the relation to the surface temperature according to equation (21).

$$\mathrm{E}_{\alpha-\mathrm{pinene}} = \mathrm{E}_{25}\, exp(0.16(ST - 25)) \qquad (22)$$

The standard emission potential was set to 25°C of surface temperature (ST) (E_{25} = $3.6*10^{-8}$ g m^{-2} s^{-1}).
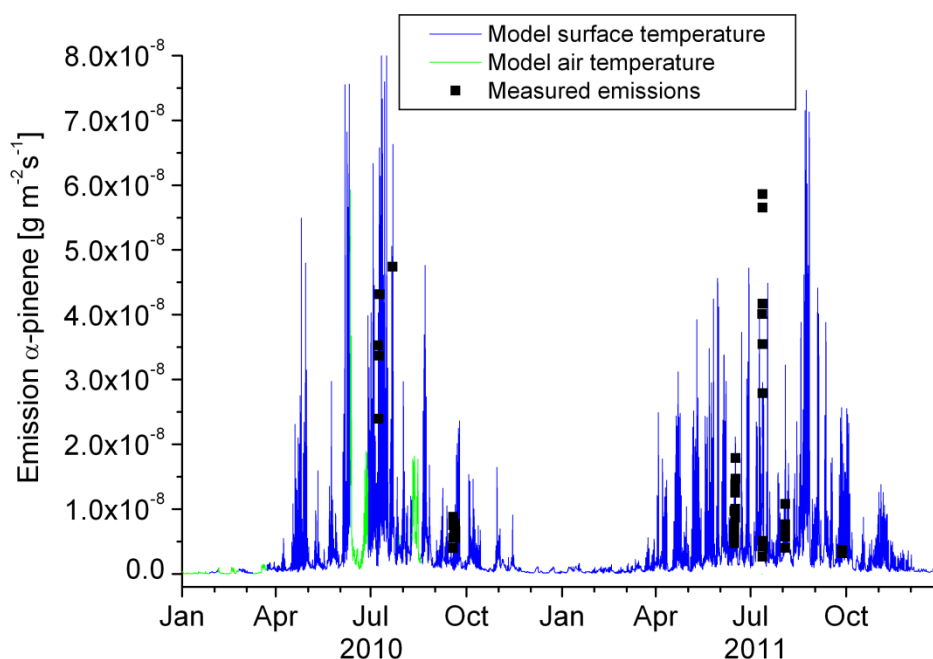
Figure 88. Emission of α-pinene modeled by the surface temperature algorithm (blue) and gap filling by the air temperature algorithm (green). Measured emissions are presented in black squares.

The modeled emission of α-pinene was close to zero in the wintertime, which is in agreement with the very low observed air concentration during the winter (see Figure 65). In the summer the source strength is low at night and on cold days. On warm summer days the emission of α-pinene could reach values of up to 80 ng/(m^{2}s). The total annual emission of α-pinene for the years 2010 and 2011 was 0.11 ± 0.05 g/m^2 (uncertainty results from the variation in the observed emission data from the model

(see Figure 84) and the gap filling, see below). Scaled up to the wind-throw area, the total emission sums up to 29 ± 14.5 kg α-pinene per year.

Due to errors in the power supply or failures of the data processing at the central station Lackenberg the surface temperature was not available in same periods of the year 2010 (01.01. -27.01.; 04.02. -24.2.; 09.03. -23.3.; 11.06. -28.06.; 09.08. -18.08.). These time intervals make up 11.9 % of the total measurement period and 23.3 % in the year 2010 only. These gaps in the emission model were filled by an air temperature controlled algorithm according to equation (23).

$$\mathrm{E}_{\alpha-\mathrm{pinene}} = \mathrm{E}_{20}\, exp(0.24(AT - 20)) \tag{23}$$

E_{20} is the standard emission potential at an air temperature of 20°C ($3.1 \ast 10^{-8}$ $g\, m^{2}\, s^{1}$) and AT is air temperature.

This model was derived from the relation of the emission of α-pinene and the air temperature measured at the satellite station (see Figure 95 in the appendix). It was shown in Figure 29 in chapter 2.3 that the air temperature at the satellite station agreed well with the one at the central station Lackenberg so both represent the air temperature in the wind-throw area. The emission of α-pinene modeled by both algorithms matched well (Figure 89, low bias of $4.35 \ast 10^{-10}$ g/(m^2s) and slope 0.999). The coefficient of determination is low due to the low determination of the single models based either on surface temperature or on air temperature. Since only 11.9% of the data is affected and the difference between the models is low, the gap filling should not be a source of high errors when estimating annual emissions.
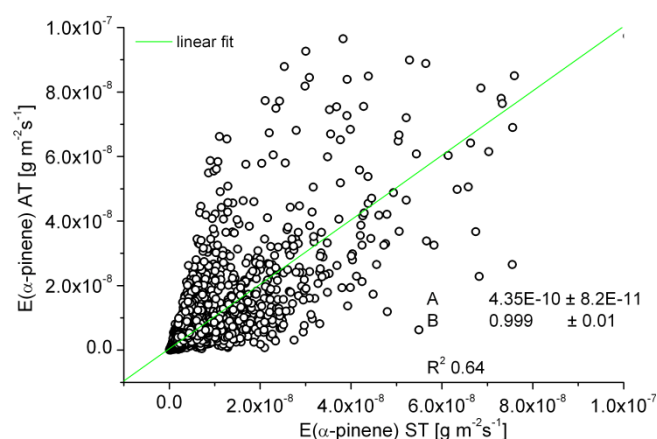
Figure 89. Emission of α-pinene modeled by the air temperature algorithm (AT) versus emission of α-pinene modeled by the surface temperature algorithm (ST). 6163 data points from 01.01.2010-31.12.2011.

4.3.10. The monoterpene content of the dead wood at the Lackenberg site

The endogenous monoterpene content of dead wood material differed very strongly between tree compartments and even within the same structures (Table 28) (see section 3.1.9 for sampling procedure). The amount of monoterpenes was highest in the stem wood with an average content of 2500 µg per gram dry-weight, low amounts were found in the branch wood (79 µg/g$_{(DW)}$). The content in the 3 needle samples was very low and for most monoterpenes below the limit of detection. The only detectable terpene in the needle extract was camphene in low traces with an average of 35 ng/g$_{(DW)}$. Camphene is also reported to be the dominant terpene in needles of Norway spruce (Persson et al., 1996; Ghirardo et al., 2010). Due to the fact that the wind-throw was caused by the storm Kyrill in January 2007, almost all needles were already decomposed, when the samples were taken in summer 2011. The few needles that were found in sheltered places represented no relevant monoterpene pool in the year 2011.

Table 28. Monoterpene content in stem wood and branch wood collected in summer 2011 at the Lackenberg. Values in µg/g$_{(DW)}$. Stem wood samples include bark and 1 cm of the sapwood. Diameter of branch wood was 1-3 cm.

monoterpene	stem wood			branch wood		
	mean	min.	max.	mean	min.	max.
α-pinene	1137	1	13914	43	2	90
β-pinene	696	0	13748	30	1	107
camphene	183	0	1925	3	0	7
limonene	186	0	1982	2	0	8
Δ^3-carene	103	0	993	3	0	13
myrcene	193	0	2162	0	0	0
total	2499	(N=26)		79	(N=10)	

The high variability in the monoterpene content of dead stem wood is caused by the function and the storage of monoterpenes in the tree. The terpenes are not homogeneously distributed within the wood, but stored in discrete resin ducts (see Figure 85). If the tree is injured, the resin is produced in larger amounts and transported to the injured regions (Trapp and Croteau, 2001). This leads to an additional accumulation of large amounts of monoterpene-containing resin in the affected areas. The dead wood at the Lackenberg exhibits lots of these monoterpene-rich wood spots, because of the injuries of the trees caused by the

wind-throw damages and by bark beetle bore holes. The exposition of the dead wood to the harsh weather conditions at the upland of the Bavarian Forest can have led to a fast depletion of the monoterpene pool of unsheltered wood, which explains the very low content in some samples.

In the stem wood of the dead spruces, the monoterpene pool was dominated by α-pinene and β-pinene, followed by camphene, limonene, Δ^3-carene and myrcene (Figure 90, left). p-cymene and eucalyptol could not be quantified in this experiment due to limitations in the analysis setup. Literature values of the content of monoterpenes in spruce wood differ strongly, but the pinenes are generally reported to be the most important substances (Figure 90, right). The total monoterpene content listed here, cannot directly be compared to the values of the present work, because they are based on fresh-mass, not on dry-weight. The conversion factor dry-weight/ fresh-mass is approximately 0.5. If this conversion factor is considered, the mean of the monoterpene content of the stem wood determined in this work is still in the range of values for living spruce material.

monoterpene	Persson	Sallas	Ghirardo
tissue	xylem	stem of seedlings	bark
α-pinene	54%	21.2%	29.2%
β-pinene	31.7%	28.4%	49.4%
camphene	1.1%	1.9%	8.8%
limonene	3.3%	32.8%	5.3%
Δ^3-carene	2.5%	9.7	/
myrcene	1.8%	3.6%	7.2%
total content	/	1026 µg/g$_{(FW)}$	1600 µg/g$_{(FW)}$

Pie chart (left) labels: α-pinene, β-pinene, camphene, limonene, Δ^3-carene, myrcene. Values: 27.9%, 7.33%, 7.45%, 4.12%, 7.73%, 45.5%.
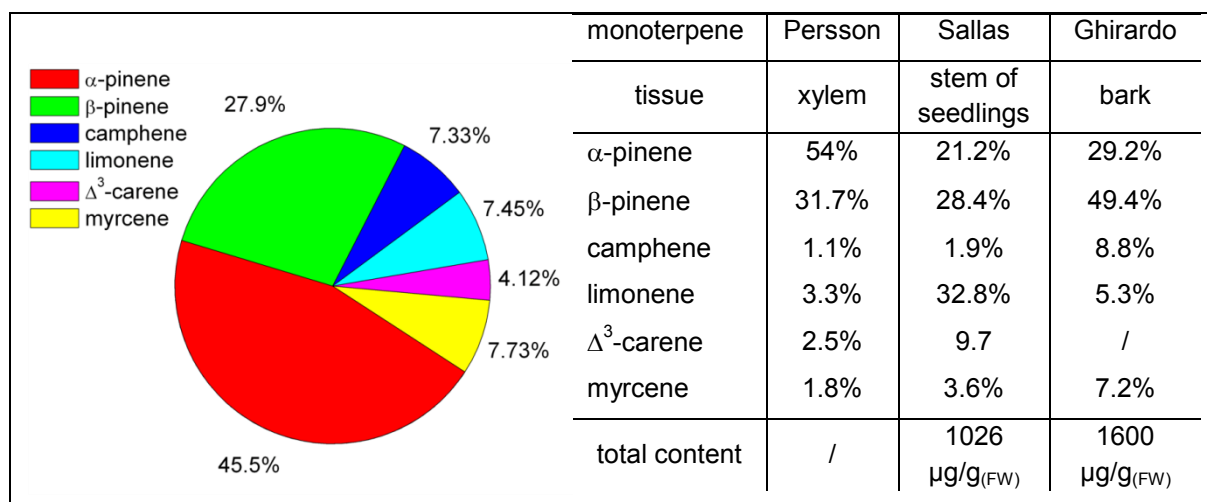
Figure 90. Left: Average endogenous monoterpene pattern in stem material of dead wood collected at the Lackenberg 2011, (N=26). Right: Literature values of monoterpene content in different tissues of Norway spruce. Data from Persson et al., 1996, Sallas et al., 2003 and Ghirardo et al. 2010.

The monoterpene pattern of the air concentration (see chapter 4.3.1), of the average emission (see chapter 4.3.8), and of the pool of the dead wood depict a very similar picture (Table 29). Small deviances can be explained by the different data collection periods (2009-2011 for the air concentration, 2010-2011 for the emission, 2011 for the pool) and the compounds eucalyptol and p-cymene, which were not quantifiable in the content measurement, and limonene, which could not be measured in the flux

determination. Myrcene, which was detected in the dead wood, was not measured in the air, most likely because of its very short atmospheric lifetime of a few minutes (see Table 3).

Nevertheless, the similarity of the 3 monoterpene patterns provide additional confidence in the results presented in this work and is another indication for the dead wood as the main source of monoterpenes in the wind-throw area.

Table 29. Monoterpene composition of the air, the emission and the dead wood determined in the present work.

monoterpene	air concentration	emission	content
α-pinene	35.1%	35.2%	45.5%
β-pinene	30.0%	26.4%	27.9%
eucalyptol	21.6%	23.9%	/
Δ^3-carene	4.4%	3.9%	4.1%
p-cymene	4.0%	8.5%	/
limonene	3.6%	/	7.4%
camphene	2.0%	2.1%	7.3%
myrcene	/	/	7.2%

4.3.11. Determination of the total monoterpene pool in the wind-throw area Lackenberg

The total dead tree biomass at the Lackenberg site was divided into stem mass (including stem wood, bark and stumps) and branch mass (including branches and fine roots). This differentiation was done, because of the very different monoterpene content in the different plant parts (Table 28). The monoterpene pool in both compartments was calculated from the biomass per square meter (2.6 kg/m^2 for stem mass and 1.6 kg/m^2 for branch mass, see chapter 2.1.3) and the monoterpene content per gram dead wood (2500 µg/g$_{(DW)}$ for stem mass and 79 µg/g$_{(DW)}$ for branch mass, Table 28) to be 6.6 g/m^2 for stem mass and 0.13 g/m^2 for branch mass. The total monoterpene pool stored in the dead wood in the whole wind-throw area therefore was 1800 kg.

A more relevant estimate for the amount of monoterpenes that is available for emission is calculated by the active mass of the dead wood. The terpenes which are

stored inside the stems cannot be emitted due to a high diffusion resistance of the wood. The mass of dead wood which can directly emit monoterpenes was calculated based on the assumption that only the outer 2 cm of the wood can contribute to the emission. Thus the calculation of the stem biomass by allometric functions (see appendix) was performed a second time with stem diameters reduced by 4 cm. The difference between the initial mass and the second biomass calculation was used as the mass of stem wood that acts as the monoterpene source. The fraction of active stem mass under this assumption results in approximately 12% of the total stem mass. The active branch mass was set to 90% of the total mass, since most of the branches had a diameter below 3 cm and thus can be treated as an almost completely accessible pool. The monoterpene amount directly available for emission results in 0.9 g/m^2 or 13% of the initial value.

This value should be treated with high caution since some approximations were necessary to estimate it. The determination of the biomass is limited in its accuracy by the applicability of the allometric functions and the uncertainties of the aerial photo analysis. The natural high variability in the monoterpene content of the dead wood material offers another source of errors, because small terpene-rich damaged spots can contribute largely to the total monoterpene content.

4.3.12. Comparison of the α-pinene emission and the storage pool in the dead wood

The α-pinene amount stored in the dead wood at the Lackenberg can be calculated the same way as the total monoterpene content, which is described in the previous chapter. The resulting pool of α-pinene is 3.1 g/m^2 for the total mass of dead wood and 0.4 g/m^2 if only the active fraction is considered. If the latter value is used, the existing pool can last approximately 4 more years, if the emission strength of α-pinene stays constant at the level of 2011 (0.11 g/m^2, see section 4.3.9). Since the active pool can be replenished by the storage pool inside the stems and the emission might decrease, the dead wood might be a source of monoterpenes for a few decades at lower rates. The newly emerging spruce population at the Lackenberg will grow and it will account for the larger fraction of the monoterpene emission in the future, but the contribution of the dead wood might still be substantial in the next few years.

5. Summary and conclusions

This study constitutes the first measurements of the emission and concentration dynamics of monoterpenes above a wind-throw disturbed spruce forest ecosystem. The national parks "Bavarian Forest" and "Berchtesgaden" offered excellent conditions for these investigations in nearly pristine and unmanaged wind-throw areas. In contrast to common practice, the dead wood remained on site in these protected areas. The measurement sites were two wind-throw areas of 27 ha (Lackenberg, Bavarian Forest) and 3 ha (Kühroint, Berchtesgaden), which were equipped with meteorological observation stations and monoterpene sampling facilities. The air concentration of terpenes in the years 2009-2011 was determined by sampling on adsorption tubes and analysis by gas chromatography-mass spectroscopy.

In Kühroint, the monoterpene composition of the air was dominated by α- and β-pinene, which represented almost ¾ of the total monoterpene loading. The residual was formed by Δ^3-carene, eucalyptol, limonene, p-cymene and camphene. The highest total loading of monoterpene in the air was measured in August 2010 with 649.3 pmol/mol. In the wintertime and summer nights the monoterpene levels in ambient air were usually below 10 pmol/mol. The monoterpene concentration in the air showed a daily cycle, following mainly the surface temperature with a variable time shift, where the highest levels were reached in the afternoon. Since the vegetation in the wind-throw area Kühroint is diverse and in addition to the dead wood there are living spruce, maple, willow and larch, parts of the measured monoterpenes are likely to originate from the living vegetation.

In the Lackenberg area of the Bavarian Forest National Park, similarly to the Kühroint site, dominant substances were α- and β-pinene. However, at 21.6%, the fraction of eucalyptol on the total monoterpene loading of the air was considerably higher. A possible explanation is the living vegetation at the Kühroint site (Norway spruce, sycamore maple, goat willow and European larch), which may be a relevant source of monoterpenes with a different emission mix to the dead wood. 15% of the monoterpene composition in air was made up by limonene, p-cymene, camphene and Δ^3-carene. The highest observed ambient monoterpene level was 655 pmol/mol in summer 2009. The monoterpene concentration in the air above the wind-throw area Lackenberg showed a prominent daily cycle and can be described very

precisely in terms of the surface temperature, which closely resembles the temperature of the source in the dead trees. This relation was described mathematically by an exponential dependence of the monoterpene level on the surface temperature. The exponential behavior was interpreted as an Arrhenius type diffusion limited emission of the volatiles out of a pool in the dead wood into the atmosphere. The concentration of monoterpenes in the air was overall decreasing from 2009 to 2010, which indicated a smaller source in the area, probably due to a depletion of the monoterpene pool in the dead wood. This result strongly attributes the dead wood as the main monoterpene source in the wind-throw area.

Due to its dimension and large scale homogeneity, the wind-throw area Lackenberg was very suitable for micrometeorological flux measurements. Two methods, based on the flux-gradient relations, were used to quantify monoterpene emissions in summer and autumn 2010 and 2011: the modified Bowen ratio method, and the surface layer gradient technique. The emissions measured by the two techniques showed a reasonably good correlation and followed a daily cycle, in general showing maximal values at noon. Highest observed emissions were 59 ng/(m^{2}s) for α-pinene, 39 ng/(m^{2}s) for β-pinene, 29 ng/(m^{2}s) for eucalyptol, 18 ng/(m^{2}s) for p-cymene, 8.1 ng/(m^{2}s) for Δ^3-carene and 4.4 ng/(m^{2}s) in the case of camphene, all measured on the same day in July 2011. This sums up to a maximal monoterpene emission of 158 ng/(m^{2}s). Thus, even four years after the storm event, the wind-throw was still a significant source of monoterpenes, with a source strength comparable to the one of living spruce ecosystems (e.g., Christensen et al., 2000; Grabmer et al., 2004; Graus et al., 2006).

The emission of monoterpenes was modeled in terms of the surface temperature using the exponential algorithm developed by Guenther et al., 1993, leading to a very good fit of the measured data in the daily cycle. Other than the surface temperature, no meteorological variables were found to be driving parameters for the emission of terpenes.

A model based on this algorithm, derived from all measured emission values was used to calculate the total emission of α-pinene in the years 2010 and 2011. The result showed the high variability in the emission of monoterpenes: the emission can be very high on warm summer days (up to 80 ng$_{(\alpha\text{-pinene})}$/(m^{2}s)), but is generally low in the winter time or at cold nights. The annual α-pinene emission at the Lackenberg

site was determined at 0.11 ± 0.05 g/m^2 in both years 2010 and 2011, which sums up to 29 kg of α-pinene emitted from the total wind-throw area per year.

The monoterpene content of the dead wood at the Lackenberg measured in summer 2011 was still very high and in the range of that in living spruce material. The relative mix of monoterpenes in the air, in the emission, and in the dead wood was very similar. This clearly identifies the dead wood as the main source of monoterpenes in the wind-throw area.

Up to now dead vegetation has hardly been considered as a significant source of natural VOCs. Large regions in Central Europe, but especially in North America and Russia, are affected by bark beetles infestations (Raffa et al., 2008), which lead to vast areas of dead wood. Clearly, in such regions, this so far unaccounted source needs to be considered in models of surface VOC emissions.

In natural forests the amount of dead wood can reach up to 40% of the total woody biomass (Siitonen, 2001). The source strength for monoterpenes of this dead wood is not negligible, as shown here. However, VOC emission inventories do not account for such a source so far. Thus, including this (so far unrecognized) dead wood source in the emission modeling of reactive trace gases in forest ecosystems bears the potential to substantially improve regional and global biogenic VOC emission estimates.

To assess the role of wind-throws on a global scale is extremely difficult. The global monoterpene emission from coniferous trees is approximately 25 Tg carbon per year (Lathiere et al., 2006). With a global dead wood fraction of about 13% (FAO, 2010), and emission properties of the dead wood similar to that of living conifers (as suggested by the present study), a total of over 3 Tg carbon per year is estimated to be emitted globally in coniferous forests by dead wood alone.

The total global monoterpene emission is estimated at about 120 TgC/a (Guenther et al., 1996; Arneth et al., 2008; Laothawornkitkul et al., 2009), and the largest fraction of this emission (approximately 60 TgC) is likely to come from the tropical region (Lathiere et al., 2006). However, with current knowledge, these emission estimates are not well constrained, since they are based on only few in-situ VOC emission studies and few ecosystem types in the tropics (Geron et al., 2002; Rinne et al., 2002; Karl et al., 2004; Greenberg et al., 2004; Langford et al., 2010). Nevertheless, it is plausible to assume that dead wood in tropical rain forests, with their fast turnover rates, contributes strongly to monoterpene emissions. Daring to extrapolate

from such scarce and ill-constrained data, we conclude that global estimates of monoterpene emissions, based on living biomass alone, underestimate the true total by 10-20%.

In answer to the main research questions of this study (section 1.8), the principal results are summarized as:

- Wind-throw areas are potentially strong sources of monoterpenes (up to 158 $ng/(m^2s)$), with emission magnitudes similar to living forests.

- The monoterpene air concentration in the wind-throw area is high on summer days (observed up to 649.3 pmol/mol), and low in winter and cold summer nights (below 10 pmol/mol), and shows a clear daily and seasonal course, following that of the surface temperature closely.

- The emission of monoterpenes can be described reasonably well by an exponential model, depending on the surface temperature only.

- The annual emission of α-pinene calculated by this model is 29 ± 14.5 kg in the wind-throw area (27 ha), even four years after the storm event

- The total pool of α-pinene in the dead wood of the wind-throw area (determined four years after the event) is approximately 830 kg; so the area is expected to remain a source of monoterpenes, at least for the next few years.

- The two different wind-throw areas in the national parks Bavarian Forest and Berchtesgaden showed overall similar monoterpene air composition patterns; individual differences can be attributed to more living vegetation at the Berchtesgaden site.

Appendices

Additional data and information to the work presented in the previous chapters, lists of the abbreviations, figuresn and tables used in the work can be found here in the appendices.

A1   Information for chapter 2. Site description

<u>Additional meteorological data collected at the measurement sites</u>

The following figures show meteorological data collected at the central stations Lackenberg and Kühroint. Data is presented as measured as 10-minute averages without gap filling. Missing data is mainly caused by technical failure.
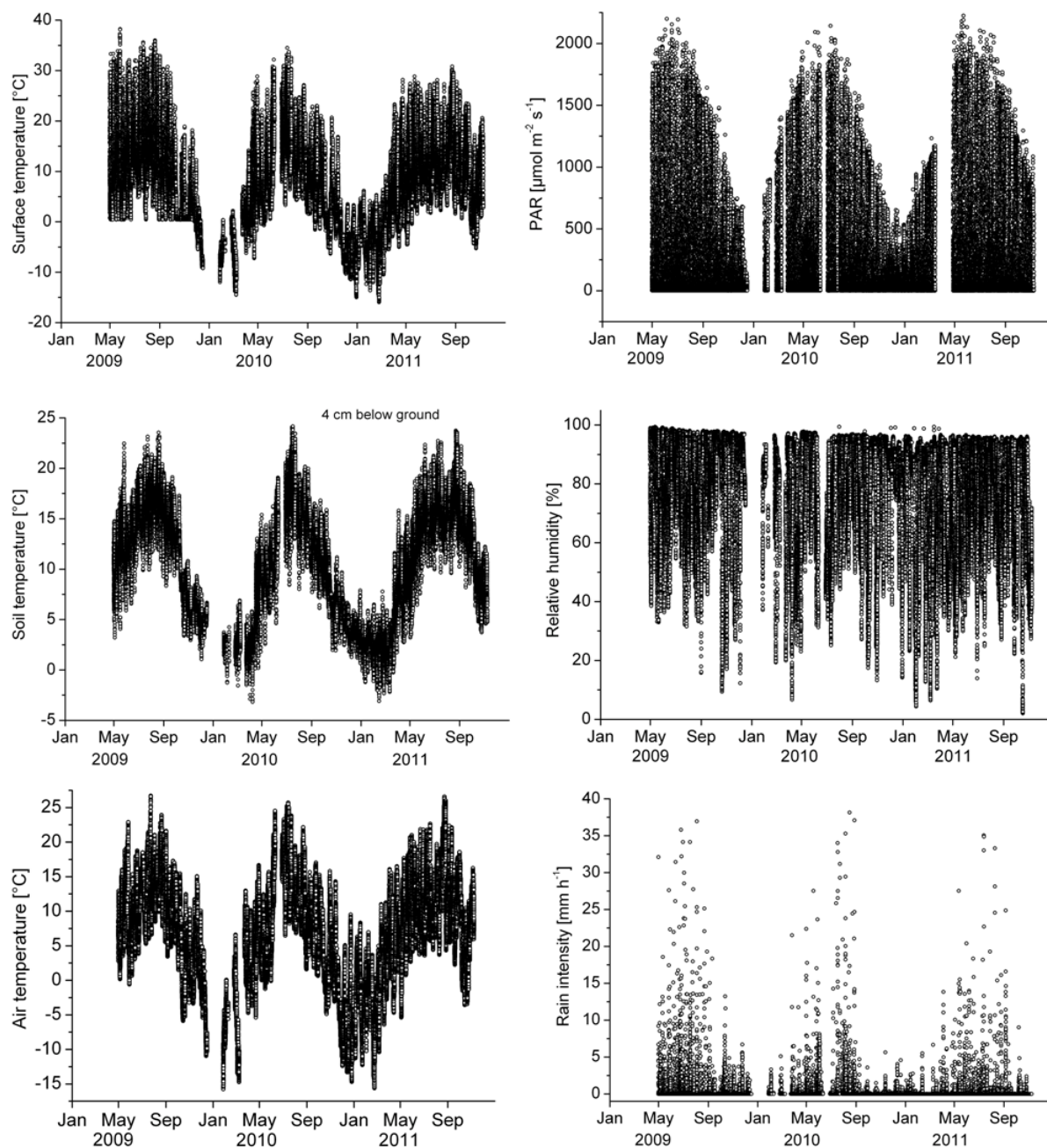
Figure 91. Meteorological data at the central station Lackenberg 2009-2011. Measurement interval: 10 minutes. The sensor of the surface temperature was replaced at the 20.11.2009, because it was not capable to measure temperatures below 0°C.
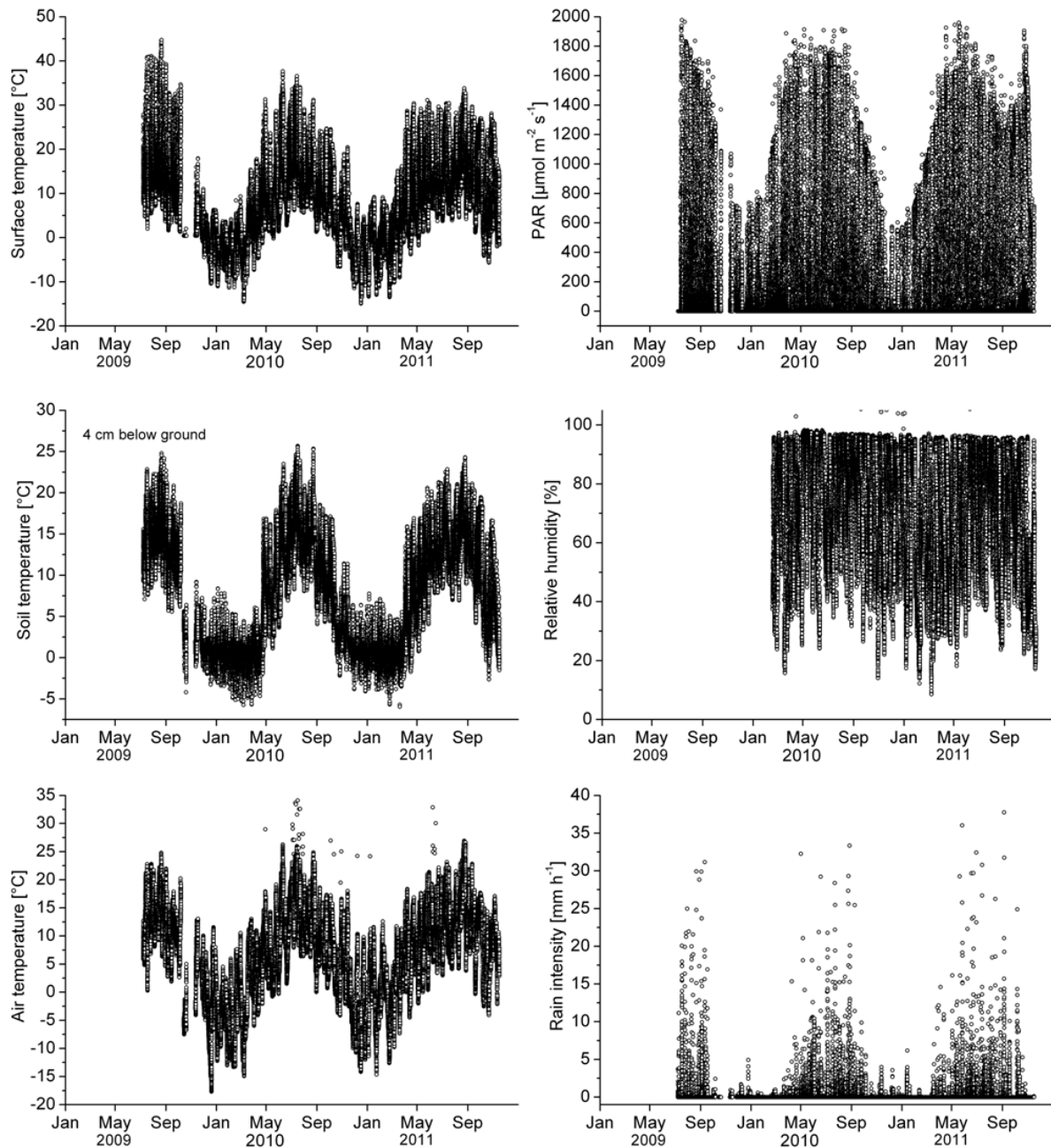
Figure 92. Meteorological data at the central station Kühroint 2009-2011. Measurement interval: 10 minutes. The sensor of the surface temperature was replaced at the 18.11.2009, because it was not capable to measure temperatures below 0°C.

<u>Allometric tree functions</u>

Allometric functions (Repola, 2009) used to calculate the amount of tree biomass on the Lackenberg site. The functions describe Norway spruce trees in boreal forests of Finland which are assumed to be very similar to the ones found in the upper regions of the Bavarian Forest National Park.

The masses of living branches and dead branches were summed up to a total branch mass in the calculation in this work.

Stem wood: $m_S = exp\left(b_0 + b_1 \frac{d_{Ski}}{d_{Ski}+14} + b_2 \ln(h_{ki}) + b_3 h_{ki} + u_k + e_{ki}\right)$

Stem bark: $m_{Sb} = exp\left(b_0 + b_1 \frac{d_{Ski}}{d_{Ski}+18} + b_2 \ln(h_{ki}) + u_k + e_{ki}\right)$

Living branches: $m_{lb} = exp\left(b_0 + b_1 \frac{d_{Ski}}{d_{Ski}+13} + b_2 \frac{h_{ki}}{h_{ki}+5} + u_k + e_{ki}\right)$

Dead branches: $m_{db} = exp\left(b_0 + b_1 \frac{d_{Ski}}{d_{Ski}+18} + \ln(h_{ki}) + u_k + e_{ki}\right)$

Stump: $m_{stump} = exp\left(b_0 + b_1 \frac{d_{Ski}}{d_{Ski}+26} + u_k + e_{ki}\right)$

Roots: $m_R = exp\left(b_0 + b_1 \frac{d_{Ski}}{d_{Ski}+24} + u_k + e_{ki}\right)$

Where mass is in kg, d_{Ski} = 2+1.25*d, d is the tree diameter in breast height in cm, h_{ki} is the tree height in m. Mass of roots is the mass of roots with a diameter > 1cm.

Table 30. Parameters for the calculation of biomass of Norway spruce. Values from Repola 2009.

	Stem wood	Stem bark	Living branches	Dead branches	Stump	Roots
b_0	-3.655	-4.349	-3.914	-5.467	-3.962	-2.295
b_1	7.942	9.879	15.22	6.252	11.725	10.649
b_2	0.907	0.274	-4.35	1.068	-	-
b_3	0.018	-	-	-	-	-
u_k	0.006	0.016	0.022	0.256	0.065	0.105
e_{ki}	0.008	0.036	0.089	0.335	0.058	0.114

A2   Information for chapter 4. Results
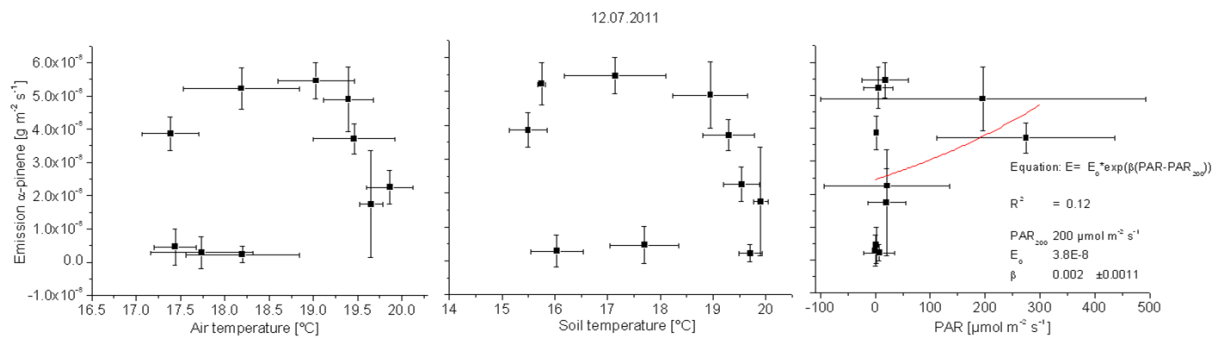
Figure 93. Relation of the emission of α-pinene calculated by the mean bulk conductance and meteorological parameters at the Lackenberg 12.07.2011. Error bars of the emission represent the uncertainty calculated by error propagation. Error bars of the meteorological quantities represent their range in the 60 minute measurement interval.
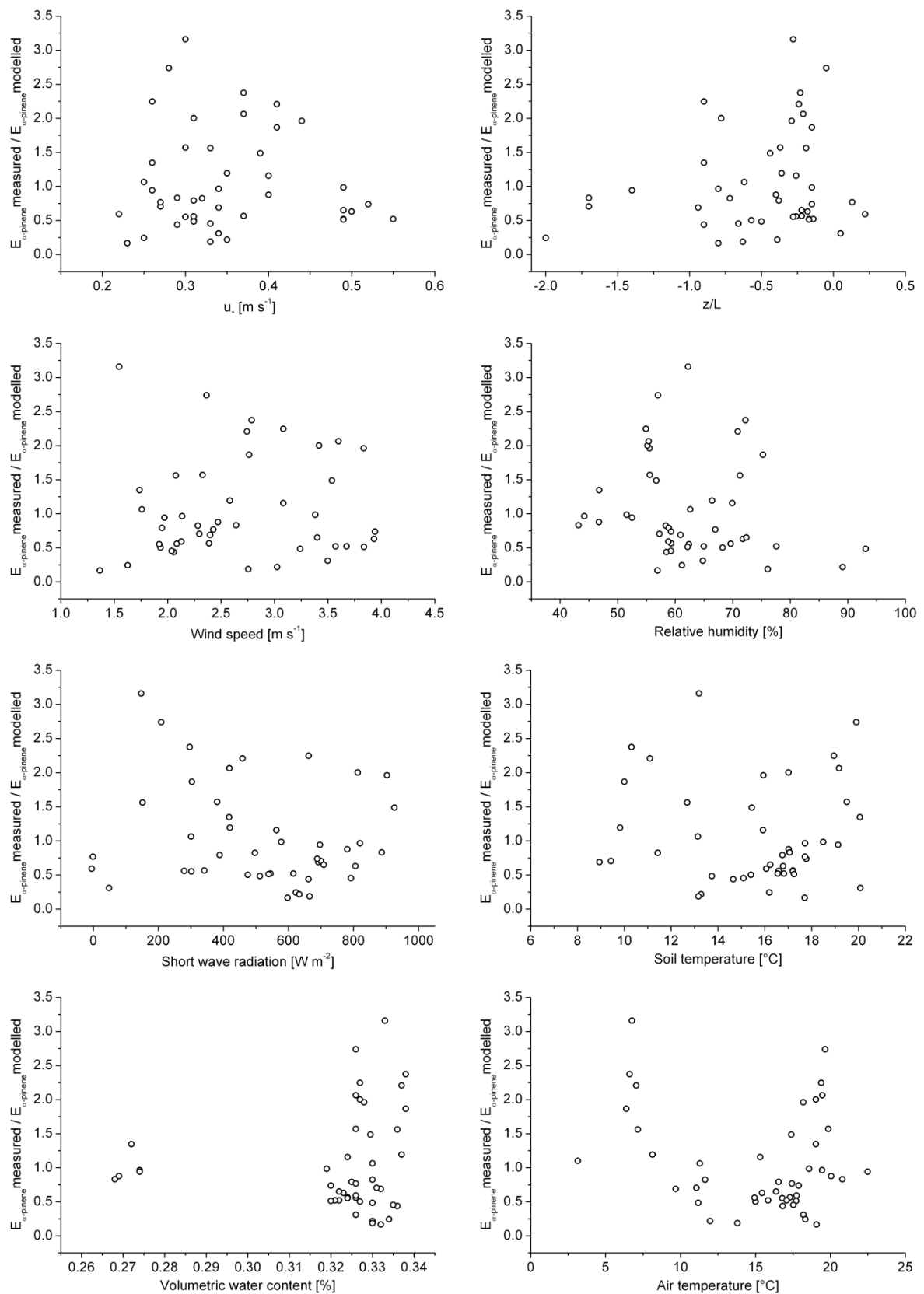
Figure 94. Relation of different meteorological parameters and the surface temperature normalized emission of α-pinene at the Lackenberg in the years 2010 and 2011. Data selected according to quality criteria (see chapter 3.2.4).
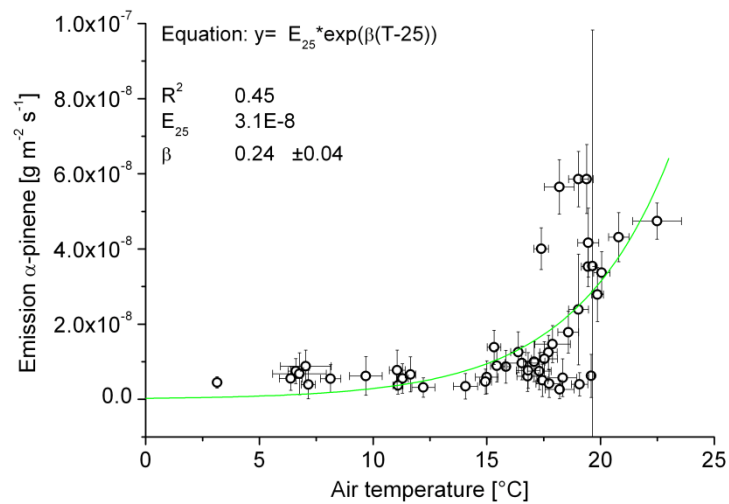
Figure 95. Relation of the air temperature and the emission of α-pinene calculated by the mean bulk conductance at the Lackenberg in the years 2010 and 2011. Data selected according to quality criteria (see chapter 3.2.4). Error bars of the emission represent the uncertainty calculated by error propagation. Error bars of the air temperature represent the range of air temperature in the measurement interval.

A3   List of abbreviations and symbols

Acetyl-CoA	acetyl coenzyme-A
AT	air temperature
AWS	Bavarian Avalanche Warning Service
BioVOC	biogenic volatile organic compound
c	concentration
CCN	cloud condensation nuclei
CO_2	carbon dioxide
d	zero-plane displacement height
DMADP	dimethylallyl diphosphate
EC	eddy covariance
F	vertical flux
G	soil heat flux
g	gravitational acceleration
GDP	geranyl diphosphate
GC	gas chromatography
H_2O	water
HTs	sensible heat flux
IDP	isopentenyl diphosphate
K	eddy diffusivity
L	Obukhov length
LvE	latent heat flux
LOD	limit of detection
MBO	2-methyl-3-butene-2-ol
MBR	modified Bowen ratio method
MEP	2-C-methyl-D-erythritol 4-phosphate
min	minute
MS	mass spectrometry
MVA	mevalonate
MW	molecular weight
NMHC	non-methane hydrocarbons
ng	nanogram, 10^{-9} gram
PAR	photosynthetic active radiation

PCC	Pearson correlation coefficient
pmol	picomol, 10^{-12} mol
ppt	parts per trillion
RF_i	the response factor of the analyte i
R_{net}	net radiation
R_G	incoming short wave radiation
SLG	surface layer gradient technique
SOA	secondary organic aerosol
ST	surface temperature (radiation temperature)
T	temperature
UTC	Coordinated Universal Time
u_*	friction velocity
VOC	volatile organic compound
w	vertical wind speed
z	height
z_0	roughness length
Δ	general denotation of a difference
κ	von Kármán constant (0.4)
λ	atmospheric bulk conductance
ξ	scalar (e.g. CO_2, H_2O, VOC, temperature…)
φ	universal functions
Φ	integrated forms of the universal function

A4   List of figures and captions

A5   List of tables

References

Alvarado, A., E. C. Tuazon, S. M. Aschmann, R. Atkinson and J. Arey, Products of the gas-phase reactions of O(P-3) atoms and O-3 with alpha-pinene and 1,2-dimethyl-1-cyclohexene, *Journal of Geophysical Research-Atmospheres, 103*(D19), 25541-25551, 1998.

Andreae, M. O., Hegg D.A. and U. Baltensperger, Sources and Nature of Atmospheric Aerosols., in Aerosol Pollution Impact on Precipitation., edited by Levin Z. and Cotton W.R., pp. 45-89, Springer Verlag, 2009.

Arimura, G., C. Kost and W. Boland, Herbivore-induced, indirect plant defences, *Biochimica et Biophysica Acta-Molecular and Cell Biology of Lipids, 1734*(2), 91-111, 2005.

Arneth, A., R. K. Monson, G. Schurgers, U. Niinemets and P. I. Palmer, Why are estimates of global terrestrial isoprene emissions so similar (and why is this not so for monoterpenes)?, *Atmospheric Chemistry and Physics, 8*(16), 4605-4620, 2008.

Arneth, A. and U. Niinemets, Induced BVOCs: how to bug our models?, *Trends in Plant Science, 15*(3), 118-125, 2010.

Atkins, P. W., Physical Chemistry, Oxford University Press, Oxford, 1986.

Atkinson, R., Atmospheric chemistry of VOCs and NOx, *Atmospheric Environment, 34*(12-14), 2063-2101, 2000.

Atkinson, R. and J. Arey, Gas-phase tropospheric chemistry of biogenic volatile organic compounds: a review, *Atmospheric Environment, 37*, S197-S219, 2003.

Aubinet, M., C. Feigenwinter, B. Heinesch, C. Bernhofer, E. Canepa, A. Lindroth, L. Montagnani, C. Rebmann, P. Sedlak and E. Van Gorsel, Direct advection measurements do not help to solve the night-time CO2 closure problem: Evidence from three different forests, *Agricultural and Forest Meteorology, 150*(5), 655-664, 2010.

Aubinet, M., T. Vesala and D. Papale, Eddy Covariance : A Practical Guide to Measurement and Data Analysis, Springer Netherlands, Dordrecht, 2012.

Bäck, J., J. Aalto, M. Henriksson, H. Hakola, Q. He and M. Boy, Chemodiversity in terpene emissions at a boreal Scots pine stand, *Biogeosciences Discuss., 8*(5), 10577-10615, 2011.

Baldocchi, D., E. Falge, L. H. Gu, R. Olson, D. Hollinger, S. Running, P. Anthoni, C. Bernhofer, K. Davis, R. Evans, J. Fuentes, A. Goldstein, G. Katul, B. Law, X. H. Lee, Y. Malhi, T. Meyers, W. Munger, W. Oechel, K. U, K. Pilegaard, H. P. Schmid, R. Valentini, S. Verma, T. Vesala, K. Wilson and S. Wofsy, FLUXNET: A new tool to study the temporal and spatial variability of ecosystem-scale carbon dioxide, water vapor, and energy flux densities, *Bulletin of the American Meteorological Society, 82*(11), 2415-2434, 2001.

Baldocchi, D. D., B. B. Hincks and T. P. Meyers, Measuring Biosphere-Atmosphere Exchanges of Biologically Related Gases with Micrometeorological Methods, *Ecology, 69*(5), 1331-1340, 1988.

Bark beetle project I, Analyse der Borkenkäfersituation in den Nationalparken Bayerischer Wald und Berchtesgaden (Borkenkäfer-Dispersion), Bavarian State Ministry of the Environment and Public Health, UGV06070204028, 2007.

Bark beetle project II, Borkenkäferbefall auf Windwurfflächen: Prozessanalyse für Handlungsoptionen, Bavarian State Ministry of the Environment and Public Health, UGV06080204000, 2008.

Barnes, I., Becker K., Bruckmann P., Gilge S., G. Smiatek, Steinbrecher R. and Wiesen P., KOHLENWASSERSTOFFE, STICKOXIDE UND OZON - DICKE LUFT, in Chemie über den Wolken, Zeller R., 2011.

Behnke, K., B. Ehlting, M. Teuber, M. Bauerfeind, S. Louis, R. Haensch, A. Polle, J. Bohlmann and J. P. Schnitzler, Transgenic, non-isoprene emitting poplars don't like it hot, *Plant Journal, 51*(3), 485-499, 2007.

Bengtsson, L., K. I. Hodges and E. Roeckner, Storm tracks and climate change, *Journal of Climate, 19*(15), 3518-3543, 2006.

Bohlander, F. and R. Schopf, Response to pheromones, pheromone production and energetic state in Ips typographus (Coleoptera, Scolytidae), DEUTSCHEN GESELL ALLGEMEINE & ANGEWANDTE ENTOMOLOGIE, BREMEN 33, 1999.

Bohlmann, J. and C. I. Keeling, Terpenoid biomaterials, *Plant Journal, 54*(4), 656-669, 2008.

Bohlmann, J., G. Meyer-Gauen and R. Croteau, Plant terpenoid synthases: Molecular biology and phylogenetic analysis, *Proceedings of the National Academy of Sciences of the United States of America, 95*(8), 4126-4133, 1998.

Bouvier-Brown, N. C., R. Holzinger, K. Palitzsch and A. H. Goldstein, Large emissions of sesquiterpenes and methyl chavicol quantified from branch enclosure measurements, *Atmospheric Environment, 43*(2), 389-401, 2009.

Buettner, A. and P. Schieberle, Characterization of the most odor-active volatiles in fresh, hand-squeezed juice of grapefruit (Citrus paradisi Macfayden), *Journal of Agricultural and Food Chemistry, 47*(12), 5189-5193, 1999.

Burba and Anderson, A Brief Practical Guide to Eddy Covariance Flux Measurements: Principles and Workflow Examples for Scientific and Industrial Applications., Lincoln,USA, 2010.

Businger, J. A., Evaluation of the Accuracy with Which Dry Deposition Can be Measured with Current Micrometeorological Techniques, *Journal of Climate and Applied Meteorology, 25*(8), 1100-1124, 1986.

Businger, J. A., J. C. Wyngaard, Y. Izumi and E. F. Bradley, Flux-Profile Relationships in Atmospheric Surface Layer, *Journal of the Atmospheric Sciences, 28*(2), 181-&, 1971.

Butler, L. D. and M. F. Burke, Chromatographic Characterization of Porous Polymers for Use As Adsorbents in Sampling Columns, *Journal of Chromatographic Science, 14*(3), 117-122, 1976.

Calfapietra, C., S. Fares and F. Lofeto, Volatile organic compounds from Italian vegetation and their interaction with ozone, *Environmental Pollution, 157*(5), 1478-1486, 2009.

Calogirou, A., B. R. Larsen and D. Kotzias, Gas-phase terpene oxidation products: a review, *Atmospheric Environment, 33*(9), 1423-1439, 1999.

Carslaw, K. S., O. Boucher, D. V. Spracklen, G. W. Mann, J. G. L. Rae, S. Woodward and M. Kulmala, A review of natural aerosol interactions and feedbacks within the Earth system, *Atmospheric Chemistry and Physics, 10*(4), 1701-1737, 2010.

Cataldo, F., O. Ursini, E. Lilla and G. Angelini, Ozonolysis of alpha-PINENE, beta-PINENE, d- and l-Turpentine Oil Studied by Chirooptical Methods; Some Implications on the Atmospheric Chemistry of Biogenic Volatile Organic Compounds, *Ozone-Science & Engineering, 32*(4), 274-285, 2010.

Christensen, C. S., P. Hummelshoj, N. O. Jensen, B. Larsen, C. Lohse, K. Pilegaard and H. Skov, Determination of the terpene flux from orange species and Norway spruce by relaxed eddy accumulation, *Atmospheric Environment, 34*(19), 3057-3067, 2000.

Chung, S. H. and J. H. Seinfeld, Global distribution and climate forcing of carbonaceous aerosols, *Journal of Geophysical Research-Atmospheres, 107*(D19), 2002.

Constable, J. V. H., M. E. Litvak, J. P. Greenberg and R. K. Monson, Monoterpene emission from coniferous trees in response to elevated CO2 concentration and climate warming, *Global Change Biology, 5*(3), 255-267, 1999.

Copolovici, L. O., I. Filella, J. Llusia, U. Niinemets and J. Penuelas, The capacity for thermal protection of photosynthetic electron transport varies for different monoterpenes in Quercus ilex, *Plant Physiology, 139*(1), 485-496, 2005.

Curci, G., M. Beekmann, R. Vautard, G. Smiatek, R. Steinbrecher, J. Theloke and R. Friedrich, Modelling study of the impact of isoprene and terpene biogenic emissions on European ozone levels, *Atmospheric Environment, 43*(7), 1444-1455, 2009.

Davidson, E. A., K. Savage, L. V. Verchot and R. Navarro, Minimizing artifacts and biases in chamber-based measurements of soil respiration, *Agricultural and Forest Meteorology, 113*(1-4), 21-37, 2002.

Demole, E., P. Enggist and G. Ohloff, 1-Para-Menthene-8-Thiol - A Powerful Flavor Impact Constituent of Grapefruit Juice (Citrus-Paradisi Macfayden), *Helvetica Chimica Acta, 65*(6), 1785-1794, 1982.

Derwent, R. G., M. E. Jenkin, N. R. Passant and M. J. Pilling, Photochemical ozone creation potentials (POCPs) for different emission sources of organic compounds under European conditions estimated with a Master Chemical Mechanism, *Atmospheric Environment, 41*(12), 2570-2579, 2007.

Dicke, M., Behavioural and community ecology of plants that cry for help, *Plant Cell and Environment, 32*(6), 654-665, 2009.

Dicke, M., T. A. Vanbeek, M. A. Posthumus, N. Bendom, H. Vanbokhoven and A. E. Degroot, Isolation and Identification of Volatile Kairomone That Affects Acarine Predator-Prey Interactions - Involvement of Host Plant in Its Production, *Journal of Chemical Ecology, 16*(2), 381-396, 1990.

Dominguez-Taylor, P., L. G. Ruiz-Suarez, I. Rosas-Perez, J. M. Hernandez-Solis and R. Steinbrecher, Monoterpene and isoprene emissions from typical tree species in forests around Mexico City, *Atmospheric Environment, 41*(13), 2780-2790, 2007.

Donat, M., D. Renggli, S. Wild, L. Alexander, V, G. Leckebusch and U. Ulbrich, Reanalysis suggests long-term upward trends in European storminess since 1871, *Geophysical Research Letters, 38*, 2011.

Dudareva, N., F. Negre, D. A. Nagegowda and I. Orlova, Plant volatiles: Recent advances and future perspectives, *Critical Reviews in Plant Sciences, 25*(5), 417-440, 2006.

Easterling, D. R., G. A. Meehl, C. Parmesan, S. A. Changnon, T. R. Karl and L. O. Mearns, Climate extremes: Observations, modeling, and impacts, *Science, 289*(5487), 2068-2074, 2000.

EEA, Air pollution by Ozone across Europe during Summer 2009, EEA Report, 2., 2010.

Engelhart, G. J., A. Asa-Awuku, A. Nenes and S. N. Pandis, CCN activity and droplet growth kinetics of fresh and aged monoterpene secondary organic aerosol, *Atmospheric Chemistry and Physics, 8*(14), 3937-3949, 2008.

Fall R., Biogenic Emissions of Volatile Organic Compounds from Higher Plants, in Reactive Hydrocarbons in the Atmosphere, edited by C. N. Hewitt, pp. 41-96, Academic Press, San Diego, 1999.

FAO, (Food and Agriculture Organization of the United Nations), Global Forest Resources Assessment 2000, Chapter 26. Europe, UN-ECE,Geneva, 2000.

FAO, (Food and Agriculture Organization of the United Nations), Global Forest Resources Assessment 2010, Rome, 2010.

Fink, A. H., T. Brucher, V. Ermert, A. Kruger and J. G. Pinto, The European storm Kyrill in January 2007: synoptic evolution, meteorological impacts and some considerations with respect to climate change, *Natural Hazards and Earth System Sciences, 9*(2), 405-423, 2009.

Flesch, G. and M. Rohmer, Prokaryotic Hopanoids - the Biosynthesis of the Bacteriohopane Skeleton - Formation of Isoprenic Units from 2 Distinct Acetate Pools and A Novel Type of Carbon Carbon Linkage Between A Triterpene and D-Ribose, *European Journal of Biochemistry, 175*(2), 405-411, 1988.

Foken, T., Angewandte Meteorologie: Mikrometeorologische Methoden, Springer, Heidelberg, 2006.

Foken, T. and B. Wichura, Tools for quality assessment of surface-based flux measurements, *Agricultural and Forest Meteorology, 78*(1-2), 83-105, 1996.

Foken, T., The Energy Balance Closure Problem: An Overview, *Ecological Applications, 18*(6), 1351-1367, 2008.

Franceschi, V. R., P. Krokene, E. Christiansen and T. Krekling, Anatomical and chemical defenses of conifer bark against bark beetles and other pests, *New Phytologist, 167*(2), 353-375, 2005.

Friedrich, R., B. Wickert, P. Blank, S. Emeis, W. Engewald, D. Hassel, H. Hoffmann, H. Michael, A. Obermeier, K. Sch+ñfer, T. Schmitz, A. Sedlmaier, M. Stockhause, J. Theloke and F. J. Weber, Development of Emission Models and Improvement of Emission Data for Germany, *Journal of Atmospheric Chemistry, 42*(1), 179-206, 2002.

Fritsche, J., D. Obrist, M. J. Zeeman, F. Conen, W. Eugster and C. Alewell, Elemental mercury fluxes over a sub-alpine grassland determined with two micrometeorological methods, *Atmospheric Environment, 42*(13), 2922-2933, 2008.

Fuentes, J. D., B. P. Hayden, M. Garstang, M. Lerdau, D. Fitzjarrald, D. D. Baldocchi, R. Monson, B. Lamb and C. Geron, New Directions: VOCs and biosphere-atmosphere feedbacks, *Atmospheric Environment, 35*(1), 189-191, 2001.

Fuentes, J. D., M. Lerdau, R. Atkinson, D. Baldocchi, J. W. Bottenheim, P. Ciccioli, B. Lamb, C. Geron, L. Gu, A. Guenther, T. D. Sharkey and W. Stockwell, Biogenic hydrocarbons in the atmospheric boundary layer: A review, *Bulletin of the American Meteorological Society, 81*(7), 1537-1575, 2000.

Fuentes, J. D., D. Wang, H. H. Neumann, T. J. Gillespie, G. DenHartog and T. F. Dann, Ambient biogenic hydrocarbons and isoprene emissions from a mixed deciduous forest, *Journal of Atmospheric Chemistry, 25*(1), 67-95, 1996.

Gallego, E., F. J. Roca, J. F. Perales and X. Guardino, Comparative study of the adsorption performance of a multi-sorbent bed (Carbotrap, Carbopack X, Carboxen 569) and a Tenax TA adsorbent tube for the analysis of volatile organic compounds (VOCs), *Talanta, 81*(3), 916-924, 2010.

Gardiner, B., Blennow K., Carnus J.M., Fleischner P., Ingemarson F., Landmann G., Lindner M., Marzano M., Nicoll B., Orazio C., Peyron J.L., Reviron M.P., M. J. Schelhaas, Schuck A., Spielmann M. and T. Usbeck, Destructive storms in European forests: past and forthcoming impacts, European Forest Institute, [S.l.], 2010.

Geron, C., A. Guenther, J. Greenberg, H. W. Loescher, D. Clark and B. Baker, Biogenic volatile organic compound emissions from a lowland tropical wet forest in Costa Rica, *Atmospheric Environment, 36*(23), 3793-3802, 2002.

Ghirardo, A., K. Koch, R. Taipale, I. Zimmer, J. P. Schnitzler and J. Rinne, Determination of de novo and pool emissions of terpenes from four common boreal/alpine trees by 13CO(2) labelling and PTR-MS analysis, *Plant Cell and Environment, 33*(5), 781-792, 2010.

Ghirardo, A., J. Gutknecht, I. Zimmer, N. Brueggemann and J. P. Schnitzler, Biogenic Volatile Organic Compound and Respiratory CO(2) Emissions after (13)C-Labeling: Online Tracing of C Translocation Dynamics in Poplar Plants, *Plos One, 6*(2), 2011.

Goldstein, A. H., B. C. Daube, J. W. Munger and S. C. Wofsy, Automated In-Situ Monitoring of Atmospheric Nonmethane Hydrocarbon Concentrations and Gradients, *Journal of Atmospheric Chemistry, 21*(1), 43-59, 1995.

Gounaris, K., A. R. R. Brain, P. J. Quinn and W. P. Williams, Structural Reorganization of Chloroplast Thylakoid Membranes in Response to Heat-Stress, *Biochimica et Biophysica Acta, 766*(1), 198-208, 1984.

Grabmer, W., M. Graus, C. Lindinger, A. Wisthaler, B. Rappengluck, R. Steinbrecher and A. Hansel, Disjunct eddy covariance measurements of monoterpene fluxes from a Norway spruce forest using PTR-MS, *International Journal of Mass Spectrometry, 239*(2-3), 111-115, 2004.

Grabmer, W., J. Kreuzwieser, A. Wisthaler, C. Cojocariu, M. Graus, H. Rennenberg, D. Steigner, R. Steinbrecher and A. Hansel, VOC emissions from Norway spruce (Picea abies L. [Karst]) twigs in the field - Results of a dynamic enclosure study, *Atmospheric Environment, 40*, S128-S137, 2006.

Grace, J. and M. Rayment, Respiration in the balance, *Nature, 404*(6780), 819-820, 2000.

Graus, M., A. Hansel, A. Wisthaler, C. Lindinger, R. Forkel, K. Hauff, M. Klauer, A. Pfichner, B. Rappengluck, D. Steigner and R. Steinbrecher, A relaxed-eddy-accumulation method for the measurement of isoprenoid canopy-fluxes using an online gas-chromatographic technique and PTR-MS simultaneously, *Atmospheric Environment, 40*, S43-S54, 2006.

Greenberg, J. P., A. B. Guenther, G. Petron, C. Wiedinmyer, O. Vega, L. V. Gatti, J. Tota and G. Fisch, Biogenic VOC emissions from forested Amazonian landscapes, *Glob. Change Biol., 10*(5), 651-662, 2004.

Guenther, A., The contribution of reactive carbon emissions from vegetation to the carbon balance of terrestrial ecosystems, *Chemosphere, 49*(8), 837-844, 2002.

Guenther, A., C. N. Hewitt, D. Erickson, R. Fall, C. Geron, T. Graedel, P. Harley, L. Klinger, M. Lerdau, W. A. Mckay, T. Pierce, B. Scholes, R. Steinbrecher, R. Tallamraju, J. Taylor and P. Zimmerman, A Global-Model of Natural Volatile Organic-Compound Emissions, *Journal of Geophysical Research-Atmospheres, 100*(D5), 8873-8892, 1995.

Guenther, A., T. Karl, P. Harley, C. Wiedinmyer, P. I. Palmer and C. Geron, Estimates of global terrestrial isoprene emissions using MEGAN (Model of Emissions of Gases and Aerosols from Nature), *Atmospheric Chemistry and Physics, 6*, 3181-3210, 2006.

Guenther, A., P. Zimmerman, L. Klinger, J. Greenberg, C. Ennis, K. Davis, W. Pollock, H. Westberg, G. Allwine and C. Geron, Estimates of regional natural volatile organic compound fluxes from enclosure and ambient measurements, *Journal of Geophysical Research-Atmospheres, 101*(D1), 1345-1359, 1996.

Guenther, A. B., P. R. Zimmerman, P. C. Harley, R. K. Monson and R. Fall, Isoprene and Monoterpene Emission Rate Variability - Model Evaluations and Sensitivity Analyses, *Journal of Geophysical Research-Atmospheres, 98*(D7), 12609-12617, 1993.

Guenther, A. B. and A. J. Hills, Eddy covariance measurement of isoprene fluxes, *J. Geophys. Res., 103*(D11), 13145-13152, 1998.

Hakola, H., V. Tarvainen, T. Laurila, V. Hiltunen, H. Hellen and P. Keronen, Seasonal variation of VOC concentrations above a boreal coniferous forest, *Atmospheric Environment, 37*(12), 1623-1634, 2003.

Helmig, D., Ozone removal techniques in the sampling of atmospheric volatile organic trace gases, *Atmospheric Environment, 31*(21), 3635-3651, 1997.

Helmig, D., B. Balsley, K. Davis, L. R. Kuck, M. Jensen, J. Bognar, T. Smith, R. V. Arrieta, R. Rodriguez and J. W. Birks, Vertical profiling and determination of landscape fluxes of biogenic nonmethane hydrocarbons within the planetary boundary layer in the Peruvian Amazon, *Journal of Geophysical Research-Atmospheres, 103*(D19), 25519-25532, 1998.

Helmig, D. and L. Vierling, Water-Adsorption Capacity of the Solid Adsorbents Tenax-Ta, Tenax-Gr, Carbotrap, Carbotrap-C, Carbosieve-Siii, and Carboxen-569 and Water Management-Techniques for the Atmospheric Sampling of Volatile Organic Trace Gases, *Analytical Chemistry, 67*(23), 4380-4386, 1995.

Hoffmann, T., R. Bandur, U. Marggraf and M. Linscheid, Molecular composition of organic aerosols formed in the alpha-pinene/O-3 reaction: Implications for new particle formation processes, *Journal of Geophysical Research-Atmospheres, 103*(D19), 25569-25578, 1998.

Högström, U., Non-Dimensional Wind and Temperature Profiles in the Atmospheric Surface-Layer - A Re-Evaluation, *Boundary-Layer Meteorology, 42*(1-2), 55-78, 1988.

Hoyle, C. R., M. Boy, N. M. Donahue, J. L. Fry, M. Glasius, A. Guenther, A. G. Hallar, K. H. Hartz, M. D. Petters, T. Petaja, T. Rosenoern and A. P. Sullivan, A review of the anthropogenic influence on biogenic secondary organic aerosol, *Atmospheric Chemistry and Physics, 11*(1), 321-343, 2011.

Hueber, J., AutoSampler Operation Manual, Atmospheric Research Lab, University of Colorado, Boulder, pp. 12, 2009.

IPCC, (Intergovernmental Panel on Climate Change), The AR 4 Synthesis Report, edited by Pachauri R.K. and Reisinger A., pp. 24-73, Cambridge University Press, Cambridge, 2007.

Ito, A. and J. E. Penner, Historical emissions of carbonaceous aerosols from biomass and fossil fuel burning for the period 1870-2000, *Global Biogeochemical Cycles, 19*(2), 2005.

Jakus, R., F. Schlyter, Q. H. Zhang, M. Blazenec, R. Vavercak, W. Grodzki, D. Brutovsky, E. Lajzova, M. Turcani, M. Bengtsson, Z. Blum and J. C. Gregoire, Overview of development of an anti-attractant based technology for spruce protection against Ips typographus: From past failures to future success, *Anzeiger fur Schadlingskunde-Journal of Pest Science, 76*(4), 89-99, 2003.

Janson, R. W., Monoterpene Emissions from Scots Pine and Norwegian Spruce, *Journal of Geophysical Research-Atmospheres, 98*(D2), 2839-2850, 1993.

Jenkin, M. E., S. M. Saunders and M. J. Pilling, The tropospheric degradation of volatile organic compounds: A protocol for mechanism development, *Atmospheric Environment, 31*(1), 81-104, 1997.

Jimenez, J. L., M. R. Canagaratna, N. M. Donahue, A. S. H. Prevot, Q. Zhang, J. H. Kroll, P. F. DeCarlo, J. D. Allan, H. Coe, N. L. Ng, A. C. Aiken, K. S. Docherty, I. M. Ulbrich, A. P. Grieshop, A. L. Robinson, J. Duplissy, J. D. Smith, K. R. Wilson, V. A. Lanz, C. Hueglin, Y. L. Sun, J. Tian, A. Laaksonen, T. Raatikainen, J. Rautiainen, P. Vaattovaara, M. Ehn, M. Kulmala, J. M. Tomlinson, D. R. Collins, M. J. Cubison, E. J. Dunlea, J. A. Huffman, T. B. Onasch, M. R. Alfarra, P. I. Williams, K. Bower, Y. Kondo, J. Schneider, F. Drewnick, S. Borrmann, S. Weimer, K. Demerjian, D. Salcedo, L. Cottrell, R. Griffin, A. Takami, T. Miyoshi, S. Hatakeyama, A. Shimono, J. Y. Sun, Y. M. Zhang, K. Dzepina, J. R. Kimmel, D. Sueper, J. T. Jayne, S. C. Herndon, A. M. Trimborn, L. R. Williams, E. C. Wood, A. M. Middlebrook, C. E.

Kolb, U. Baltensperger and D. R. Worsnop, Evolution of Organic Aerosols in the Atmosphere, *Science, 326*(5959), 1525-1529, 2009.

Jockel, P., H. Tost, A. Pozzer, C. Bruhl, J. Buchholz, L. Ganzeveld, P. Hoor, A. Kerkweg, M. G. Lawrence, R. Sander, B. Steil, G. Stiller, M. Tanarhte, D. Taraborrelli, J. Van Aardenne and J. Lelieveld, The atmospheric chemistry general circulation model ECHAM5/MESSy1: consistent simulation of ozone from the surface to the mesosphere, *Atmospheric Chemistry and Physics, 6,* 5067-5104, 2006.

Joutsensaari, J., M. Loivamaki, T. Vuorinen, P. Miettinen, A. M. Nerg, J. K. Holopainen and A. Laaksonen, Nanoparticle formation by ozonolysis of inducible plant volatiles, *Atmospheric Chemistry and Physics, 5,* 1489-1495, 2005.

Kaimal, J. C. and J. J. Finnigan, Atmospheric boundary layer flows : their structure and measurement, Oxford University Press, New York, 1994.

Kanakidou, M., J. H. Seinfeld, S. N. Pandis, I. Barnes, F. J. Dentener, M. C. Facchini, R. Van Dingenen, B. Ervens, A. Nenes, C. J. Nielsen, E. Swietlicki, J. P. Putaud, Y. Balkanski, S. Fuzzi, J. Horth, G. K. Moortgat, R. Winterhalter, C. E. L. Myhre, K. Tsigaridis, E. Vignati, E. G. Stephanou and J. Wilson, Organic aerosol and global climate modelling: a review, *Atmospheric Chemistry and Physics, 5,* 1053-1123, 2005.

Kanakidou, M., K. Tsigaridis, F. J. Dentener and P. J. Crutzen, Human-activity-enhanced formation of organic aerosols by biogenic hydrocarbon oxidation, *Journal of Geophysical Research-Atmospheres, 105*(D7), 9243-9254, 2000.

Karl, T., M. Potosnak, A. Guenther, D. Clark, J. Walker, J. D. Herrick and C. Geron, Exchange processes of volatile organic compounds above a tropical rain forest: Implications for modeling tropospheric chemistry above dense vegetation, *Journal of Geophysical Research-Atmospheres, 109*(D18), 2004.

Kautz, M. and R. Schopf, Elevational range shifts and altered flight patterns of bark beetle populations as a response to climatic change in the Alps., (submitted), *Ecological Entomology,* 2011.

Keeling, C. I. and J. Bohlmann, Genes, enzymes and chemicals of terpenoid diversity in the constitutive and induced defence of conifers against insects and pathogens, *New Phytologist, 170*(4), 657-675, 2006.

Keenan, T., U. Niinemets, S. Sabate, C. Gracia and J. Penuelas, Process based inventory of isoprenoid emissions from European forests: model comparisons, current knowledge and uncertainties, *Atmospheric Chemistry and Physics, 9*(12), 4053-4076, 2009.

Kerminen, V. M., T. Petaja, H. E. Manninen, P. Paasonen, T. Nieminen, M. Sipila, H. Junninen, M. Ehn, S. Gagne, L. Laakso, I. Riipinen, H. Vehkamaki, T. Kurten, I. K. Ortega, M. Dal Maso, D. Brus, A. Hyvarinen, H. Lihavainen, J. Leppa, K. E. J. Lehtinen, A. Mirme, S. Mirme, U. Horrak, T. Berndt, F. Stratmann, W. Birmili, A. Wiedensohler, A. Metzger, J. Dommen, U. Baltensperger, A. Kiendler-Scharr, T. F. Mentel, J. Wildt, P. M. Winkler, P. E. Wagner, A. Petzold, A. Minikin, C. Plass-Dulmer, U. Poschl, A. Laaksonen and M. Kulmala, Atmospheric nucleation: highlights of the EUCAARI project and future directions, *Atmospheric Chemistry and Physics, 10*(22), 10829-10848, 2010.

Kesselmeier, J., P. Ciccioli, U. Kuhn, P. Stefani, T. Biesenthal, S. Rottenberger, A. Wolf, M. Vitullo, R. Valentini, A. Nobre, P. Kabat and M. O. Andreae, Volatile organic compound emissions in relation to plant carbon fixation and the terrestrial carbon budget, *Global Biogeochemical Cycles, 16*(4), 2002.

Kesselmeier, J. and M. Staudt, Biogenic volatile organic compounds (VOC): An overview on emission, physiology and ecology, *Journal of Atmospheric Chemistry, 33*(1), 23-88, 1999.

Kessler, A. and I. T. Baldwin, Defensive function of herbivore-induced plant volatile emissions in nature, *Science, 291*(5511), 2141-2144, 2001.

Kessler, A., R. Halitschke, C. Diezel and I. T. Baldwin, Priming of plant defense responses in nature by airborne signaling between Artemisia tridentata and Nicotiana attenuata, *Oecologia, 148*(2), 280-292, 2006.

Klimetzek, D. and W. Francke, Relationship Between the Enantiomeric Composition of Alpha-Pinene in Host Trees and the Production of Verbenols in Ips Species, *Experientia, 36*(12), 1343-1345, 1980.

Knudsen, J. T., R. Eriksson, J. Gershenzon and B. Stahl, Diversity and distribution of floral scent, *Botanical Review, 72*(1), 1-120, 2006.

Kormann, R. and F. X. Meixner, An analytical footprint model for non-neutral stratification, *Boundary-Layer Meteorology, 99*(2), 207-224, 2001.

Kreuzwieser, J., J. P. Schnitzler and R. Steinbrecher, Biosynthesis of organic compounds emitted by plants, *Plant Biology, 1*(2), 149-159, 1999.

Kuhn, U., M. O. Andreae, C. Ammann, A. C. Araujo, E. Brancaleoni, P. Ciccioli, T. Dindorf, M. Frattoni, L. V. Gatti, L. Ganzeveld, B. Kruijt, J. Lelieveld, J. Lloyd, F. X. Meixner, A. D. Nobre, U. Poschl, C. Spirig, P. Stefani, A. Thielmann, R. Valentini and J. Kesselmeier, Isoprene and monoterpene fluxes from Central Amazonian rainforest inferred from tower-based and airborne measurements, and implications on the atmospheric chemistry and the local carbon budget, *Atmospheric Chemistry and Physics, 7*(11), 2855-2879, 2007.

Kulmala, M., How particles nucleate and grow, *Science, 302*(5647), 1000-1001, 2003.

Kurten, T., M. Kulmala, M. Dal Maso, T. Suni, A. Reissell, H. Vehkamaki, P. Hari, A. Laaksonen, Y. Viisanen and T. Vesala, Estimation of different forest-related contributions to the radiative balance using observations in southern Finland, *Boreal Environment Research, 8*(4), 275-285, 2003.

Langford, B., P. K. Misztal, E. Nemitz, B. Davison, C. Helfter, T. A. M. Pugh, A. R. MacKenzie, S. F. Lim and C. N. Hewitt, Fluxes and concentrations of volatile organic compounds from a South-East Asian tropical rainforest, *Atmospheric Chemistry and Physics, 10*(17), 8391-8412, 2010.

Laothawornkitkul, J., J. E. Taylor, N. D. Paul and C. N. Hewitt, Biogenic volatile organic compounds in the Earth system, *New Phytologist, 183*(1), 27-51, 2009.

Lathiere, J., D. A. Hauglustaine, A. D. Friend, N. De Noblet-Ducoudre, N. Viovy and G. A. Folberth, Impact of climate variability and land use changes on global biogenic volatile organic compound emissions, *Atmospheric Chemistry and Physics, 6*, 2129-2146, 2006.

Leaitch, W. R., J. W. Bottenheim, T. A. Biesenthal, S. M. Li, P. S. K. Liu, K. Asalian, H. Dryfhout-Clark, F. Hopper and F. Brechtel, A case study of gas-to-particle conversion in an eastern Canadian forest, *Journal of Geophysical Research-Atmospheres, 104*(D7), 8095-8111, 1999.

Lelieveld, J., T. M. Butler, J. N. Crowley, T. J. Dillon, H. Fischer, L. Ganzeveld, H. Harder, M. G. Lawrence, M. Martinez, D. Taraborrelli and J. Williams, Atmospheric oxidation capacity sustained by a tropical forest, *Nature, 452*(7188), 737-740, 2008.

Lerdau, M., M. Litvak, P. Palmer and R. Monson, Controls over monoterpene emissions from boreal forest conifers, *Tree Physiology, 17*(8-9), 563-569, 1997.

Lichtenthaler, H. K., The 1-deoxy-D-xylulose-5-phosphate pathway of isoprenoid biosynthesis in plants, *Annual Review of Plant Physiology and Plant Molecular Biology, 50*, 47-65, 1999.

Lindfors, V., T. Laurila, H. Hakola, R. Steinbrecher and J. Rinne, Modeling speciated terpenoid emissions from the European boreal forest, *Atmospheric Environment, 34*(29-30), 4983-4996, 2000.

Litvak, M. E. and R. K. Monson, Patterns of induced and constitutive monoterpene production in conifer needles in relation to insect herbivory, *Oecologia, 114*(4), 531-540, 1998.

Llusia, J. and J. Penuelas, Seasonal patterns of terpene content and emission from seven Mediterranean woody species in field conditions, *American Journal of Botany, 87*(1), 133-140, 2000.

Loivamaeki, M., R. Mumm, M. Dicke and J. P. Schnitzler, Isoprene interferes with the attraction of bodyguards by herbaceous plants, *Proceedings of the National Academy of Sciences of the United States of America, 105*(45), 17430-17435, 2008.

Loreto, F., A. Forster, M. Durr, O. Csiky and G. Seufert, On the monoterpene emission under heat stress and on the increased thermotolerance of leaves of Quercus ilex L. fumigated with selected monoterpenes, *Plant Cell and Environment, 21*(1), 101-107, 1998.

Loreto, F., P. Pinelli, F. Manes and H. Kollist, Impact of ozone on monoterpene emissions and evidence for an isoprene-like antioxidant action of monoterpenes emitted by Quercus ilex leaves, *Tree Physiology, 24*(4), 361-367, 2004.

Loreto, F. and J. P. Schnitzler, Abiotic stresses and induced BVOCs, *Trends in Plant Science, 15*(3), 154-166, 2010.

Mauder, M., C. Liebethal, M. Gockede, J. P. Leps, F. Beyrich and T. Foken, Processing and quality control of flux data during LITFASS-2003, *Boundary-Layer Meteorology, 121*(1), 67-88, 2006.

Mcgarvey, D. J. and R. Croteau, Terpenoid Metabolism, *Plant Cell, 7*(7), 1015-1026, 1995.

Metzger, A., B. Verheggen, J. Dommen, J. Duplissy, A. S. H. Prevot, E. Weingartner, I. Riipinen, M. Kulmala, D. V. Spracklen, K. S. Carslaw and U. Baltensperger, Evidence for the role of organics in aerosol particle formation under atmospheric conditions, *Proceedings of the National Academy of Sciences of the United States of America, 107*(15), 6646-6651, 2010.

Meyers, T. P., M. E. Hall, S. E. Lindberg and K. Kim, Use of the modified bowen-ratio technique to measure fluxes of trace gases, *Atmospheric Environment, 30*(19), 3321-3329, 1996.

Moncrieff, J. B., Y. Malhi and R. Leuning, The propagation of errors in long-term measurements of land-atmosphere fluxes of carbon and water, *Glob. Change Biol., 2*(3), 231-240, 1996.

Monin A.S. and Obukhov A.M., Basic laws of turbulent mixing in the surface layer of the atmosphere, *Tr. Akad. Nauk SSSR, 24*(151), 163-187, 1954.

Monson, R. K., C. H. Jaeger, W. W. Adams, E. M. Driggers, G. M. Silver and R. Fall, Relationships Among Isoprene Emission Rate, Photosynthesis, and Isoprene Synthase Activity As Influenced by Temperature, *Plant Physiology, 98*(3), 1175-1180, 1992.

Montzka, S. A., M. Krol, E. Dlugokencky, B. Hall, P. Jockel and J. Lelieveld, Small Interannual Variability of Global Atmospheric Hydroxyl, *Science, 331*(6013), 2011.

Moosmüller, H., R. K. Chakrabarty and W. P. Arnott, Aerosol light absorption and its measurement: A review, *Journal of Quantitative Spectroscopy and Radiative Transfer, 110*(11), 844-878, 2009.

Munich RE, Zwischen Hoch und Tief, Wetterrisiken in Mitteleuropa, pp. 1-58, München, 2007.

Nationalparkverwaltung Berchtesgaden, Bayerisches Staatsministerium für Landesentwicklung und Umweltfragen, Nationalparkplan Berchtesgaden, München, 2001.

Nishida, N., S. Tamotsu, N. Nagata, C. Saito and A. Sakai, Allelopathic effects of volatile monoterpenoids produced by Salvia leucophylla: Inhibition of cell proliferation and DNA synthesis in the root apical meristem of Brassica campestris seedlings, *Journal of Chemical Ecology, 31*(5), 1187-1203, 2005.

Penuelas, J., J. Llusia and M. Estiarte, Terpenoids - A Plant Language, *Trends in Ecology & Evolution, 10*(7), 289, 1995.

Penuelas, J. and M. Staudt, BVOCs and global change, *Trends in Plant Science, 15*(3), 133-144, 2010.

Persson, M., K. Sjodin, A. K. BorgKarlson, T. Norin and I. Ekberg, Relative amounts and enantiomeric compositions of monoterpene hydrocarbons in xylem and needles of Picea abies, *Phytochemistry, 42*(5), 1289-1297, 1996.

Pichersky, E. and J. Gershenzon, The formation and function of plant volatiles: perfumes for pollinator attraction and defense, *Current Opinion in Plant Biology, 5*(3), 237-243, 2002.

Pio, C. A., P. A. Silva, M. A. Cerqueira and T. V. Nunes, Diurnal and seasonal emissions of volatile organic compounds from cork oak (Quercus suber) trees, *Atmospheric Environment, 39*(10), 1817-1827, 2005.

Plaza, J., L. Nunez, M. Pujadas, R. Perrez-Pastor, V. Bermejo, S. Garcia-Alonso and S. Elvira, Field monoterpene emission of Mediterranean oak (Quercus ilex) in the central Iberian Peninsula measured by enclosure and micrometeorological techniques: Observation of drought stress effect, *Journal of Geophysical Research-Atmospheres, 110*(D3), 2005.

Prieme, A., T. B. Knudsen, M. Glasius and S. Christensen, Herbivory by the weevil, Strophosoma melanogrammum, causes severalfold increase in emission of monoterpenes from young Norway spruce (Picea abies), *Atmospheric Environment, 34*(5), 711-718, 2000.

Pureswaran, D. S., R. Gries and J. H. Borden, Antennal responses of four species of tree-killing bark beetles (Coleoptera : Scolytidae) to volatiles collected from beetles, and their host and nonhost conifers, *Chemoecology, 14*(2), 59-66, 2004.

Raffa, K. F., B. H. Aukema, B. J. Bentz, A. L. Carroll, J. A. Hicke, M. G. Turner and W. H. Romme, Cross-scale drivers of natural disturbances prone to anthropogenic amplification: The dynamics of bark beetle eruptions, *Bioscience, 58*(6), 501-517, 2008.

Raisanen, T., A. Ryyppo and S. Kellomaki, Effects of elevated CO2 and temperature on monoterpene emission of Scots pine (Pinus sylvestris L.), *Atmospheric Environment, 42*(18), 4160-4171, 2008.

Ramanathan, V., P. J. Crutzen, J. T. Kiehl and D. Rosenfeld, Atmosphere - Aerosols, climate, and the hydrological cycle, *Science, 294*(5549), 2119-2124, 2001.

Reddemann, J. and R. Schopf, The importance of monoterpenes in the aggregation of the spruce bark beetle Ips typographus (Coleoptera: Scolytidae: Ipinae), *Entomologia Generalis, 21*(1-2), 69-80, 1996.

Reinhard, J., M. V. Srinivasan and S. W. Zhang, Olfaction: Scent-triggered navigation in honeybees, *Nature, 427*(6973), 411, 2004.

Repola, J., Biomass Equations for Scots Pine and Norway Spruce in Finland, *Silva Fennica, 43*(4), 625-647, 2009.

Rinne, H. J. I., A. B. Guenther, J. P. Greenberg and P. C. Harley, Isoprene and monoterpene fluxes measured above Amazonian rainforest and their dependence on light and temperature, *Atmospheric Environment, 36*(14), 2421-2426, 2002.

Rinne, J., J. P. Tuovinen, T. Laurila, H. Hakola, M. Aurela and H. Hypen, Measurements of hydrocarbon fluxes by a gradient method above a northern boreal forest, *Agricultural and Forest Meteorology, 102*(1), 25-37, 2000.

Rinne, J., T. Riutta, M. Pihlatie, M. Aurela, S. Haapanala, J. P. Tuovinen, E. S. Tuittila and T. Vesala, Annual cycle of methane emission from a boreal fen measured by the eddy covariance technique, *Tellus Series B-Chemical and Physical Meteorology, 59*(3), 449-457, 2007.

Ruuskanen, T. M., H. Hakola, M. K. Kajos, H. Hellen, V. Tarvainen and J. Rinne, Volatile organic compound emissions from Siberian larch, *Atmospheric Environment, 41*(27), 5807-5812, 2007.

Ruuskanen, T. M., P. Kolari, J. Back, M. Kulmala, J. Rinne, H. Hakola, R. Taipale, M. Raivonen, N. Altimir and P. Hari, On-line field measurements of monoterpene emissions from Scots pine by proton-transfer-reaction mass spectrometry, *Boreal Environment Research, 10*(6), 553-567, 2005.

Ruzicka, L., The Isoprene Rule and the Biogenesis of Terpenic Compounds, *Experientia, 9*(10), 357-367, 1953.

S.Dev, A.P.S.Narula and J.S.Yadav, Handbook of Terpenoids: Monoterpenoids, CRC, 1982.

Sallas, L., E. M. Luomala, J. Utriainen, P. Kainulainen and J. K. Holopainen, Contrasting effects of elevated carbon dioxide concentration and temperature on Rubisco activity, chlorophyll fluorescence, needle ultrastructure and secondary metabolites in conifer seedlings, *Tree Physiology, 23*(2), 97-108, 2003.

Scaife, A., T. Spangehl, D. Fereday, U. Cubasch, U. Langematz, H. Akiyoshi, S. Bekki, P. Braesicke, N. Butchart, M. Chipperfield, A. Gettelman, S. Hardiman, M. Michou, E. Rozanov and T. Shepherd, Climate change projections and stratosphere-troposphere interaction, *Climate Dynamics,* 1-9, 2011.

Schaub, A., J. D. Blande, M. Graus, E. Oksanen, J. K. Holopainen and A. Hansel, Real-time monitoring of herbivore induced volatile emissions in the field, *Physiologia Plantarum, 138*(2), 123-133, 2010.

Schelhaas, M. J., G. J. Nabuurs and A. Schuck, Natural disturbances in the European forests in the 19th and 20th centuries, *Glob. Change Biol., 9*(11), 1620-1633, 2003.

Schmid, H. P., H. B. Su, C. S. Vogel and P. S. Curtis, Ecosystem-atmosphere exchange of carbon dioxide over a mixed hardwood forest in northern lower Michigan, *Journal of Geophysical Research, vol.108, no.D14*, ACH6-19, 2003.

Schnitzler, J. P., R. Arenz, R. Steinbrecher and A. Lehning, Characterization of an isoprene synthase from leaves of Quercus petraea (Mattuschka) Liebl, *Botanica Acta, 109*(3), 216-221, 1996.

Schnitzler, J. P., N. Bauknecht, N. Bruggemann, W. Einig, R. Forkel, R. Hampp, A. C. Heiden, U. Heizmann, T. Hoffmann, C. Holzke, L. Jaeger, M. Klauer, M. Komenda, R. Koppmann, J. Kreuzwieser, H. Mayer, H. Rennenberg, G. Smiatek, R. Steinbrecher, J. Wildt and W. Zimmer, Emission of biogenic volatile organic compounds: An overview of field, laboratory and modelling studies performed during the 'Tropospheric Research Program' (TFS) 1997-2000, *Journal of Atmospheric Chemistry, 42*(1), 159-177, 2002.

Schnitzler, J. P., R. Steinbrecher, I. Zimmer, D. Steigner and M. Fladung, Hybridization of European oaks (Quercus ilex x Q-robur) results in a mixed isoprenoid emitter type, *Plant Cell and Environment, 27*(5), 585-593, 2004.

Schoenwitz, R., Kloos M., L. Merk and H. Ziegler, Patterns of monoterpenes stored in the needles of <i>Picea abies</i> (L.) Karst. from several locations in mountainous regions of southern Germany, *Trees - Structure and Function, 4*(1), 27-33, 1990.

Schurgers, G., A. Arneth, R. Holzinger and A. H. Goldstein, Process-based modelling of biogenic monoterpene emissions combining production and release from storage, *Atmospheric Chemistry and Physics, 9*(10), 3409-3423, 2009.

Schween, J. H., R. Dlugi, C. N. Hewitt and P. Foster, Determination and accuracy of VOC-fluxes above the pine/oak forest at Castelporziano, *Atmospheric Environment, 31*, 199-215, 1997.

Seybold, S. J., J. Bohlmann and K. F. Raffa, Biosynthesis of coniferophagous bark beetle pheromones and conifer isoprenoids: Evolutionary perspective and synthesis, *Canadian Entomologist, 132*(6), 697-753, 2000.

Sharkey, T. D., Isoprene synthesis by plants and animals, *Endeavour, 20*(2), 74-78, 1996.

Shulaev, V., P. Silverman and I. Raskin, Airborne signalling by methyl salicylate in plant pathogen resistance, *Nature, 385*(6618), 718-721, 1997.

Siitonen, J., Forest Management, Coarse Woody Debris and Saproxylic Organisms: Fennoscandian Boreal Forests as an Example, *Ecological Bulletins,*(49), 11-41, 2001.

Simon, V., L. Dumergues, P. Bouchou, L. Torres and A. Lopez, Isoprene emission rates and fluxes measured above a Mediterranean oak (Quercus pubescens) forest, *Atmospheric Research, 74*(1-4), 49-63, 2005.

Simpson, D., W. Winiwarter, G. Borjesson, S. Cinderby, A. Ferreiro, A. Guenther, C. N. Hewitt, R. Janson, M. A. K. Khalil, S. Owen, T. E. Pierce, H. Puxbaum, M. Shearer, U. Skiba, R. Steinbrecher, L. Tarrason and M. G. Oquist, Inventorying emissions from nature in Europe, *Journal of Geophysical Research-Atmospheres, 104*(D7), 8113-8152, 1999.

Singh, H. B. and P. Zimmermann, Atmospheric Distribution and Sources of Nonmethane Hydrocarbons, in Gaseous Pollutants:Characterization and Cycling, edited by J.O.Nriagu, p. 235pp, John Wiley and Sons, 1992.

Singh, H. P., D. R. Batish, S. Kaur, H. Ramezani and R. K. Kohli, Comparative phytotoxicity of four monoterpenes against Cassia occidentalis, *Annals of Applied Biology, 141*(2), 111-116, 2002.

Starokozhev, E., E. Fries, A. Cycura and W. Puettmann, Distribution of VOCs between air and snow at the Jungfraujoch high alpine research station, Switzerland, during CLACE 5 (winter 2006), *Atmospheric Chemistry and Physics, 9*(9), 3197-3207, 2009.

Staudt, M., N. Bertin, B. Frenzel and G. Seufert, Seasonal variation in amount and composition of monoterpenes emitted by young Pinus pinea trees - Implications for emission modeling, *Journal of Atmospheric Chemistry, 35*(1), 77-99, 2000.

Staudt, M. and L. Lhoutellier, Volatile organic compound emission from hohn oak infested by gypsy moth larvae: evidence for distinct responses in damaged and undamaged leaves, *Tree Physiology, 27*, 1433-1440, 2007.

Steinbrecher, Flüchtige organische Verbindungen (VOC): Der Brennstoff für die bodennahe Ozonproduktion., in Gefahrstoffe - Reinhaltung der Luft, pp. 71-73, 2011.

Steinbrecher, R., A revised parameterization for emission modelling of isoprenoids for boreal plants, edited by H. H. a. J. R. K.Hauff, 1999.

Steinbrecher, R., G. Eichstadter, W. Schurmann, L. Torres, B. Clement, V. Simon, D. Kotzias, R. Daiber and J. Vaneijk, Monoterpenes in Air Samples - European Intercomparison Experiments, *International Journal of Environmental Analytical Chemistry, 54*(4), 283-297, 1994.

Steinbrecher, R., M. Klauer, K. Hauff, W. R. Stockwell, W. Jaeschke, T. Dietrich and F. Herbert, Biogenic and anthropogenic fluxes of non-methane hydrocarbons over an urban-impacted forest, Frankfurter Stadtwald, Germany, *Atmospheric Environment, 34*(22), 3779-3788, 2000.

Steinbrecher, R., G. Smiatek, R. Koble, G. Seufert, J. Theloke, K. Hauff, P. Ciccioli, R. Vautard and G. Curci, Intra- and inter-annual variability of VOC emissions from natural and semi-natural vegetation in Europe and neighbouring countries, *Atmospheric Environment, 43*(7), 1380-1391, 2009.

Stull, R. B., An introduction to boundary layer meteorology, Kluwer, Dordrecht [u.a.], 1988.

Trapp, S. and R. Croteau, Defensive resin biosynthesis in conifers, *Annual Review of Plant Physiology and Plant Molecular Biology, 52*, 689-724, 2001.

Ulbrich, U. and M. Christoph, A shift of the NAO and increasing storm track activity over Europe due to anthropogenic greenhouse gas forcing, *Climate Dynamics, 15*(7), 551-559, 1999.

Ulbrich, U., J. G. Pinto, H. Kupfer, G. C. Leckebusch, T. Spangehl and M. Reyers, Changing northern hemisphere storm tracks in an ensemble of IPCC climate change simulations, *Journal of Climate, 21*(8), 1669-1679, 2008.

Usbeck, T., T. Wohlgemuth, M. Dobbertin, C. Pfister, A. Burgi and M. Rebetez, Increasing storm damage to forests in Switzerland from 1858 to 2007, *Agricultural and Forest Meteorology, 150*(1), 47-55, 2010.

Van Den Boom, C. E. M., T. A. Van Beek, M. A. Posthumus, A. De Groot and M. Dicke, Qualitative and quantitative variation among volatile profiles induced by Tetranychus urticae feeding on plants from various families, *Journal of Chemical Ecology, 30*(1), 69-89, 2004.

Vancanneyt, G., C. Sanz, T. Farmaki, M. Paneque, F. Ortego, P. Castanera and J. J. Sanchez-Serrano, Hydroperoxide lyase depletion in transgenic potato plants leads to an increase in aphid performance, *Proceedings of the National Academy of Sciences of the United States of America, 98*(14), 8139-8144, 2001.

Vickers, C. E., J. Gershenzon, M. T. Lerdau and F. Loreto, A unified mechanism of action for volatile isoprenoids in plant abiotic stress, *Nature Chemical Biology, 5*(5), 283-291, 2009a.

Vickers, C. E., J. Gershenzon, M. T. Lerdau and F. Loreto, A unified mechanism of action for volatile isoprenoids in plant abiotic stress, *Nature Chemical Biology, 5*(5), 283-291, 2009b.

Walker, J. T., W. P. Robarge, Y. Wu and T. P. Meyers, Measurement of bi-directional ammonia fluxes over soybean using the modified Bowen-ratio technique, *Agricultural and Forest Meteorology, 138*(1-4), 54-68, 2006.

Wallach, O., Zur Kenntniss der Terpene und ätherischen Oele, *Justus Liebigs Annalen der Chemie, 238*(1-2), 78-89, 1887.

Wallach, O., Ueber Terpene und Campher, *Ber. Dtsch. Chem. Ges., 24*(1), 1525-1579, 1891.

Wang, Y. H., D. J. Jacob and J. A. Logan, Global simulation of tropospheric O-3-NOx-hydrocarbon chemistry 3. Origin of tropospheric ozone and effects of nonmethane hydrocarbons, *Journal of Geophysical Research-Atmospheres, 103*(D9), 10757-10767, 1998.

Went, F. W., Blue Hazes in the Atmosphere, *Nature, 187*(4738), 641-643, 1960.

<u>Erklärung</u>

Ich erkläre an Eides statt, dass ich die der Fakultät Wissenschaftszentrum Weihenstephan für Ernährung, Landnutzung und Umwelt der Technischen Universität München zur Promotionsprüfung vorgelegten Arbeit mit dem Titel:

"Emission and abundance of biogenic volatile organic compounds in wind-throw areas of upland spruce forests in Bavaria"

am Lehrstuhl für Atmosphärische Umweltforschung unter der Anleitung und Betreuung durch Professor Dr. Hans Peter Schmid und Dr. Rainer Steinbrecher ohne sonstige Hilfe erstellt und bei der Abfassung nur die gemäß § 6 Abs. 5 angegebenen Hilfsmittel benutzt habe.

Ich habe die Dissertation in dieser oder ähnlicher Form in keinem anderen Prüfungsverfahren als Prüfungsleistung vorgelegt.

Ich habe den angestrebten Doktorgrad noch nicht erworben und bin nicht in einem früheren Promotionsverfahren für den angestrebten Doktorgrad endgültig gescheitert.

Die Promotionsordnung der Technischen Universität München ist mir bekannt.

München, den

                                                            Benjamin Wolpert

Acknowledgements

Garmisch-Partenkirchen, April 2012

Benjamin Wolpert

CURRICULUM VITAE

BENJAMIN WOLPERT

Kreuzstrasse 3

82467 Garmisch-Partenkirchen

Tel.:   0049 8821 183285

e-mail: benjamin.wolpert@kit.edu

born 14.12.1981 in Garmisch-Partenkirchen, Germany

EDUCATION

2008-2012	Dissertation at the Technical University Munich (TUM), Center of Life and Food Sciences Weihenstephan in collaboration with the Karlsruhe Institute of Technology (KIT), Institute of Meteorology and Climate Research, Department of Atmospheric Environmental Research
	Thesis: "Emission and abundance of biogenic volatile organic compounds in wind-throw areas of upland spruce forests in Bavaria"
	Supervisors: Professor Dr. H.P. Schmid and Dr. Rainer Steinbrecher
10/2007-12/2007	Project "Screening of gas sensitive inorganic ion conductors" in collaboration with Siemens VDO at the University of Regensburg
2001-2007	Diploma in Chemistry, University of Regensburg
	Diploma Thesis: "Development of conductometric ammonia gas sensors based on inorganic copper compounds"
	Main subject: Analytical Chemistry Minor subjects: Inorganic chemistry, Organic chemistry
1992-2001	Werdenfels Gymnasium, Garmisch-Partenkirchen

PUBLICATIONS

<u>Peer reviewed journals</u>

B. Wolpert, M. Leitl, A. Pfitzner, V. M. Mirsky, *Chemosensitive properties of electrically conductive Cu(I) compounds at room temperature*, Sens. actuat. B: Chem, 134, 2, (2008) 839-842

B. Wolpert, O. S. Wolfbeis, V. M. Mirsky, *Gas sensing properties of electrically conductive Cu(I) compounds at elevated temperatures*, Sens. actuat. B: Chem, 142, 2, (2009), 446-450

B. Wolpert, R. Steinbrecher, M. Lindauer, M. Mauder, H.P. Schmid, *Dead wood is a strong source of monoterpenes in a disturbed forest ecosystem,* Agr. Forest Meteorol. submitted, (2012)

<u>Oral presentations:</u>

B. Wolpert, R. Steinbrecher, M. Lindauer, H.P. Schmid, (2011), *Investigations on biogenic organic compounds in wind throw areas in Bavarian national parks*, International workshop on biogenic volatile organic compound emissions models and their applications. Lancaster, England

B. Wolpert, R. Steinbrecher, M. Lindauer, H.P. Schmid, (2011), *Monoterpene fluxes in a wind-throw disturbed forest ecosystem in the National Park Bavarian Forest.* Project meeting of the network "Große Ohe". Spiegelau, Germany

B. Wolpert, R. Steinbrecher, M. Lindauer, M. Mauder, H.P. Schmid, (2010), *Environmental control on BioVOC levels in disturbed forest ecosystems.* Research actualities in Bohemian/Bavarian Forest. Srni, Czech Republic

<u>Posters:</u>

B. Wolpert, R. Steinbrecher, M. Lindauer, H.P. Schmid, (2011), *Monoterpene fluxes above a wind-throw disturbed upland spruce forest ecosystem*. ILEAPS conference, Garmisch-Partenkirchen, Germany

B. Wolpert, H.P. Schmid, R. Steinbrecher, (2010), *Investigations on biogenic volatile organic compounds (BioVOC) in wind throw areas of Norway spruce forests in Bavarian National Parks.* Gordon Research Conference on Biogenic Hydrocarbons & the Atmosphere, Les Diablerets, Switzerland

B. Wolpert, R. Steinbrecher, H.P. Schmid, (2012), *Dead wood in a disturbed forest ecosystem is a strong source of monoterpenes*. Gordon Research Conference on Biogenic Hydrocarbons & the Atmosphere, Lewiston, Maine, USA